



Joseany de Moraes Santos Almeida

**Development of electro-analytical methods
using electrochemical carbon-based sensors
for determination of trifloxystrobin, gentamicin
and lapachol**

Tese de Doutorado

Thesis presented to the Programa de Pós-graduação em Química of PUC-Rio in partial fulfillment of the requirements for the degree of Doutor em Química.

Advisor: Prof. Ricardo Queiroz Aucélio

Co-Advisor: Prof^a. Andrea Rosane da Silva

Rio de Janeiro
March 2018



Joseany de Moraes Santos Almeida

**Development of electro-analytical methods
using electrochemical carbon-based sensors
for determination of trifloxystrobin,
gentamicin and lapachol**

Thesis presented to the Programa de Pós-graduação em Química of PUC-Rio in partial fulfillment of the requirements for the degree of Doutor em Química. Approved by the undersigned Examination Committee.

Prof. Ricardo Queiroz Aucélio

Advisor

Departamento de Química - PUC-Rio

Prof^a. Andrea Rosane da Silva

Co-advisor

CEFET/RJ

Prof^a. Silvia Helena Pires Serrano

USP

Prof. Renato Camargo Matos

UFJF

Prof. Felipe Silva Semaan

UFF

Prof. Nicolás Adrián Rey

Departamento de Química - PUC-Rio

Prof. Jones Limberger

Departamento de Química - PUC-Rio

Prof. Márcio da Silveira Carvalho

Vice Dean of Graduate Studies Centro Técnico Científico –
PUC-Rio

Rio de Janeiro, March 16th 2018

Joseany de Moraes Santos Almeida

PhD candidate in the Chemistry Graduate Program at Pontifícia Universidade Católica do Rio de Janeiro (PUC-Rio). Masters degree in Analytical Chemistry concluded at the Universidade Federal do Maranhão (UFMA), in 2013. She concluded specialization in Food Sanitary Surveillance at UFMA in 2012. Bachelor in Chemistry at UFMA in 2010. She also has experience in the field of Analytical Chemistry (Electroanalytical methods and Electrochemical Sensors).

Bibliographic data

Almeida, Joseany de Moraes Santos

Development of electro-analytical methods using electrochemical carbon-based sensors for determination of trifloxystrobin, gentamicin and lapachol / Joseany de Moraes Santos Almeida; advisor: Ricardo Queiroz Aucélio; co-advisor: Andrea Rosane da Silva – 2018.

135 f.: il. color. ; 30 cm

Tese (doutorado) – Pontifícia Universidade Católica do Rio de Janeiro, Departamento de Química, 2018.

Inclui bibliografia

1. Química – Teses. 2. Voltametria. 3. Amperometria. 4. Diamante dopado com boro. 5. Eletrodo de grafite-epoxi. I. Aucélio, Ricardo Queiroz. II. Da Silva, Andrea Rosane. III. Pontifícia Universidade Católica do Rio de Janeiro. Departamento de Química. IV. Título.

CDD: 540

Acknowledgment

To God, first, by the force of moving on;

To my advisor Dr. Ricardo Queiroz Aucélio for his guidance, encouragement, support, friendship and dedication, you are my inspiration;

To my co-advisor Andrea Rosane da Silva for her collaboration and help in the development of doctoral work, encouragement and friendship.

To the CNPq and PUC-Rio for granting the doctoral scholarship, instituting scholarship and encouraging research;

To FAPERJ and CNPq for the funding that maintained this research.

To the Professors Aldaléa Marques and Edmar Marques for starting me in the academic world of research and for the confidence, opportunity and incentive dedicated to me, both of you to my eternal gratitude.

To the students of scientific initiation, Isabela, Barbara, Ana Beatriz and Bianca, for supporting the accomplishment of the research, the dedication given to the projects and for the friendship established during the period of work together.

To the members of the evaluation committee for their availability and for having accepted the invitation;

To the graduate department of chemistry of PUC-Rio for the opportunity and research support. In particular, the Professors whose teachings provided me with great academic growth.

To my parents Maria and José Carlos, brothers Joseana and Carlos Wendel and my sister-in-law Kleude for their patience, encouragement and motivation;

To all my family that has always been by my side in the joyful hours and the difficult ones too;

To all the friends of the postgraduate course, especially my great friends Druval Santos de Sá for being a great gift in my life and for helping me so much in this work, and friends Raquel Martins, Glaucia Olivatto. In special I thank Carlos Toloza for being my best friend and laboratory partner, I am your fan and wish you a lot of success, you can be whatever you want in this life, I admire you a lot.

To my cousin Fernando Almeida and friends Veronica Diniz and Fernando (Nando) for the friendship.

To Ana Paula, my friend and laboratory companion for all the help and availability granted, for the encouragement, motivation and happy moments and fun together.

To Dr. Alessandra Licursi for all the teachings transmitted and for her kindness, solidarity, and friendship dedicated to me.

To the friends and technician of the LEEA Claudiomar Franco, Luis Maqueira, Larissa Madeira, Igor Pinto, Jarol Miranda, Marlin Pedrozo, Sônia Gomes, Leila, Junior and Paulo Santos, always willing to help me in the laboratory;

To Guilherme Schardong, for the companionship, friendship, support, encouragement, trust and help, you are my strength.

To Anna De Falco for your help, patience and encouragement in the final stretch of this work. You are very special.

To Juliano Xavier, a great friend who has always believed in my potential and has been with me in the most difficult moments during this doctorate. There were many talks and advices and I will keep them forever in my heart, you are an example of persistence, motivation and victory. Thank you for always being my friend.

To friends Leticia, Luis, Renan, Thais and Neto, for the fun Saturdays and friendship.

To all the people who have passed through my life and influenced me in some way, but they were not mentioned.

Abstract

Almeida, Joseany de Moraes Santos; Aucélio, Ricardo Queiroz (advisor); Da Silva, Andrea Rosane (Co-advisor). **Development of electro-analytical methods using electrochemical carbon-based sensors for determination of trifloxystrobin, gentamicin and lapachol.** Rio de Janeiro, 2018. 135p. Tese de Doutorado - Departamento de Química, Pontifícia Universidade Católica do Rio de Janeiro.

The present work aimed to develop electroanalytical methods using graphite-epoxy and boron-doped diamond electrodes for the determination of the antibiotic gentamicin sulfate, substances of biological interest (naphthoquinones) and the pesticide trifloxystrobin. Boron doped diamond (BDD) features attractive electrochemical detection characteristics that are useful in analytical applications based on voltammetry and amperometry. It has a wide potential window in aqueous solutions that allowed the quantification of the fungicide trifloxystrobin (in +1744 mV versus Ag/AgCl_(KCl_{sat})) by square-wave voltammetry (SWV) in Britton-Robinson buffer (0.04 mol L⁻¹, pH 4.00) / acetonitrile 70/30% v/v electrolyte medium. The analyte addition curve was constructed using 40 mV pulse amplitude, 30 Hz frequency, 20 mV step potential. The instrumental limit of detection was 1.4×10^{-7} mol L⁻¹ and the linear dynamic range covered three orders of magnitude (from 10⁻⁷ to 10⁻⁵ mol L⁻¹). Recoveries of about 80% in orange juice samples and 92.4 to 104.0% in water samples. A study to evaluate potential interferences was carried out in the presence of other fungicides. Diagnostic studies indicated that the oxidation of trifloxystrobin in aqueous medium, on the surface of the BDD, is irreversible, involving two steps, each of them with two electrons. UV degradation of trifloxystrobin was studied using the proposed voltammetric method and degradation kinetics with a half-life of 1.07 min was established. Batch injection amperometry (BIA) with BDD (operating at +2000 mV) was used to develop a method for the determination of gentamicin sulfate. Solid phase extraction (SPE) using a cartridge packed with a molecular imprinting polymer made with kanamycin as the template molecule, was used to improve the selectivity. The acetate buffer (0.01 mol L⁻¹; pH 4.40) was used as supporting electrolyte. Oxidation of gentamicin sulfate occurred right after the

analyte (60 μL solution) comes into contact with the surface of the electrode. The SPE cartridge packed with MIP was very efficient in retaining the analyte when compared to the one packed with the corresponding non-printed polymer (NIP). The analytical curve was linear, the instrument accuracy was less than 3% and the limit of quantification was $2.7 \times 10^{-6} \text{ mol L}^{-1}$. The analytical frequency was 90 measurements h^{-1} and no memory effect was observed between sequential measurements. The performance of the proposed method was compared with that obtained by HPLC-UV and molecular absorption spectrophotometry (both after chemical derivatization of the analyte with o-phthalaldehyde or with ninhydrin). The method was applied in injectable pharmaceutical formulations and in simulated samples, with recoveries close to 100%. For the determination of lapachol SWV was employed using a graphite-epoxy electrode made in the laboratory. The electrolytic medium used was an aqueous solution containing the cationic surfactant CTAB ($1.2 \times 10^{-4} \text{ mol L}^{-1}$), phosphate buffer ($4.0 \times 10^{-2} \text{ mol L}^{-1}$, pH 6.00) and KNO_3 (1.0 mol L^{-1}). The cationic surfactant improved the diffusion and interaction of the analyte with the electrode, producing a reversible process that improved the total current measured by the system. The lapachol signal was measured at -470 mV after preconcentration at 400 mV for 140 s, using a 30 Hz frequency, 40 mV pulse amplitude with a step potential of 20 mV. The instrumental limit of detection was 0.029 mg L^{-1} and the dynamic linear range comprised two orders of magnitude. In the presence of β -lapachone (structural isomer), the selectivity was obtained by the first-order derivative of the SWV signal. The determination of lapachol in ethanolic extract of *Tabebuia impetiginosa* was carried out after a simple separation of the analyte by thin layer chromatography. The results are statistically similar (with 95% confidence level) with those performed through HPLC-UV. Studies for the simultaneous determination of beta-lapachone and alpha-lapachone were also successfully performed.

Keywords

Voltametry; Amperometry; Boron-doped diamond; Graphite-epoxy electrode; Trifloxystrobin; Naphtoquinones; Gentamicin.

Resumo

Almeida, Joseany de Moraes Santos; Aucélio, Ricardo Queiroz; Da Silva, Andrea Rosane. **Desenvolvimento de métodos eletroanalíticos utilizando sensores eletroquímicos baseados no carbono para determinação de trifloxistrobina, gentamicina e lapachol.** Rio de Janeiro, 2018. 135p. Tese de Doutorado, Departamento de Química, Pontifícia Universidade Católica do Rio de Janeiro.

O presente trabalho teve como objetivo o desenvolvimento de métodos eletroanalíticos empregando elétrodos de grafite-epóxi e diamante dopado com boro para a determinação do antibiótico sulfato de gentamicina, substâncias de interesse biológico (naftoquinonas) e do pesticida trifloxistrobina. O diamante dopado com boro (DDB) apresenta características atraentes de detecção eletroquímica que são úteis em aplicações analíticas baseadas em voltametria e amperometria. Possui uma ampla janela de potencial em soluções aquosas que permitiu a quantificação do fungicida trifloxistrobina (em +1744 mV versus Ag/AgCl_(KCl_{sat})) por voltametria de onda quadrada (SWV), em um tampão Britton-Robinson (0,04 mol L⁻¹, pH 4,00)/acetonitrila 70/30% v/v. A curva de adição de analito foi obtida usando amplitude de pulso 40 mV, frequência de 30 Hz, passo de potencial de 20 mV. O limite instrumental de detecção foi de $1,4 \times 10^{-7}$ mol L⁻¹ e a faixa linear dinâmica abrangeram três ordens de grandeza (10^{-7} a 10^{-5} mol L⁻¹). As amostras foram analisadas com recuperações de cerca de 80% em amostras de suco de laranja e de 92,4 a 104,0% em amostras de água. Um estudo para avaliar potenciais interferentes foi realizado na presença de outros fungicidas. Estudos diagnósticos indicaram que a oxidação da trifloxistrobina em meio aquoso na superfície do DDB é irreversível, envolvendo duas etapas, cada um com dois elétrons. A degradação UV da trifloxistrobina foi avaliada utilizando o método eletroquímico proposto e a cinética de degradação estabelecida com meia-vida de 1.07 min. A amperometria por injeção em batelada (BIA do inglês *batch-injection analysis*) com o DDB (operando a +2000 mV) foi utilizada para desenvolver um método para a determinação de sulfato de gentamicina. A extração em fase sólida (SPE do inglês *solid-phase extraction*), utilizando um cartucho empacotado com um polímero impresso molecularmente, tendo a canamicina como molécula molde, foi utilizada para melhorar a seletividade. O tampão acetato (0,01 mol L⁻¹;

pH 4,4) foi utilizado como eletrólito suporte. A oxidação do sulfato de gentamicina ocorreu logo após a injeção do analito (60 µL) que entra em contato com a superfície do eletrodo. O cartucho de SPE foi muito eficiente na retenção do analito quando comparado com o polímero não-impresso correspondente (NIP). A curva analítica apresentou resposta linear, a precisão instrumental foi inferior a 3% e o limite de quantificação foi de $2,7 \times 10^{-6} \text{ mol L}^{-1}$. A frequência analítica foi de 90 medições h^{-1} e nenhum efeito de memória foram observados entre as medidas sequenciais. O desempenho do método proposto foi comparado com o obtido por HPLC-UV e com espectrofotometria de absorção molecular (ambos após derivação química do analito com *o*-ftalaldeído ou com ninhidrina). O método desenvolvido neste trabalho foi aplicado em formulações farmacêuticas injetáveis e em amostras simuladas, com recuperações próximas de 100%. Para a determinação do lapachol foi utilizada a SWV usando um eletrodo de grafite-epoxi feito no laboratório. O meio eletrolítico utilizado foi uma solução aquosa contendo o surfactante catiônico CTAB ($1,2 \times 10^{-4} \text{ mol L}^{-1}$), tampão fosfato ($4,0 \times 10^{-2} \text{ mol L}^{-1}$, pH 6,0) e KNO_3 ($1,0 \text{ mol L}^{-1}$). O surfactante catiônico melhorou a difusão e a interação do analito com o eletrodo, produzindo um processo reversível que melhorou a corrente total medida pelo sistema. O sinal do lapachol foi medido a -470 mV, após pré-concentração a 400 mV durante 140 s, usando frequência de 30 Hz, amplitude de pulso de 40 mV com passo de potencial de 20 mV. O limite instrumental de detecção foi de 0,029 mg L^{-1} e a faixa linear dinâmica abrangeu duas ordens de grandeza. Na presença de β -lapachona (isômero estrutural), a seletividade foi obtida pela derivada de primeira ordem do sinal SWV. A determinação do lapachol em extrato etanólico de *Tabebuia impetiginosa* foi realizada após uma simples separação do analito por cromatografia em camada fina. Os resultados são similares estatisticamente (com nível de confiança de 95%) com os realizados através de HPLC com detecção absorciométrica. Estudos para determinação simultânea de β -lapachona e α -lapachona também foram realizados com sucesso.

Palavras-chave

Voltametria; Amperometria; Diamante dopado com boro; Eletrodo de grafite-epoxi; Trifloxistrobina; Naftoquinonas; Gentamicina.

Table of contents

1.1	Contextualization of Work	21
1.2	Thesis structure	22
1.3	Objectives	23
1.3.1	General objective	23
1.3.2	Specific objectives	24
2	Theoretical fundamentals	25
2.1	Carbon Based Sensors	25
2.2	Electrochemical Techniques	30
2.2.1	Cyclic voltammetry	30
2.2.2	Square-wave voltammetry	31
2.2.3	Batch injection analysis with amperometric detection	34
3	Materials and Methods	38
3.1	Instrumentation	38
3.2	Reagents and Materials	41
3.3	Construction and characterization of the graphite-epoxy electrode	43
3.4	Electrode electroactive area estimation	43
3.5	Treatment of the BDD electrode surface	44
3.5	Solutions, standard solutions and sample preparation	45
3.6	Characterization of the water samples	47
3.7	Preparation of the molecular imprinted polymer using kanamycin as a template	48
3.8	Solid phase extraction using the molecular imprinted polymer	49
3.9	Thin-layer chromatography for determination lapachol, α -lapachone and β -lapachone	50
3.10	Voltammetric measurements of trifloxystrobin, gentamicin, lapachol, α -lapachone and β -lapachone	51
3.11	Study of trifloxystrobin degradation under UV exposure	53
3.12	Chromatographic analysis	53
4	Electrooxidation of trifloxystrobin at the boron-doped diamond electrode: electrochemical mechanism, quantitative determination and degradation studies	55
4.1	Introduction	55

4.3 Results	58
4.3.1 Preliminary studies	58
4.3.2 Oxidation process	60
4.3.3 Optimization of experimental and instrumental conditions	63
4.3.4 Analytical figures of merit	64
4.3.5 Application of method	68
4.3.6 UV-induced trifloxystrobin degradation	70
4.4. Partial conclusion	74
5 Kanamicin-template imprinted polymer based solid-phase extraction and batch-analysis amperometry for gentamicin determination	76
5.1 Introdução	76
5.3 Results	80
5.3.1 Preliminary studies	80
5.3.2 Electrochemical qualitative study	80
5.2 Optimization of parameters for measurements using batch injection amperometry	82
5.3 Analytical determination of gentamicin and figures of merit for the BIA-amperometric method	84
5.4 Interference study	86
5.4.1 Substances commonly found in gentamicin veterinary formulations	86
5.4.2 Solid-phase extraction studies using the cartridge packed with the aminoglycoside-selective molecularly imprinted polymer	86
5.5 Application of the BIA-amperometric method	89
5.6 Partial conclusion	91
6 Voltammetric determination of lapachol in the presence of lapachones and in ethanolic extract of <i>Tabebuia impetiginosa</i> using an epoxygraphite composite electrode	92
6.1 Introduction	92
6.2 Results	94
6.2.1 Preliminary studies	94
6.2.1.1 Electroactive area	94
6.2.1.2 Influence of CTAB on the electroanalytical process at different pH values	95
6.2.1.3 Mechanistic studies in aqueous medium containing CTAB	97
6.3.2 Optimization of experimental and instrumental conditions for analysis using SWV	100

6.3.3 Analytical determination of lapachol	102
6.3.3.2 Interference from other naphthoquinones and determination of lapachol in ethanolic extract of <i>T. impetiginosa</i>	104
6.3.4 Preliminary studies aiming the selective determination of α -lapachone and β -lapachone	107
6.3.5 Partial conclusion	111
7 Conclusion	112
8 Future works	114
9 References	116
A Published papers	133
B Participation in Congress	135

List of figures

Figure 2.1. Illustration of a potential application in square-wave voltammetry, where: a is the pulse width; ΔE_s is the scan increment and τ is the time	32
Figure 2.2. a) Schematic diagram of the first BIA cell: A - working electrode; B - auxiliary electrode; C - reference electrode; D - micropipette tip; E - hole to fill the cell; F - stir bar; G - drain. b) Stages involved in an injection into the BIA	35
Figure 3.1. Interior of the photoreactor with six UV mercury lamps connected	39
Figure 3.2. Electrochemical Teflon cell constructed in the laboratory: (A) Platinum auxiliary electrode; (B) Reference electrode of $\text{Ag}/\text{AgCl}_{(\text{sat})}$; (C) Working electrode of BDD	40
Figure 3.3. 1) Schematic representation of the BIA-amperometry cell: (A) $\text{Ag}/\text{AgCl}(\text{KCl}_{(\text{sat})})$ reference electrode; (B) auxiliary electrode; (C) Combitip® electronic micropipette plastic tip; (D) Teflon bar used as stirrer; (E) copper plate to establish electrical contact with the potentiostat; (F) Rubber sealing ring; (G) BDD electrode. 2) Photograph of the cell used in BIA-amperometry	41
Figure 3.4. Field-emission scanning electron microscopy image of the polished surfaces of graphite-epoxy composite electrodes (Acceleration voltage of 1.0 kV; resolution of 10 μm)	44
Figure 3.5. (A) Cyclic voltammograms at different potential scanning velocities for the ferricyanide / ferrocyanide system in a $1.0 \times 10^{-3} \text{ mol L}^{-1}$ solution of $\text{K}_3[\text{Fe}(\text{CN})_6]$ / $0,5 \text{ mol L}^{-1}$ of K_2SO_4 . (B) Curve of the variation of the peak current with the square root of the potential sweep speed. Data extracted from Figure 3.5A	44
Figure 3.6. Steps for the synthesis and cleaning of the molecularly imprinted polymer (kanamycin-MIP) and non-imprinted polymer (NIP)	48
Figure 3.7. Infrared spectrum of (a) kanamycin sulfate (black). (b) kanamycin-MIP after clean-up to remove the kanamycin template (red) and (c) NIP (blue)	49
Figure 3.8. Scheme of the solid phase extraction for gentamicin sulfate using the kanamycin-MIP packed cartridge coupled in the outlet of a flow system.	50
Figure 3.9. Thin-layer chromatograms of lapachones before (A) and (B) after the run	51
Figure 4.1. Chemical structure of trifloxistrobin	56
Figure 4.2. CV of trifloxystrobin ($8.0 \times 10^{-4} \text{ mol L}^{-1}$ or 0.33 g L^{-1}) on BDD electrode in BR buffer (0.040 mol L^{-1} , pH 4.0)/ACN 70/30%	

v/v. (A) Complete cycle from +1200 to +2300 mV potential range: (1) 1st cycle, (2) 5th cycle, (3) 11th cycle, (4) blank. (B) For the first oxidation peak: (1) 1st cycle, (2) 5th cycle, (3) 11th cycle, (4) 19th cycle and (5) blank. (C) For the second oxidation peak: (1) 1st cycle, (2) 3rd cycle, (3) 5th cycle and (4) blank. (D) Influence of pH on the first voltammetric (SWV) trifloxystrobin ($4.0 \times 10^{-5} \text{ mol L}^{-1}$ or 16 mg L^{-1}) oxidation peak area (with maximum at +1744 mV). Scan rate of 100 mV s^{-1} for CV

59

Figure 4.3. (A) and (B) CV data of a solution with $4.0 \times 10^{-4} \text{ mol L}^{-1}$ (0.16 g L^{-1}) trifloxystrobin: Peak current (I_p) versus square root of the scan rate (\sqrt{v}) representation for (A) oxidation peak with maximum at +1740 mV ($R^2 = 0.989$) and (B) oxidation peak with maximum at +2010 mV ($R^2 = 0.990$); (C) Sequence of cyclic voltammograms obtained at different scan velocities. Experimental conditions: BR buffer (pH 4.0; 0.040 mol L^{-1})/ACN (70/30% v/v) and scan rate from 10 to 400 mV s^{-1}

60

Figure 4.4. CV study (trifloxystrobin $4.0 \times 10^{-4} \text{ mol L}^{-1}$ or 0.16 g L^{-1}) of the logarithm of peak current intensity ($\log I_p$) in function of the logarithm of the scan velocity ($\log v$) for: (A) the first oxidation peak ($R^2 = 0.988$) and (B) the second oxidation peak ($R^2 = 0.980$). SWV peak current (I_p) in function of frequency for (C) first oxidation peak ($R^2 = 0.996$) and (D) second oxidation peak ($R^2 = 0.992$). Detail presents the potential (E_p) in function of the logarithm of the frequency ($\log f$) for: (C) first oxidation peak ($R^2 = 0.981$) and (D) second oxidation peak ($R^2 = 0.988$)

61

Figure 4.5. Proposed trifloxystrobin electrochemical oxidation mechanism mediated by BDD

63

Figure 4.6. (A) SWV response with DDB as the working electrode: Concentration of trifloxystrobin: (1) blank; (2) $1.0 \times 10^{-5} \text{ mol L}^{-1}$ (4.1 mg L^{-1}); (3) $2.0 \times 10^{-5} \text{ mol L}^{-1}$ (8.2 mg L^{-1}); (4) $3.0 \times 10^{-5} \text{ mol L}^{-1}$ (12.2 mg L^{-1}); (5) $4.0 \times 10^{-5} \text{ mol L}^{-1}$ (16.3 mg L^{-1}); (6) $5.0 \times 10^{-5} \text{ mol L}^{-1}$ (20.4 mg L^{-1}); (7) $6.0 \times 10^{-5} \text{ mol L}^{-1}$ (24.5 mg L^{-1}); (8) $7.0 \times 10^{-5} \text{ mol L}^{-1}$ (28.6 mg L^{-1}); (9) $8.0 \times 10^{-5} \text{ mol L}^{-1}$ (32.7 mg L^{-1}); (10) $9.0 \times 10^{-5} \text{ mol L}^{-1}$ (36.8 mg L^{-1}); (11) $1.0 \times 10^{-4} \text{ mol L}^{-1}$ (40.8 mg L^{-1}). (B) Analytical curve ($R^2 = 0.998$) and (C) Voltammograms showing the difference between the signal produced by (1) blank and (2) trifloxystrobin at a concentration equivalent to the LOQ ($4.6 \times 10^{-7} \text{ mol L}^{-1}$ or 0.19 mg L^{-1}). Experimental conditions indicated in Table 1

66

Figure 4.7. UV exposure of trifloxystrobin: (A) Analyte percent degradation in function of time; (B) The relationship between the inverse of the concentration of trifloxystrobin and time ($R^2 = 0.987$). Instrumental parameters of the analyte determination indicated in Table 1

71

Figure 4.8. (A) GC chromatogram for the degraded solution trifloxystrobin. (B) Mass spectrum of one of the isomers of trifloxystrobin (RT = 14.64 min)

72

Figure 4.9. Mass spectrum for the product degradation corresponding to: (A) RT = 34.00 min and (B) RT = 52.07 min 73

Figure 5.1. Structures of gentamicin sulfate C_{1A}, C₂ and C₁ 77

Figure 5.2. (A) Gentamicin sulfate cyclic voltammetry on BDD electrode: (a) supporting electrolyte and (b) gentamicin sulfate (B) Sequence of cyclic voltammograms (1200 to 2100 mV) under no forced convective transport: (a) supporting electrolyte; (b) 1th cycle; (c) 20th cycle and (d) 40th cycle. (C) Square root of scan rate (\sqrt{v}) in function of analyte peak current (I_p). (D) Analyte peak current measured by SWV in function of applied frequency (f). Experimental conditions: Electrolyte support: acetate buffer (0.2 mol L⁻¹, pH 4.0). SWV parameters: amplitude = 40 mV; frequency = 30 Hz; step potential = 2 mV; Cyclic voltammetry parameters: $v = 100$ mV s⁻¹; amplitude = 40 mV; gentamicin sulfate (338 mg L⁻¹) 81

Figure 5.3. (A) Gentamicin sulfate SWV voltammograms in acetate buffer 0.01 in the pH 4.0; a-blank, (b-g) 56.4 - 338.1 mg L⁻¹ in the range additions. (B) Gentamicin sulfate hydrodynamic voltammograms in acetate buffer 0.01 mol L⁻¹ in the pH range from 3.8 to 5.4 obtained from the peak current as a function of the applied potential pulses (1400 - 2200 mV). Stirring speed: 600 rpm; injection volume: 80 μ L gentamicin sulfate 5.07 mg L⁻¹. (C) The effect of sample volume on the peak current for gentamicin (from 10 to 100 μ L): (a) Blank and (b) Gentamicin sulfate 9.0×10^{-8} mmol. (D) Effect of variation in the injection rate of the peak current. Supporting electrolyte: acetate buffer 0.01 mol L⁻¹ pH = 4.4 and work potential 2000 mV 83

Figure 5.4. (A) Successive sample introductions of a solution containing (a) 2.8 mg L⁻¹ and (b) 11.3 mg L⁻¹ of gentamicin sulfate. Electrolyte: 0.01 mol L⁻¹ acetate buffer solution pH 4.40; injected volume: 60 μ L; stirring rate: 600 rpm. (B) Response BIA-amperometry system with BDD electrode for injections in triplicate (a) 2.8; (b) 3.9; (c) 5.1; (d) 11.3, and (d) 22.5 mg L⁻¹ solution of gentamycin standard. (C) Analytical curve with equation of $Y = (1.1 \times 10^{-6} \pm 5.1 \times 10^{-8} \text{ mg L}^{-1} \mu\text{A}) X + (1.6 \times 10^{-6} \pm 3.3 \times 10^{-7})$ and $R^2 = 0.988$ for increasing concentrations of gentamicin. (D) Analytical responses for gentamicin showing signal saturation. Instrumental parameters: see Table 1 85

Figure 5.5. Study of the saturation capacity (225.4 mg L⁻¹ or 4.0×10^{-4} mol L⁻¹) of the SPE cartridge packed with kanamycin -MIP in the retention of gentamicin sulfate. Fractions of 1 mL analyzed in the BIA-amperometry system 89

Figure 6.1. Chemical structures of (1) lapachol, (2) α -lapachone and (3) β -lapachone 92

Figure 6.2. Cyclic voltammetry of the redox process of lapachol in aqueous media at different pH in the (a) absence and (b) presence of CTAB. (A) Tris-HCl buffer ($4.0 \times 10^{-2} \text{ mol L}^{-1}$, pH 9.0); (B) phosphate buffer ($4.0 \times 10^{-2} \text{ mol L}^{-1}$, pH 6.0) and (C) acetate buffer ($4.0 \times 10^{-2} \text{ mol L}^{-1}$, pH 4.0). $v = 100 \text{ mV s}^{-1}$ 97

Figure 6.3. (A) Sequential cyclic scans (line a-k) for lapachol at 100 mV s^{-1} at 72.7 mg L^{-1} of lapachol. (B) Cyclic scans at rate of $10\text{-}100 \text{ mV s}^{-1}$ for lapachol in presence of CTAB $1.2 \times 10^{-4} \text{ mol L}^{-1}$ by check the reversibility of the redox process. (C) Study of the $\log v \times \log I_p$ (29.1 mg L^{-1}) of lapachol; $v = 10$ to 1000 mV s^{-1} . Experimental conditions: phosphate buffer ($4.0 \times 10^{-2} \text{ mol L}^{-1}$; pH 6), $1.2 \times 10^{-4} \text{ mol L}^{-1}$ CTAB, KNO_3 (1 mol L^{-1}) in aqueous medium at $v = 100 \text{ mV s}^{-1}$ 98

Figure 6.4. (A) Study of $\log f \times E_p$ in the range from 10 - 90 Hz; (B) Study of $\sqrt{f} \times I_p$ in the range from 10 to 90 Hz; (C) Study of $\text{pH} \times E_p$ in the pH range from 5 to 9, using SWV using 29.1 mg L^{-1} of lapachol 99

Figure 6.5. Voltammetric responses from 72.7 mg L^{-1} of lapachol in aqueous media in presence of CTAB before CMC ($8.1 \times 10^{-4} \text{ mol L}^{-1}$), at CMC ($1.0 \times 10^{-3} \text{ mol L}^{-1}$) and after CMC ($1.5 \times 10^{-3} \text{ mol L}^{-1}$). (A) Cyclic voltammetry (anodic peak); (B) cyclic voltammetry (cathodic peak) and (C) square-wave cathodic voltammetry. Experimental conditions: phosphate buffer ($4.0 \times 10^{-2} \text{ mol L}^{-1}$; pH 6), KNO_3 (1 mol L^{-1}) in aqueous medium at $v = 100 \text{ mV s}^{-1}$. 100

Figure 6.6. SWV signal (measured using graphite-epoxy electrode) dependence upon: (A) deposition time; (B) pulse amplitude (a) and (C) pulse frequency (f). Electrolyte support: CTAB ($1.2 \times 10^{-4} \text{ mol L}^{-1}$), phosphate buffer ($4.0 \times 10^{-2} \text{ mol L}^{-1}$; pH 6) and KNO_3 (1.0 mol L^{-1}) in aqueous medium. Lapachol concentration of 0.388 mg L^{-1} . 101

Figure 6.7. SWV analytical addition curves of lapachol covering the concentration range from 0.097 mg L^{-1} to 0.485 mg L^{-1} and using: (A) graphite-epoxy electrode and (B) glassy carbon electrode (GCE). Experimental conditions of Table 1. (C) Background signal measured using the graphite-epoxy electrode (GEE) and the glass carbon electrode (GCE) 103

Figure 6.8. Voltammograms of mixtures containing lapachol (4.8 mg L^{-1}) and its isomers: (A) mixture with α -lapachone and (B) mixture with β -lapachone. Concentrations indicated for the isomer: a) blank; b) 0 mg L^{-1} ; c) 4.8 mg L^{-1} ; d) 7.3 mg L^{-1} and e) 9.7 mg L^{-1} . (C) First derivative of the voltammetric response for a) lapachol from $97 \text{ } \mu\text{g L}^{-1}$ to $775 \text{ } \mu\text{g L}^{-1}$ and b) β -lapachone from $97 \text{ } \mu\text{g L}^{-1}$ to $388 \text{ } \mu\text{g L}^{-1}$. Optimized experimental conditions (Table 6.1) 104

Figure 6.9. (A) Sequential cyclical voltammograms (line a-o) for α -lapachone and β -lapachone (both at $4.0 \times 10^{-4} \text{ mol L}^{-1}$)

at 100 mV s^{-1} . (B) The cyclic voltammetry using ν from $40\text{-}100 \text{ mV s}^{-1}$ for α -lapachona and β -lapachona in the presence of CTAB $1.2 \times 10^{-4} \text{ mol L}^{-1}$. (C) Study concerning $\sqrt{f} \times I_p$ in the f range from 10 to 200 Hz using phosphate buffer ($4.0 \times 10^{-2} \text{ mol L}^{-1}$ and $\text{pH } 6$), CTAB ($1.2 \times 10^{-4} \text{ mol L}^{-1}$), KNO_3 (1 mol L^{-1}) at $\nu = 100 \text{ mV s}^{-1}$

109

Figure 6.10. SWV analytical addition curves of α -lapachone and β -lapachone covering the concentration range from $1.0 \times 10^{-6} \text{ mol L}^{-1}$ to $1.3 \times 10^{-6} \text{ mol L}^{-1}$ using: (A) graphite-epoxy electrode and (B) glassy carbon electrode (GCE)

110

List of tables

Table 4.1. Experimental conditions selected for the square-wave voltammetric determination of trifloxystrobin using the BDD	65
Table 4.2. Evaluation the interference imposed by other strobilurin and triazole fungicides in the trifloxystrobin ($1.0 \times 10^{-5} \text{ mol L}^{-1}$ or 4.1 mg L^{-1}) electroanalytical signal ^a (n = 3)	68
Table 4. 3. Recoveries for trifloxystrobin (n=3 in two different days) in analyte fortified samples ($7.0 \times 10^{-6} \text{ mol L}^{-1}$ or 2.9 mg L^{-1})	70
Table 4. 4. Some figures for electroanalytical methods for the determination of strobilurin and electrophoretic separation of strobilurins using absorbance measurement for detection	75
Table 5.1. BIA-amperometry chosen experimental conditions to determine gentamicin	84
Table 5.2. Recoveries for the gentamicin sulfate determination in simulated samples and in pharmaceutical formulation using BIA-amperometry (n = 3)	90
Table 5.3. Comparative results for gentamicin sulfate determination in pharmaceutical formulation samples using the proposed method and the one based on the use of HPLC	91
Table 6.1. Conditions for the SWV determination of lapachol	102
Table 6.2. Lapachol concentration (analysed in three days, n=3 replicates) in wood <i>T. impetiginosa</i> (Pink Ipê) and in commercial extracts after separation by TLC	106
Table 6. 3. Determination of lapachol in samples of heartwood of Pink Ipê	106

List of abbreviations

AMG	Aminoglycoside
APTMS	(3-aminopropyl) trimethoxysilane
AuNPs	Gold nanoparticles
BDD	Boron-doped diamond
BIA	Batch injection analysis
BR	Britton-Robinson
CMC	Critical micellar concentration
CTAB	Hexadecyltrimethylammonium Bromide
CV	Cyclic voltammetry
EDTA	Ethylenediaminetetracetic acid
FIA	Flow-injection analysis
GC	Gas chromatography
GCE	Glass carbon electrode
GC-MS	Gas chromatography-mass spectrometry
GPC	Gel permeation chromatography
HPLC	High performance liquid chromatography
IC	Inorganic carbon
LLE	Liquid-liquid extraction
LLME	Liquid-liquid microextraction
LOD	Limit of detection
LOQ	Limit of quantification
MIP	Molecular imprinted polymer
NIP	Non-imprinted polymer
OPA	o-phthalaldehyde
QDs	Quantum dots
RDE	Rotating disc electrode
RSD	Relative standard deviation
SPE	Solid phase extraction
SPME	Solid phase microextraction
LSPR	Localized surface plasmon resonance
SWV	Square-wave voltammetry
TC	Total carbon
TEOS	Tetraethyl orthosilicate
TLC	Thin layer chromatography
TOC	Total organic carbon

“If I have seen further than others, it is by
standing upon the shoulders of giants.”
Isaac Newton

1

Introduction

1.1

Contextualization of Work

Trifloxystrobin, a fungicide from the strobilurins class, is considered to be less toxic and with fast degradation, under field conditions, than other commonly used pesticides. Despite that, analytical methods are required to allow the evaluation of human and environment exposure to such substance. Gentamicin sulfate is an aminoglycoside widely used to treat lung, eye and skin infections. Due to its collateral effects, even to lower administered amounts, analytical methods are required to guarantee proper quantities of gentamicin sulfate in medicines. Lapachol is an important naphthoquinone because of its bactericidal and anti-tumor capabilities. Since several commercial plant extracts claim to contain lapachol, selective methods are required to actually confirm its presence. In this context, electrochemical methods are excellent options since they rely on cost-effective instrumentation enabling the detection of very low quantities of analyte often with adequate selectivity, when proper experimental conditions are adjusted and/or when associated with separation methods. The choice of the working electrode (sensor) is crucial to enable sensitive analytical response, reproduction of measured signals and sharp peaks in function of either the applied potential (voltammetry) or time (amperometry), improving selectivity.

Carbon-based electrodes are known to be very versatile, robust and to mediate or participate very effectively in a myriad of redox processes. The boron-doped diamond (BDD) electrode has a wide working potential range and the ability to electrocatalyze reactions from molecules very resistant to oxidation and/or reduction. The epoxy-graphite electrode has a noticeable capability to pre-concentrate analytes, increasing the detection capacity and to be easily constructed with simple and readily available materials.

The BDD electrode was used to enable sensitive analytical responses for either trifloxystrobin or gentamicin, allowing reliable and sensitive analytical

results. Using the BDD electrode and voltammetry, it was possible to study the redox mechanism and to evaluate the thermal and UV-induced degradation of trifloxystrobin. The BDD electrode enabled high analytical frequency (measurements h^{-1}) in the analysis of gentamicin containing samples using batch-injection analysis with amperometric detection. Studies using the graphite epoxy electrode were performed for lapachol and other naphthoquinones such as α -lapachone and β -lapachone. It was possible to improve the sensitivity and detection of lapachol in comparison with other reported analytical methods also promoting some selective capability to discriminate different naphthoquinones.

1.2

Thesis structure

This thesis is structured in seven chapters. In Chapter 1, a brief contextualization of the work, its structure and their objectives are presented.

In Chapter 2, we present the characteristics of the BDD and carbon-composite electrode, revising the literature for recent works addressing the use of such electrochemical sensors and also presenting theoretical fundamentals on the employed electroanalytical techniques.

Chapter 3 contains detailed information about the employed instrumentation, materials and reagents also presenting the procedures used to prepare solutions and samples and the developed analytical protocols involving the analytical methods developed.

The results of our work were divided in to three chapters, each of them referring to either a work previously published in a scientific journal or a manuscript submitted for publication. A brief specific introduction about target-analytes and on the importance of their study is presented at the beginning of each chapter, followed by the presentation of results and partial conclusion on the subject.

In Chapter 4 we present the results obtained for the determination of trifloxystrobin by square-wave voltammetry (SWV) using the BDD electrode: i) the study of the oxidation mechanism of trifloxystrobin; ii) the optimization of experimental and instrumental conditions for the SWV determination of

trifloxystrobin; the analytical figures of merit and a study of potential interferences on the analytical signal; iii) the application of the proposed method in the analysis of commercial samples of orange juice and natural waters and v) a study concerning the thermal and UV-induced degradations of trifloxystrobin.

In Chapter 5, we show the results obtained for the determination of gentamicin sulfate using batch-injection analysis (BIA) with amperometric detection using the BDD electrode. The following are presented: i) optimization of the experimental and instrumental conditions for the gentamicin sulfate determination by BIA; ii) the analytical figures of merit; iii) the gentamicin sulfate containing sample treatment using a kanamycin-imprinted polymer and iv) the application of the BIA-amperometric method in the analysis of gentamicin sulfate based veterinary drugs.

In Chapter 6, we show the method developed for the determination of lapachol by SWV with a graphite-epoxy electrode as follows: i) a preliminary study aiming the maximization of the lapachol electrochemical response in a surfactant organized medium; ii) a brief study of the redox mechanism of lapachol; iii) the optimization of the instrumental and experimental conditions for determination of lapachol by SWV; iv) the determination of lapachol in the presence of other naphthoquinones in plant extracts after thin-layer chromatography; v) a brief study on the possibility of the selective voltammetric determination of naphthoquinones in synthetic mixtures.

Finally, in Chapter 7 we present the final conclusions of our work, as well as directions for future works.

1.3 Objectives

1.3.1 General objective

The goal of this Thesis was to develop electroanalytical methods using carbon-based sensors (BDD and graphite-epoxy electrodes) applying them to the determination of analytes of biological, environmental and pharmacological interest, also making efforts to study the electrochemical mechanisms involved.

1.3.2

Specific objectives

- ✓ To study conditions that provide adequate electrochemical responses for the determination of analytes trifloxistrobin, gentamicin sulfate and lapachol ;
- ✓ To investigate the interaction of the sensors with analytes, the redox processes and, when possible, to propose the mechanism of reaction;
- ✓ Adjust instrumental parameters in order to obtain the best possible analytical response;
- ✓ Study the possible interferences;
- ✓ Obtain the analytical figures of merit;
- ✓ Apply the proposed methods in real and/or simulated/fortified samples to determine the analytes and, when necessary, to study strategies to eliminate interferences;
- ✓ To compare the performance of the developed methods with traditionally methods reported in the literature or by performing controlled recovery tests.

2 Theoretical fundamentals

2.1 Carbon Based Sensors

The prime working electrodes used in amperometry and voltammetry were the ones based on mercury, a toxic metal liquid that has been restricted in use because of environmental and health concerns. Working electrodes evolved substantially from pure metal electrodes and alloys to pure or composite materials and pastes. Carbon based electrodes are extensively used as electrochemical sensors since they can be operated at potential windows favorable to promote redox processes of a myriad of chemical species at a wide range of pH values. They are cost-effective devices that are easy to construct, to handle and to modify [1]. More recently, different nanostructured materials, including the ones of carbon (carbon nanotubes for instance) have been used to improve sensitivity and selectivity in determinations, also providing long-term stability in analytical responses. According to the intended application, there is also the possibility of transient or permanent chemical modifications in electrode substrates by electrodeposition, adsorption by ionic, and / or covalent interactions, among others [2].

An advanced carbon material called nanocrystalline boron-doped diamond (BDD) has become a very reliable and useful working electrode in voltammetry/amperometry because of its high electrochemical stability and wide potential window, covering, in aqueous solutions, the range of ± 2200 mV, due to its ability to shift the redox potential of water and dissolved oxygen. This characteristic allows the monitoring of electrolytic reactions of chemical species at larger relative potentials than those normally achieved using the glass carbon electrode (GCE) or graphite paste electrodes. The high O_2 overvoltage gives the BDD a high oxidative power, which promotes the effective electrolytic degradation of organic substances (sometimes referred to as "combustion") with formation of CO_2 and H_2O due to the production of large amounts of hydroxyl

radical (from water) on the surface of the BDD [3,4]. BDD is a material with high chemical and physical stability, enabling the work under extreme conditions, for example, in strongly acidic medium. In addition, it has good biocompatibility, a low capacitive current (noise) response and a lower sensitivity to the dissolved oxygen in solution, not requiring, in many cases, de-oxygenation of the electrolyte support [5]. Such properties make BDD suitable to be used in electroanalytical methods. However, when operating the BDD electrode at such high potentials, many chemical species can undergo redox processes, increasing the risk of interferences [5,6].

The BDD has been applied as working electrode in electroanalytical studies/determinations of pesticides from the strobilurin class using Ag/AgCl_(KCl_{sat}) as reference electrode [7-9]. Kresoxim-methyl was determined using square wave voltammetry (SWV) using the BDD electrode by Dornellas *et al.*, in 2013 [7]. The irreversible oxidation of the pesticide was observed and the measurements were carried out with anodic sweep (from +1000 mV to +1750 mV with a peak maximum at +1420 mV) in acetate buffer solution (pH 4.0; 0.050 mol L⁻¹). The obtained signal generated a linear response covering two-orders of magnitude, starting at 270 µg L⁻¹. The recoveries found in fortified samples (grape juice) after solid phase extraction (SPE), ranged from 91.6% to 105.3%. The electrochemical study of pyraclostrobin was also performed by the same author [8]. The quasi-reversible oxidation process was identified by cyclic voltammetry with two well-defined oxidation peaks (around +1300 mV and at +1650 mV). Analytical determination was performed by SWV with current measured at +1280 mV using acetate buffer (pH 4.0; 0.050 mol L⁻¹) as supporting electrolyte. The response was linear and covered two orders of magnitude starting at the limit of detection (LOD) of 320 µg L⁻¹. The recovery values obtained in fortified samples of water and grape juice were between 94 and 102%. Dimoxystrobin was determined by BIA-amperometry [9]. In this approach, a few microliters of analyte solution were added, by means of an electronic micropipette, directly to the surface of the BDD electrode in such a way that the analyte contained in the injected zone underwent oxidation, generating a transient peak. The monitoring was made at +1900 mV in Britton-Robinson buffer (pH 2.0, 0.040 mol L⁻¹). The method presented high analytical frequency (180 injections h⁻¹), good precision

(RSD <3%, n = 10), and a detection limit of 124 $\mu\text{g L}^{-1}$. The recovery in natural waters fortified with the analyte were between 80 and 105%.

The DDB electrode has also been used for the determination of a myriad of other chemical substances. Some very recent works (published in 2018) are interesting to mention. Deroco *et al.* developed a unique electroanalytical method for the simultaneous quantification of two dyes (indigo carmine and alura red) by coupling flow injection and multiple pulse amperometry. The limits of detection (LOD) were 40.0 nmol L^{-1} (for indigo carmine) and 7.0 nmol L^{-1} (for alura red) enabling up to 153 determinations h^{-1} . The method was successfully applied for the quantification of these dyes in commercial sweets [10]. Alpar *et al.* used the BDD to perform the selective and simultaneous determination of 5-O-caffeoyloquinic acid, which is the main compound of chlorogenic acids in coffee, vanillin and caffeine using adsorptive redissolution square-wave voltammetry. The effect of the pretreatment (anodically or cathodically) of the BDD electrode was investigated in detail on the voltammetric redissolution of the analytes. The cathodic pretreatment was considered the best option, leading to higher peak currents and better separation of analyte peaks. Analytical curves were obtained for the simultaneous determination of the analytes with LOD of 4.0×10^{-7} (5-O-caffeoyloquinic acid) 3.8×10^{-7} (vanillin) and 1.5×10^{-7} mol L^{-1} (caffeine) with the proposed method applied in commercial samples of foods and beverages [11]. The BDD was used for the detection of Sb^{3+} using differential pulse anodic redissolution voltammetry. Interferences due to the presence of other ions, especially As^{3+} , were eliminated using NaH_2PO_4 as supporting electrolyte with addition of ethylenediaminetetracetic acid (EDTA) as selective complexing agent for Sb^{3+} . The LOD was 1.1×10^{-7} mol L^{-1} and the proposed method was applied to natural water from ancient antimony mines [12].

Adams, in 1958, introduced carbon-based composite materials [1,13,14] that present differentiated properties due to the synergy of the precursor materials [15]. Carbon-based electrodes made of composite materials usually consist of graphite powder mixed in different proportions of an insulating phase, producing a homogeneous mixture at a macroscopic level, but microscopically heterogeneous and with clearly defined zones [16]. The mechanical characteristics of the material are generally controlled by the selected insulation phase. Among the insulating materials reported in the production of such type of electrodes are

organic solvents [1], mineral oil [17], paraffin [18], poly (4-vinylpyridine) [19], epoxy [20] and polyurethane resins [21,22]. Generally the solid composite electrodes present greater mechanical stability than paste electrodes [23] and have been used in a wide range of both pH and potential, besides presenting good conductivity, low cost, mechanical stability, easiness to restore electrode surface, possibility to include chemical modifiers in its composition and compatibility with non-aqueous solvents. Chemical modifications, for instance with surfactants, might improve the sensitivity and selectivity towards specific analytes. Using graphite-composite electrodes, improvements in signal-to-noise ratios, with consequent LOD, have been demonstrated [24, 25].

There are several reported approaches to prepare composite materials to be used as electrodes, among them: i) thermoformation of a homogeneous mixture of solids [26]; ii) mechanical compression of a powder mixture to obtain pellets [27]; iii) *in situ* polymerization of a monomer, or mixture of monomers, when mixed with graphite [28]; iv) liquification of a mixture of materials at high temperature to achieve an homogenous system before cooling it down to obtain a solid composite [29]; and v) dispersing graphite in a polymer, dissolved in a suitable volatile organic solvent, followed by the evaporation of the solvent [30].

Epoxy-type resins are polymers consisting of monomers or prepolymers that react with a curing agent to produce thermo-resistant and highly efficient plastics. Epoxides have been widely accepted in electrical, structural and protective applications because of a combination of properties such as hardness, adhesion and chemical resistance. The most common commercial epoxy resins are ethers derived from bisphenol A and epichlorohydrin [31]. The performance of the resins for hardness, stiffness and high temperature resistance is due to the presence of bisphenol A.

A composite electrode prepared by mixing a commercial epoxy resin (Araldite®) and graphite powder was proposed for Calixto *et al.*, 2008 to be used in didactic experiments as these electrode could be easily prepared by the students. These electrodes were applied in simple experiments to demonstrate the effect of the composite composition on the conductivity and in the voltammetric response. The possibility of using the composite electrode in quantitative analysis was also demonstrated [39].

There are many examples of the use of graphite-epoxy electrodes, varying from the determination of metal ions [32], covering the determination of many chemical species of biochemical and pharmaceutical importance such as the simultaneous determination of dopamine and ascorbic acid [33], melamine [34], atenolol [35] and urea [20], ultimately used in the latest developments in electronic tongue systems [36]. Graphite-epoxy composites were developed by Alegret *et al.* [37], and optimized as conducting plastic materials. These rigid and easily mechanized composites have been used to construct electrochemical sensors and biosensors in different sizes and shapes. All-solid-state potentiometric sensors and biosensors have been developed using graphite-epoxy conducting substrates. The procedure has been extended to CHEMFET and ENFET sensors. It has been found out that enzymes retain their bioactivity within the graphite-epoxy matrices. Different biocomposites have been prepared and applied as amperometric transducers [37].

In 2006, Cervini [38] applied composite electrodes made of graphite (60% w/w) and polyurethane of vegetal origin in the voltammetric and amperometric determination of hydroquinone, paracetamol and atenolol. Hydroquinone was determined by SWV and flow injection analysis (FIA) with chronoamperometry as detection technique achieving LOD values of 283 nmol L⁻¹ and 100 µmol L⁻¹ respectively. The determinations of paracetamol in pharmaceutical formulations were made by differential pulse voltammetry (LOD of 3.9 µmol) with the rotating disc electrode made of the composite (LOD of 2.6 µmol) and by FIA-chronoamperometry (LOD of 6.7 µmol). Atenolol was determined in pharmaceutical formulations by differential pulse voltammetry (LOD of 3.2 µmol) and by FIA-chronoamperometry (LOD of 18.1 µmol).

Semaan *et al.* developed a composite of polyurethane-graphite electrode for the determination of furosemide in pharmaceuticals by SWV. There was no need for constant renewing of the electrode surface since analyte did not adsorb on the electrode material [25]. Azevedo *et al.*, (2015) presented results regarding the development and characterization of graphite-epoxy composites to be used in electroanalysis. Such composites were preliminary studied by termogravimetry, atomic force microscopy and X-ray diffraction and cyclic voltammetry (CV). Authors found that best electroanalytical responses were obtained using 65% (w/w) of graphite [40]. Most recently, Balbin-Tamayo *et al.* evaluated the

proportions of graphite and epoxy to prepare composite electrodes modified with deoxyribonucleic acid (DNA) [41]. Electrodes were characterized by CV, electrochemical impedance spectroscopy and field emission scanning electron microscopy. The best electrochemical responses (using SWV) towards guanine monophosphate and adenine were obtained using graphite/epoxy resin/hardener at a 3.3/2.5/1.0 w/w/w proportion with traces of DNA.

2.2 Electrochemical Techniques

2.2.1 Cyclic voltammetry

Cyclic voltammetry is the most commonly used technique to acquire informations about electrochemical processes. This technique rapidly provides information about the thermodynamics of redox processes, the kinetics of heterogeneous electron transfer reactions and on chemical reactions coupled to adsorptive processes [2,42].

In CV, a potential is applied at a constant rate, producing a linear potential variation as a function of time, starting from an initial potential value, until reaching a final one, when the potential sweep is reversed until the starting potential is reached again. These two scan steps produce a cycle that may be repeated as many times as necessary. As the current, measured during the process, is plotted in function of the applied potential, the so-called cyclic voltammogram is obtained. In CV, the oxidation and reduction processes of the target chemical species occur at the working electrode and produce, in a reversible redox system, features represented by the anodic peak current (I_{pa}) that occurs at a maximum anodic peak potential (E_{pa}) and the cathodic peak current (I_{pc}) that occur at a maximum anodic peak potential (E_{pc}) [43].

The peak current values (I_p) depend upon several parameters indicated in Eq. 1., where n is the number of electrons, in mol, involved in the half-reaction; A is the electrode area of the electrode (cm^2); C is the concentration of the electroactive species (mol L^{-1}); D is the diffusion coefficient of the species in the medium ($\text{cm}^2 \text{s}^{-1}$) and v is the sweep velocity (V s^{-1}).

$$I_p = (2.686 \times 10^5) n^{3/2} ACD^{1/2} v^{1/2} \quad (\text{Eq. 1})$$

From Eq. 1 it is also possible to calculate the electrode area of the working electrode. In this case, if a linear relationship between peak current and the square root of the scan velocity is found, one can obtain information about the nature of the involved electrochemical process (reversibility, irreversibility and or *quasi*-reversibility) [43]. CV also provides information about the redox mechanism and the mass transport of an electroactive species. The electrochemical reversibility is associated with the rapid exchange of electrons between the electroactive species and the electrode. When the electroactive species has a reversible redox mechanism, a linear relationship is established between the square root of the potential scanning velocity and peak current (both anodic and cathodic). For a diffusion-controlled mass transport, the linear relationship is established between the value of current peak (cathodic or anodic) and the square root of the potential scan velocity. In systems with mass transport controlled by adsorption, such a relationship is not linear. This information, together with others obtained by square-wave voltammetry, makes possible the understanding of the redox reaction mechanisms and mass transport [43]. CV is mainly used in exploratory studies and its application in quantitative determinations is limited in terms of sensitivity, mainly due to the interference of the capacitive current in the resulting final current (due to the application of a continuous or pseudo-continuous linear potential scan). In some situations, the signal-to-noise ratio can be improved by sampling at a specific time each potential variation increment, so that an experiment similar to cyclic voltammetry is made but with potential variation in defined increments. In this case, the quantitative application may be feasible, but still having limitations in terms of sensitivity [43,44].

2.2.2

Square-wave voltammetry

Square wave voltammetry (SWV) is a technique in which the acquisition of the current resulting from the redox process comes from the overlapping of a square-shaped pulse over a potential linear ramp, forming a ladder with a characteristic pulse amplitude (a), scan increment (ΔE_s) and duration (τ). In

Figure 2.1 the form of application of the potential in square-wave voltammetry is presented. The frequency of the square-wave, in Hz, is equal to $1/\tau$. Current measurement is performed at two points along the square-wave pulse. The first measurement (position 1 in Figure 2.1) is at the end of the direct pulse (direct scanning) and the second measurement (position 2 in Figure 2.1) is made in the reverse direction of the scanning [45,46].

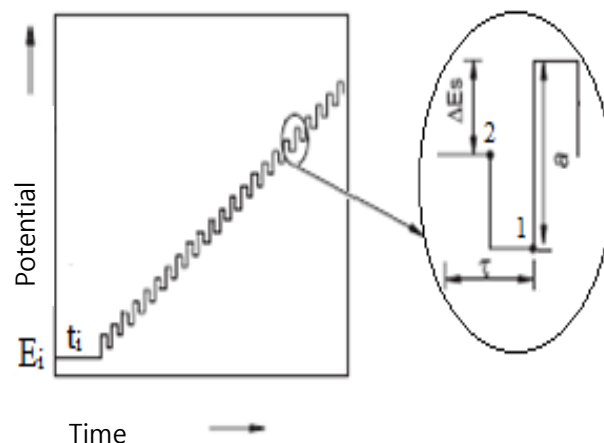


Figure 2.1. Illustration of a potential application in square-wave voltammetry, where: a is the pulse width; ΔE_s is the scan increment and τ is the time. Source: Adapted from SOUZA, *et al.*, 2003 [45].

SWV allows faster measurements because of the high frequency of pulse application. The scan velocity in a SWV is given as a function of the potential sweep increment (ΔE_s) and the frequency (f) of application of the potential pulses [45,46]. In addition, due to the time-delayed current sampling, the influence of capacitive current (noise) is greatly reduced. The SWV mathematical models can be used to study redox mechanisms involving the electroactive species that interact with the working electrode, allowing the calculation of important parameters such as the number of electrons involved in the redox process. Therefore, this technique is an important tool for the study of electrolytic induced processes [45,47].

In the study of redox mechanisms by SWV, irreversible systems are characterized by a linear relationship between the peak current (I_p) and the frequency (f) of the pulses, as shown in Equation 2, where K_r is a rate constant of the redox process [45].

$$I_p = K_{\nu} f \quad (\text{Eq. 2})$$

Therefore, Eq. 2 indicates that for irreversible redox systems, the increase of frequency tends to improve the sensitivity of the analytical response. In irreversible reactions, a linear relationship between E_p and the logarithm of the frequency ($\log f$) is found. This makes possible calculate the electron transfer coefficient (α) or the number of electrons (n) involved in the redox process using the angular coefficient, as shown in Eq. 3, where R is the ideal gas constant, T is the temperature and F is the Faraday constant [43,45].

$$\Delta E_p / \Delta \log f = -2,3RT / \alpha n F \quad (\text{Eq. 3})$$

Another important fact observed in irreversible redox reactions is that the half-height width ($\Delta E_{p/2}$) is independent of the amplitude of the pulses. The value of the peak width at half height of current intensity is an indicator used to calculate the quantity of electrons, in mol, involved in the reaction, as indicated in Eq. 4 [43,45].

$$\Delta E_{p/2} = (65.5 + 0.5) / \alpha n \quad (\text{Eq. 4})$$

As the electron transfer coefficient approaches a characteristic value of $\alpha = 0.5$, Eq. 4 is simplified (Eq. 5) [43,45].

$$\Delta E_{p/2} = 127 / n \quad (\text{Eq. 5})$$

Coefficient values lower than 0.5 indicate that the electronic transfer occurs very rapidly from the electrode to the electroactive species. Coefficients with lower values may also indicate a structural change in the redox products generated at the electrode surface, causing a barrier to electronic transfer. The values of α greater than 0.5 may occur in redox reactions involving more than one stage. The approximation of the electron transfer coefficient to 0.5 is acceptable when considering irreversible redox systems with only one electron transfer stage and with generation of products that do not interfere in the efficiency of electron transfer [43,45]. Another important information that can be obtained from mathematical models in SWV is the concentration of adsorbed species (Γ) on the

surface of the working electrode. This can be calculated by Eq. 6, where Γ is obtained from the angular coefficient of the linear relationship obtained between I_p and a [48]. The angular coefficient, q , is the active surface area of the electrode (in cm^{-2}), n is the quantity of electrons (mol), α is the electron transfer coefficient, F is the Faraday constant (in A s mol^{-1}), a is the amplitude of the square wave pulse (in V), f is the applied pulse frequency (in Hz) and ΔE_s is the scan increment (in V).

$$I_p/a = (5 \pm 1) 10^2 q \alpha n^2 F f \Delta E_s \Gamma \quad (\text{Eq. 6})$$

In *quasi*-reversible redox systems, no linear behavior is found in the relationship between I_p and frequency of pulse. In reversible systems, the linear relationship occurs when the peak current is monitored as a function of the square-root of f [45].

2.2.3

Batch injection analysis with amperometric detection

Amperometry relies on the measurement of the magnitude of the current produced by the analyte undergoing the redox process at a fixed applied potential in function of time. In general, in order to take advantage of the characteristics of the process, this type of determination is made in flow regime associated with liquid chromatography and FIA. Batch Injection Analysis (BIA) is often coupled with amperometric detection [49-52], although it has been associated with detection techniques such as absorption spectrophotometry [53] calorimetry [54], fluorimetry [55,56], potentiometry [57,58] and voltammetry [59,60].

In BIA, small volumes of the analyte are injected, with the aid of an electronic micropipette, directly onto the surface of the working electrode immersed in a large volume cell containing supporting electrolyte. The contact between the injected analyte zone and the surface of the electrode results in transient signals similar to those obtained in FIA. BIA cannot be fully automated as FIA but, despite that, it present characteristics analogous to FIA such as high analytical frequency, simplicity, use of small sample volumes (typical of ultra-trace analysis) and repeatability. In contrast, since BIA is not fully automated, relying on sample introduction using micropipete, it does not require pumps,

connection tubes and valves that keep the mobile phase constantly flowing to carry the analyte zone [9, 61]. In Figure 2.2a it is shown the schematic of a traditional BIA system, consisting of a cell was made of acrylic and the micropipette tip at a 2 mm distance from the surface of the working electrode [61]. The steps involved are outlined in Figure 2.2b: The sample solution is injected (in volumes on the order of microliters) through an electronic micropipette forming a zone that comes in direct contact with the electrode, thus producing a measurable current. Then the injected zone disperses in the supporting electrolyte achieving infinite dilution, reducing the measured current to baseline. As the transport of the zone to the electrode is reproducible and the zone dispersion is fast, the analytical response is transient. Signal intensity drop may be slower in systems where the analyte tends to adsorb onto the surface of the electrode, requiring mechanical agitation of the electrolyte to aid in the cleaning of the electrode surface. After adjusting the experimental conditions and before the saturation limit of the analytical response, the signal intensity obtained in a BIA-amperometry system is proportional to the concentration of the analyte in the solution volume injected onto the surface of the electrode [62].

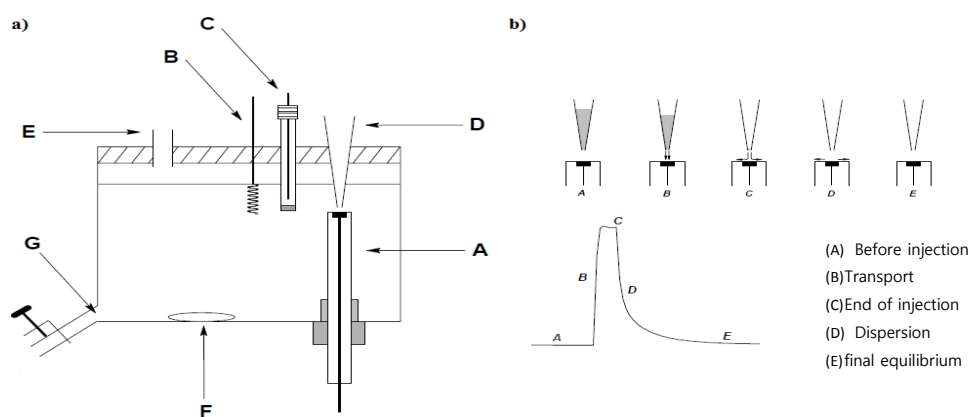


Figure 2.2. a) Schematic diagram of the first BIA cell: A - working electrode; B - auxiliary electrode; C - reference electrode; D - micropipette tip; E - hole to fill the cell; F - stir bar; G - drain. b) Stages involved in an injection into the BIA. Source: DORNELLAS, 2014 [9].

It was demonstrated that BIA cells of volumes from 40 to 200 mL are sufficient to enable analyte dilution enough to bring the measured signal back to baseline and enabling to perform a relatively large series of analyzes. The

parameters that influence the signal response in an analytical method based on BIA are the injection rate of the solution; the volume of the injected solution and, if necessary, the need for agitation and its speed [62].

BIA-amperometry has been used for the analysis of several types of samples such as fuels [49-51], foods [52] and drugs [63-65]. Stefano *et al.*, 2017 proposed a sensitive amperometric determination of omeprazole on screen-printed electrodes using BIA. A screen-printed electrode containing a multiwalled carbon nanotube modified electrode coupled to the BIA system provided an analytical method with a low LOD (9 nmol L^{-1}), high precision (1.3%) and excellent sample throughput (120 h^{-1}). The analytical system presented portable characteristics that enable application for *on-site* analysis [66]. Cardozo *et al.*, in 2017, employed BIA with multiple pulse amperometric detection of sildenafil. A sequence of three potential pulses in function of time (+1.3, +1.6 and +2.1 V) were applied on a BDD while reproducible injections were performed on a BIA cell. The chemical profile of the drug combined three ratios between the peak currents obtained in each amperogram: $R_1 = ip_{a1.6V}/ip_{a1.3V}$, $R_2 = ip_{a2.1V}/ip_{a1.6V}$, $R_3 = ip_{a2.1V}/ip_{a1.3V}$. This simple protocol allowed the discrimination between reference and generic formulations, also allowing the detection of counterfeit drugs adulterated with caffeine, dipyron, paracetamol and tadalafil. For comparison, screening of these samples was also performed using square-wave voltammetry combined with a chemometric method (principal component analysis), in which was achieved similar discrimination [67].

In 2017, Silva *et al.* developed a fast and simple procedure for simultaneous determination of propyphenazone, paracetamol and caffeine using BIA with multiple pulse (50 ms duration) amperometric detection. Three potentials were selected for the analysis: +0.90 V to only oxidize paracetamol; +1.20 V: to oxidize both paracetamol and propyphenazone without the interference from caffeine; +1.60 V to oxidize all three analytes. The sample aliquot (150 μL) was directly injected onto the BDD electrode surface immersed in a BIA cell and quantification was achieved by calculating the increment of signals obtained in the selected potentials. The analytical characteristics of the proposed method include high analytical frequency ($75 \text{ injections h}^{-1}$), good stability ($\text{RSD} < 3.9\%$; $n = 10$), and low detection limits (down to 0.1 mg L^{-1}).

The proposed method yielded similar results to those obtained by liquid chromatography at a 95% confidence level [68].

Rocha *et al.*, 2018, employed solenoid micropumps to introduce samples in a BIA system. It was possible to operate in a stopped flow mode resulting in low background noise levels, which would not be possible under continuous flow conditions. As a proof-of-concept, BIA coupled with amperometric and square-wave voltammetric (SWV) detection were used to quantify dopamine using anodic-stripping voltammetric detection for metal ions. The micro-pump provided injections of 14 mL of solution per pulse at $512 \mu\text{L s}^{-1}$ over the electrode during electrochemical measurement. Moreover, fast injections of analyte or electrolyte were programmed during deposition or conditioning steps of anodic stripping voltammetry aiming analyte preconcentration or electrode surface cleaning. The proposed system improved limits of detection and sensitivity precision and sample throughput in comparison with traditional BIA systems due to enhanced mass transfer and consequent reduced dispersion of analyte. It was possible to control injections without analyst intervention. The work opened new possibilities of applications of the BIA system, including on-line sample treatment (derivatization or dilution steps) [69].

3

Materials and Methods

3.1

Instrumentation

The electrochemical studies were made using a potentiostat/galvanostat (μ -AUTOLAB Type III, Metrohm, The Netherlands) interfaced to a personal computer and operating in the voltammetric modes (square-wave voltammetry, cyclic voltammetry), amperometric mode and in the galvanostatic chronopotentiometric mode.

UV-vis absorption spectra were acquired on a Perkin Elmer Lambda 35 double-beam spectrophotometer using 1 cm quartz cuvettes. Gas chromatography experiments were made on a model TRACE 1300 ISQ single quadrupole gas chromatographic system (Thermo Scientific, USA) with mass spectrometry detection. A chromatographic open tube column DB-5MS (60 m \times 0.25 mm and 0.25 μ m from J&W Scientific, USA) was used. Liquid chromatography was made on a model 1200 high performance liquid chromatographic system (Agilent Technologies, Japan) equipped with absorption photometric detection, a column oven (kept at 30°C) and an Eclipse XDB-C18 column (250 \times 4.6 mm and 5 μ m average particle size, USA) from Agilent. Solid-phase extraction (SPE) was partially automated using a flow system model FIALab-2500 (FIALab[®] Instruments with a software version 1.0607). A pH meter (model mPA-210, MS Tecnon, Brazil) with a pH-combined glass electrode with an Ag/AgCl (in saturated KCl) reference electrode was used. A total carbon analyser, model TOC-V CNP, Shimadzu, was used to determine the organic, inorganic and the total carbon present in water samples.

A lab-made photochemical reactor was used to expose trifloxystrobin solutions to the UV radiation (253 and in the range between 296-313 nm [70,71]). The reactor consisted of six mercury lamps (germicide mercury lamp of 6 W) placed at the internal side of a cylindrical structure (reaction chamber) covered

with aluminium foil in order to reflect radiation inside the reactor chamber (Figure 3.1) Only two of the lamps, in opposite sides, were kept on during the experiment. The quartz tubes were placed in a rotatory turret enabling them to receive the same radiance exposure from the lamps during a rotation cycle (five cycles per minute).



Figure 3.1. Interior of the photoreactor with six UV mercury lamps connected.

The working electrodes were: i) 1.0 cm^2 polycrystalline BDD (p-doped; 1.0-1.5 micrometer thick; $6000\text{-}8000 \text{ mg kg}^{-1}$ boron doping) from Adamant Technologies, Switzerland and ii) A graphite-epoxy working electrode constructed following the work of Balbin-Tamayo *et al.* (briefly described later in the text) [41]. A glass carbon electrode (GCE) was also used in some comparative experiments. The Ag/AgCl (KCl_{sat}) electrode was used as reference and a platinum wire was used as the auxiliary electrode.

In electrochemical experiments, the solutions were placed in a laboratory-made cylindrical cell made of Teflon (15 mL total volume), as indicated in Figure 3.2, or made of borosilicate (15 mL total volume) with Teflon lids (that allowed access of three electrodes to the solution) for the voltammetric analyzes.

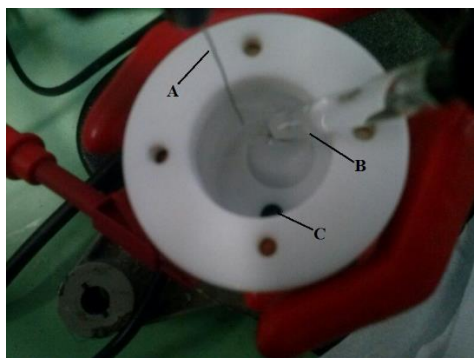


Figure 3.2. Electrochemical Teflon cell constructed in the laboratory: (A) Platinum auxiliary electrode; (B) Reference electrode of $\text{Ag}/\text{AgCl}_{(\text{sat})}$; (C) Working electrode of BDD.

A cell made of Teflon (250 mL total volume) was used in amperometric studies with the cell lid containing four openings (Figure 3.3): one for the reference electrode ($\text{Ag}/\text{AgCl}_{(\text{sat})}$), one for the auxiliary electrode (Pt wire), a third to insert the tip of the electronic micropipette and the last one to place a Teflon bar stir, coupled to a micromotor, which serve to agitate the solution. The BDD working electrode was positioned in the bottom of the cell over a copper plate used to establish electrical contact with the potentiostat. The distance between the tip of the micropipete and the surface of BDD was approximately 2.0 mm.

The introduction of standard and samples in voltammetric analyzes were made using a manual micropipete (from Brand, Germany) with adjustable volumes from 10 to 100 μL and from 100 to 1000 μL . For BIA, an electronic micropipette (model BRND705000, Handy Step, USA) was used (1 μL to 5 mL). The ultrasonic bath was the USC 1800 model from Unique (Brazil) and used in cleaning of material, homogenizing of the samples and degassing of solvents. The pH measurements were made on a pH meter model mPA 210, version 2.3 supplied by Tecnoyon (Brazil). The electrode for pH measurement was a glass membrane conjugated with an $\text{Ag}/\text{AgCl}(\text{KCl}_{(\text{sat})})$ reference electrode. Conductivity measurements were made using a model MA150, MS conductivimeter (Technoyon) with a two parallel plate Pt electrode.

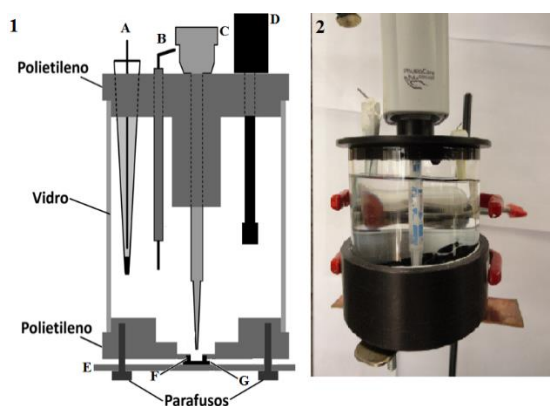


Figure 3.3. 1) Schematic representation of the BIA-amperometry cell: (A) Ag/AgCl(KCl_(sat)) reference electrode; (B) auxiliary electrode; (C) Combitip® electronic micropipette plastic tip; (D) Teflon bar used as stirrer; (E) copper plate to establish electrical contact with the potentiostat; (F) Rubber sealing ring; (G) BDD electrode. 2) Photograph of the cell used in BIA-amperometry. Source: Adapted from TORMIN *et al.*, 2011 [50].

3.2 Reagents and Materials

All solutions were prepared using ultrapure water (resistivity less than 18 MΩ cm) obtained from a water purifier Milli-Q Gradient System A10 (Millipore, USA). Fluoxastrobín (99.0%), kresoxim-methyl (99.0%), trifloxystrobín (99.0%), picoxystrobín (99.0%), tebuconazole (99.0%) and ciproconazole (99.0%) were from Riedel-de-Haen (Germany). Acetonitrile, boric acid, hydrochloric acid, sulphuric acid, phosphoric acid, sodium hydroxide, acetic acid, sodium acetate, ammonium acetate, potassium nitrate, bromhexine hydrochloride, monobasic sodium phosphate and dibasic sodium phosphate were obtained from Merck (Germany). Kanamycin sulphate, (3-aminopropyl) trimethoxysilane (APTMS), tetraethyl orthosilicate (TEOS), *o*-phthalaldehyde (OPA), 2-mercaptoethanol, hexadecyltrimethylammonium bromide (CTAB), sodium metabisulfite, anhydrous di-sodium ethylenodiamino tetracetic acid (EDTA), methylparaben, propylparaben, eritromicin, neomycin and streptomycin were purchased from Sigma-Aldrich (USA). Gentamicin sulfate standard was also obtained from Sigma-Aldrich being composed, according instructions, by the maximum percent values of 45% for gentamicin sulfate C₁ (M = 575.6 g mol⁻¹), 30% for gentamicin sulfate C_{1a} (M = 547.5 g mol⁻¹) and for 35% of gentamicin sulfate C₂ (M = 561.6 g mol⁻¹).

Adjusting percentages by factor 110 (sum of maximum percentages indicated for each type of gentamicin) it was assumed: 41% of gentamicin sulfate C₁; 27% of gentamicin sulfate C_{1a} and 32% of gentamicin sulfate C₂. Therefore, the weighted molar mass of gentamicin sulfate used to calculate the molar concentration of the standards was 563.5 g mol⁻¹. Hexane, methyl alcohol and ethanol (all of them HPLC grade) were obtained from Tedia (Brazil). Chloroform was from Isofar (Brazil), potassium ferrocyanide was from Autolabor (Brazil) and Tris.HCl buffer was from Synth, Brazil.

Lapachol (142-143°C), α -Lapachone (140°C), β -lapachone (155°C) and β -lapachone 3- sulfonic acid (158-160°C) were obtained following procedures described in the literature [72-74] with all of the obtained naphthoquinones purified and characterized by measuring melting points and using spectroscopic techniques (infrared and nuclear magnetic resonance) with results agreeing with literature data [75-77].

Spectroscopic grade graphite powder was from Ringsdorff-Werke GMBH (Germany). Alumina paste (1 μ m) was from Fortel (Brazil). Nitrogen (ultra pure; 5.0) gas used in the purging of solutions was obtained from Linde-gases (Brazil). Thin-layer chromatographic silica gel plates (60 F254) were purchased from Merck. PTFE syringe filters (0.45 μ m) were from Whatman (UK). Bond Elut C-18 SPE cartridge (3.0 mL and 500.0 mg; Varian, USA) was used for clean up of samples (juice, river water and lake water). The resin used in the preparation of the epoxy-graphite electrode was the Araldite Professional[®] adhesive kit (Brascola LTDA). It is composed of a formulated epoxy resin, which has a clear-gray liquid appearance and a hardener with a greenish-looking appearance. Usually the mixture of these components is made by the ratio 1:1, it is possible to handle it for about 90 min and the total cure time of the mixture is 24 h. Solvent free, room temperature or hot cure.

Water samples were obtained from the Rodrigo de Freitas Lagoon (Rio de Janeiro, Brazil), from the Rainha Creek (Rio de Janeiro, Brazil). In addition, tap water and commercial mineral water were also analysed. Fermented soy orange juice sample were bought in the local market. Three pharmaceutical formulations of gentamicin (injectable solutions for veterinary use) were purchased in local drugstores and labeled as Sample A, Sample B and Sample C, containing, according to the formulation instructions, respectively, 44 mg mL⁻¹, 40 mg mL⁻¹

and 80 mg mL⁻¹ of gentamicin sulfate. Information on injectable formulations of gentamicin [78,79] indicated that each 1 mL of the formulation contains the following excipients: sodium metabisulfite (between 2.9 and 3.2 mg) and anhydrous di-sodium EDTA (0.1 mg) as stabilizers, methylparaben (1.8 mg) and propylparaben (0.2 mg) as preservatives. The pH values of the pharmaceutical formulations A and B were between 2.6 and 3.4, respectively. Commercial plant extracts (Pau d'arco, supposedly from *T. impetiginosa*) were purchased in drugstores. The natural heartwood of *T. impetiginosa* (Pink Ipê) was purchased in a local store.

3.3

Construction and characterization of the graphite-epoxy electrode

For the construction of graphite-epoxy electrode, it was used a procedure indicated in literature [41], with minor adjustments. The epoxy resin and the hardener (from the Araldite kit) were mixed, in equal quantities, before the addition of the graphite powder. These components were mixed in order to achieve a homogeneous composite constituted of about 3% m/m of the resin-hardener mixture and 97% m/m graphite. Before the graphite-epoxy composite became hard, it was introduced, about 10 mm, into the tip of a 1 mm diameter glass capillary where a copper wire was inserted, establishing the electrical contact between the copper wire and the composite. After 24 h, the surface of the composite was polished using a sandpaper (1200 and then 600 grit) followed by a final polishing using a 1 µm alumina suspension. The microscopic image of the polished composite is shown in Figure 3.4.

3.4

Electrode electroactive area estimation

The experiment to determine the electroactive area of the BDD electrode was similar to the one performed by Dornellas as the same system was used in this present work. The BDD plate has with a surface area of 0.10 cm². Part of the surface was not in contact with the solution due to the geometry of the cell bottom hole and the isolation using a rubber o`ring that left only the working electrode area of 0.035 cm².

The active graphite-epoxy electrode surface area was determined using CV measurements (from -250 to +650 mV in the 20-100 mV s⁻¹ scan rate range) of a K₄[Fe(CN)₆] solution (1.0 × 10⁻³ mol L⁻¹) using KNO₃ solution (0.5 mol L⁻¹) as support electrolyte (Figure 3.5). The value found was equal to 0.019 cm².

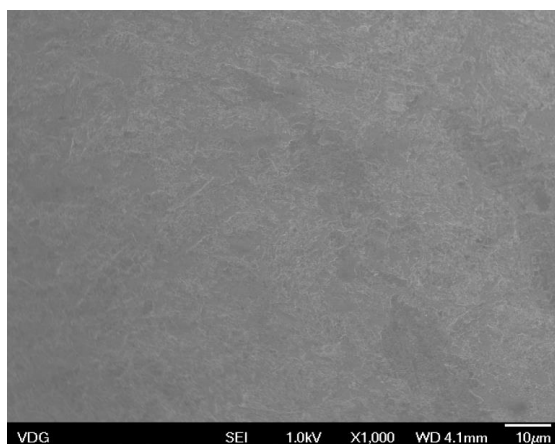


Figure 3.4. Field-emission scanning electron microscopy image of the polished surfaces of graphite-epoxy composite electrodes (Acceleration voltage of 1.0 kV; resolution of 10 µm).

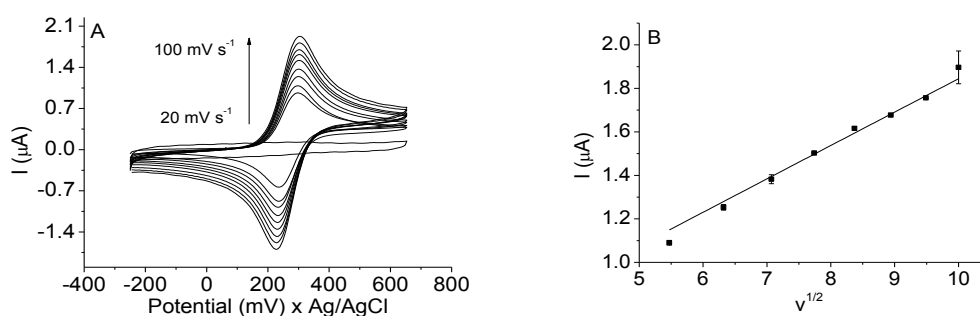


Figure 3.5. (A) Cyclic voltammograms at different potential scanning velocities for the ferricyanide / ferrocyanide system in a 1.0 × 10⁻³ mol L⁻¹ solution of K₃[Fe(CN)₆]/ 0,5 mol L⁻¹ of K₂SO₄. (B) Curve of the variation of the peak current with the square root of the potential sweep speed. Data extracted from Figure 3.5A.

3.5 Treatment of the BDD electrode surface

Pretreatment of the BDD (activation procedure) was performed daily prior to analysis using galvanostatic chronopotentiometry. Initially, the BDD was immersed in H₂SO₄ 0.10 mol L⁻¹ and subjected to an anodic pretreatment by applying a current of +0.01 A, during 1000 s, then a cathodic pretreatment was

made with -0.01 A, during 1000 s. In addition, a sequence of 10 voltammetric cycles (100 mV s^{-1}) was applied from -500 to $+1500$ mV, until signal stabilisation in H_2SO_4 0.10 mol L^{-1} .

3.6

Solutions, standard solutions and sample preparation

Trifloxistrobin stock solution ($1.0 \times 10^{-3} \text{ mol L}^{-1}$ or 0.41 g L^{-1}) was prepared in acetonitrile and, when required, diluted in Britton-Robinson (BR) buffer (0.040 mol L^{-1} ; pH 4.0) to prepare standards of lower concentrations. A standard stock solution of gentamicin sulfate (563.5 mg L^{-1}) was prepared by dissolving the gentamicin standard in acetate buffer. For the electrochemical measurements, standard stock solutions were prepared daily before work from the dilution aliquots of the standard stock solution of gentamicin sulfate in 10 mL with acetate buffer (0.01 mol L^{-1} pH 4.4). Appropriate amounts of each naphthoquinone (lapachol, α -lapachone and β - lapachone) were used to prepare standard stock solutions of $1.0 \times 10^{-2} \text{ mol L}^{-1}$ and $1.0 \times 10^{-4} \text{ mol L}^{-1}$ in methanol. More diluted naphthoquinone solutions were prepared by proper dilution of the stock solutions with methanol.

The OPA stock solution (derivative reagent) was prepared, in 10.00 mL glass volumetric flask, by adding 0.0536 g of OPA, 2 mL of methanol, 40 μL of 2-mercaptoethanol with the final volume adjusted with borate buffer (0.4 mol L^{-1} ; pH 9.5). This solution was stored in the dark. Gentamicin sulfate derivatized standards was made in 2 mL vials by adding 400 μL of gentamicin sulfate stock solution (from 2.5 mg L^{-1} to 20 mg L^{-1}) in borate buffer (0.4 mol L^{-1} ; pH 9.5) then adding 150 μL of the OPA stock solution. The derivatized samples solutions were prepared in a similar form.

Appropriate quantities of the potential interferents sodium metabisulfite, anhydrous di-sodium EDTA, methylparaben and propylparaben were used to prepare individual stock solutions, using ultrapure water, at $1 \times 10^{-3} \text{ mol L}^{-1}$. Aliquots of these solutions were used for prepare a more diluted stock solutions ($4 \times 10^{-4} \text{ mol L}^{-1}$ or 22.5 mg L^{-1}) using acetate buffer pH 4.4.

BR buffer (0.040 mol L^{-1}), consisting of a mixture of boric acid, phosphoric acid and acetic acid, was prepared in water and the pH adjusted by adding appropriate amounts of sodium hydroxide 1 mol L^{-1} . Acetate buffer was

prepared by dissolution of sodium acetate and the pH 4.4 was adjusted with acetic acid. The borate buffer 0.4 mol L^{-1} solution, at pH 9.5, was prepared from the boric acid solution 0.4 mol L^{-1} , with pH adjusted by the addition of sodium hydroxide (6.0 mol L^{-1}). Phosphate buffer 0.2 mol L^{-1} at pH 7.4 was prepared through the dilution of monobasic phosphate 0.2 mol L^{-1} and solution sodium hydroxide 0.2 mol L^{-1} . The working electrolytic solution contained final concentrations of the following components: phosphate buffer ($4.0 \times 10^{-2} \text{ mol L}^{-1}$; pH 6.0), potassium nitrate (1.0 mol L^{-1}) and the cationic surfactant CTAB ($1.2 \times 10^{-4} \text{ mol L}^{-1}$) in ultrapure water.

Supporting electrolytes were: 10 mL of BR buffer (0.040 mol L^{-1} ; pH 4.0) for trifloxystrobin; 50 mL of acetate buffer (0.01 mol L^{-1} pH 4.4) for gentamicin sulfate and 5 mL total volume consisting of 1 mL of a mixture of phosphate buffer ($4.0 \times 10^{-2} \text{ mol L}^{-1}$; pH 6.0), 1 mL of potassium nitrate (1.0 mol L^{-1}) and 10 μL of a CTAB solution ($1.2 \times 10^{-4} \text{ mol L}^{-1}$), adjusting the final volume with ultrapure water.

For trifloxystrobin, the samples of mineral water, tap water, water from the Rainha Creek and the water from the Rodrigo de Freitas Lagoon did not require any pretreatment prior to analysis. Volume of 5.00 mL of water samples were fortified with two pesticide concentration levels ($5 \times 10^{-6} \text{ mol L}^{-1}$ or 2.0 mg L^{-1} and $7.0 \times 10^{-6} \text{ mol L}^{-1}$ or 2.9 mg L^{-1}). After analyte fortification, 1.00 mL of each water samples was introduced into the electrochemical cell that contained 10.0 mL of supporting electrolyte. For orange juice, a fraction of 2.5 mL of sample was diluted in ultrapure water to 5.0 mL and fortified with trifloxystrobin. These samples were loaded into a Bond Elut C-18 SPE cartridge (3.0 mL and 500.0 mg) Varian, USA) and washed with 20.0 mL of ultrapure water. The cartridge had been previously treated with 2.0 mL of acetonitrile, followed by 2.0 mL of water. The retained analyte was eluted with acetonitrile (1.0 mL) and then diluted to 2.0 mL with ultrapure water. An aliquot of 1.00 mL of this eluted solution was added to the electrochemical cell containing 10.0 mL of supporting electrolyte.

For gentamicin sulfate total components determination, the dilution of veterinary use pharmaceutical formulation samples (A, B and C) were prepared in 10,00 mL glass volumetric flasks by adding 51.2 μL of pharmaceutical formulation A or 56.3 μL of pharmaceutical formulation B or 28.2 μL of the

pharmaceutical formulation C with final volume completed with ultrapure water. The simulated sample was prepared at one concentration levels (16.9 mg L^{-1}) from the dilution of a gentamicin standard in acetate buffer 0.04 mol L^{-1} pH 4.4. The dilution of the pharmaceutical formulations samples for the HPLC analysis (according reference from literature [80]) were made by preparing an intermediary solution, in 25.00 mL glass volumetric flasks, by adding of 500 μL of sample (sample A, B or C) with final volume adjusted with ultrapure water. The final sample solution was made, in 10.00 mL glass volumetric flasks, by adding of 100 μL of the intermediary solution with final volume adjusted by adding borate buffer solution (0.4 mol L^{-1} ; pH 9.5).

As described by Lima *et al.* [82] the commercial Pau d'arco (250 mg of the inner bark powder per capsule) was extracted with ethanol in an ultrasonic bath (5 min), then the extract was passed through syringe filter ($0.45 \mu\text{m}$) and collected in a 10.00 mL volumetric flask, and stored in the dark and under refrigeration. The heartwood of *T. impetiginosa* (Pink Ipê) was finely grinded (about 1 g). Then, portions of 125 mg of the resultant powder were extracted with ethanol (as described above) and stored in 10.00 mL volumetric flasks. All sample extracts were made in triplicate.

3.7 Characterization of the water samples

Natural water samples were analysed in order to obtain the total organic carbon (TOC), total carbon (TC) and inorganic carbon (IC) values. For the Rainha Creek water (sweet water), results were 8.68 mg L^{-1} (TOC), 9.68 mg L^{-1} (TC) and 0.99 mg L^{-1} (IC). The water from the Rodrigo de Freitas Lagoon (a mixture of seawater and sweet water coming from several water streams) was analysed after a 1:1 dilution with ultrapure water. The results (after correcting for the dilution factor) indicated 9.50 mg L^{-1} (TOC), 10.51 mg L^{-1} (TC) and 1.01 mg L^{-1} (IC). The pH of the Rainha Creek water and Rodrigo de Freitas Lagoon water samples were, respectively, 6.95 and 7.63 with their conductivities of $144.6 \mu\text{S cm}^{-1}$ and 12.94 mS cm^{-1} .

3.8

Preparation of the molecular imprinted polymer using kanamycin sulfate as a template

The molecular imprinted polymer (MIP) using kanamycin sulfate as template (Kanamycin-MIP) was synthesized based on the procedure described by Khan *et al.* [83]. Briefly, in a glass recipient it was added 500 mg of kanamycin sulfate, 6 mL of deionized water, 400 μL of aqueous solution of HCl 1 mol L⁻¹ (as catalyst), 3200 μL of APTMS and 2650 μL of TEOS). The mixture was heated, at 40 °C, under magnetic stirring until the appearance of turbidity. The obtained gel was cooled to room-temperature and kept at ambient temperature for 12 h to ensure dryness of the material. The polymer was crushed and washed with 1 L of deionized water and 300 mL of methanol to remove the kanamycin sulfate template. This cleaning process was repeated two more times. The extraction of kanamycin sulfate was monitored by BIA-amperometry (the developed method). Finally, the polymer was sieved to obtain regular size distribution of particles with diameters between 106-50 μm . The kanamycin-MIP was then stored at room temperature. The corresponding non-imprinted polymer (NIP) was prepared in the same manner except for addition of kanamycin sulfate. In Figure 3.6 the synthesis and clean-up procedures for MIP and NIP are illustrated.

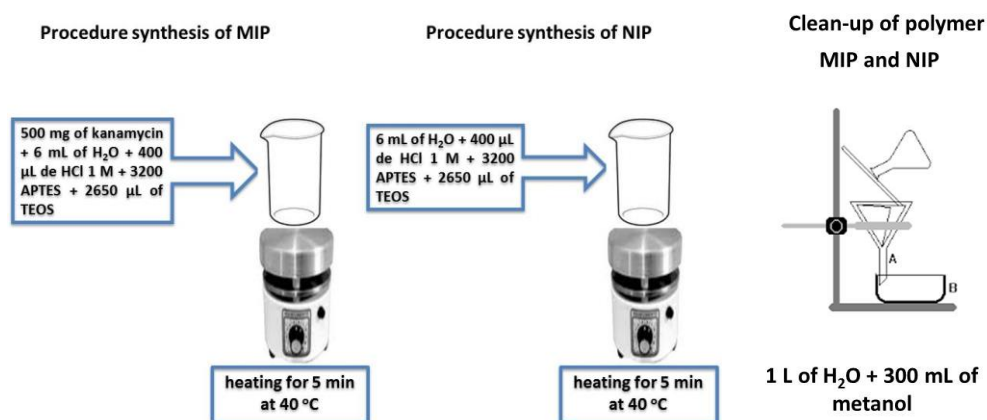


Figure 3.6. Steps for the synthesis and cleaning of the molecularly imprinted polymer (kanamycin-MIP) and non-imprinted polymer (NIP).

In Figure 3.7, the infrared spectrum of the MIP is shown (after cleaning up) and compared to the spectrum of the kanamycin sulfate (template). In the infrared spectrum of the MIP it can be seen that the characteristic peaks of

kanamycin are absent after cleaning. The characteristic infrared bands from the polymer are the dominant ones: 3307 cm^{-1} (stretching of N-H (NH_2) from the APTMS); $2956\text{-}2889\text{ cm}^{-1}$ (stretching of C-H (CH_2) from the APTMS); 1120 and 1033 cm^{-1} (stretching of C-O from ether and Si-O-Si stretching) and 781 cm^{-1} (Si-C stretching) [84].

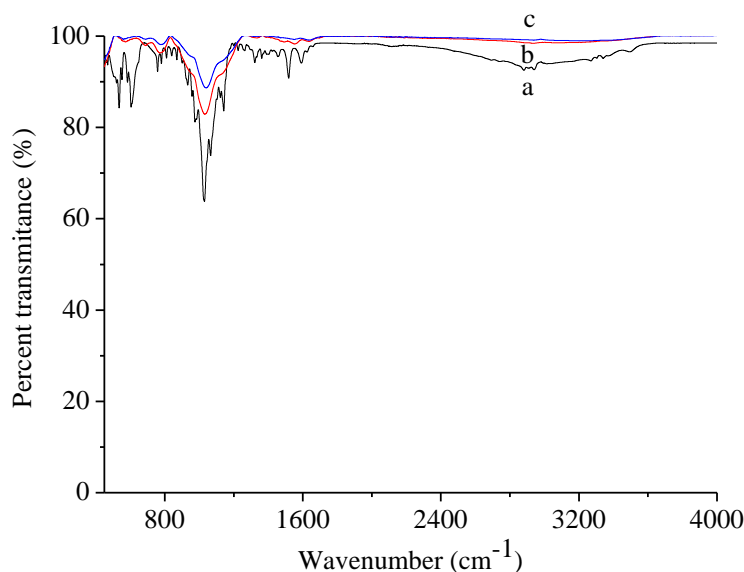


Figure 3.7. Infrared spectrum of (a) kanamycin sulfate (black). (b) kanamycin-MIP after clean-up to remove the kanamycin template (red) and (c) NIP (blue).

3.9

Solid phase extraction using the molecular imprinted polymer

In order to manufacture the cartridges packed with either kanamycin-MIP or NIP, 70 mg of polymer was loaded into a 1 mL micropipette tips (previously prepared by placing a small amount of cotton to cap the micropipette outlet to avoid loss of polymer). The cartridge was adjusted in the outlet tubing of a flow system in order to semi-automatize the solid phase extraction (SPE). Before using, the cartridges were conditioned with ultrapure water. The SPE process was made by loading the cartridges with 40 μL of stock solutions, interfering substances or samples, leaving it to rest for 1 h (equilibration time). Then, 5 mL of ultrapure water (in each cartridge) was added with a controlled flow of 1 mL min^{-1} . Finally, the elution of was made with 1 mL of acetate buffer (0.01 mol L^{-1} ; pH 3.5).

Aliquots of 60 μL of the eluates were added to the electrochemical cell to perform measurements. After extraction, the cartridge went through a cleanup step with a flow (1 mL min^{-1}) of water (approximately 50 mL at $40 \text{ }^\circ\text{C}$) and then with 5 mL methanol to ensure complete cleanup of the cartridge to be used for subsequent extraction. A single cartridge was used throughout the development of the work. In Figure 3.8, the semi-automated SPE procedure for gentamicin using the cartridge packed with the kanamycin-MIP is illustrated.

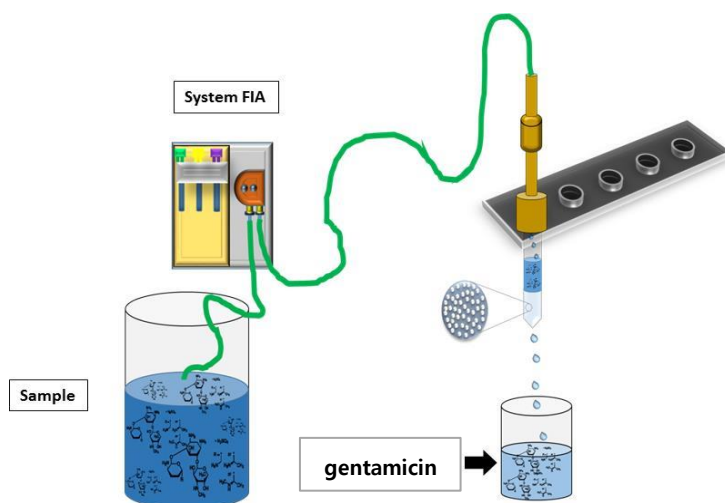


Figure 3.8. Scheme of the solid phase extraction for gentamicin sulfate using the kanamycin-MIP packed cartridge coupled in the outlet of a flow system.

3.10

Thin-layer chromatography for determination lapachol, α -lapachone and β -lapachone

Thin-layer chromatography (TLC) procedure was the one described by Lima and co-authors [82]. Aliquots of 20 μL of naphthoquinone stock solution ($1.0 \times 10^{-2} \text{ mol L}^{-1}$ or $1.0 \times 10^{-3} \text{ mol L}^{-1}$) or aliquots of 40 μL of alcoholic extract samples were spotted on the TLC plates allowing the spot to dry at room-temperature. Then, the plates were placed in a revelation chamber containing the mobile phase (chloroform:hexane 8:2 v/v). Mixtures containing lapachol, α -lapachone and β -lapachone (equimolar proportion) were spotted on TLC plate to evaluate the separation of lapachol from the other naphthoquinones. Lapachol presented the higher retention factor value ($R_F = 0.78$) being completely separated (Figure 3.9) from the other naphthoquinones. The area of the TLC plate

containing the lapachol spot was removed and then the analyte was extracted with 3 mL of methanol (under 5 min of ultrasonic treatment). The eluted solution was filtered in a syringe filter. Then, 5 mL methanol was passed through the filter to wash it. These solutions were collected in the same vial and evaporated (in a boiling water-bath) until a dry residue is left. The dry residue was re-dissolved in methanol (1.00 mL) from where it was collected an aliquot of 250 μL to be added to the electrochemical cell, in order to perform voltammetric measurements. TLC spots from an unused plate (about 1 g) were also treated in the same way in order to evaluate any potential interference imposed by any residue from the plate.

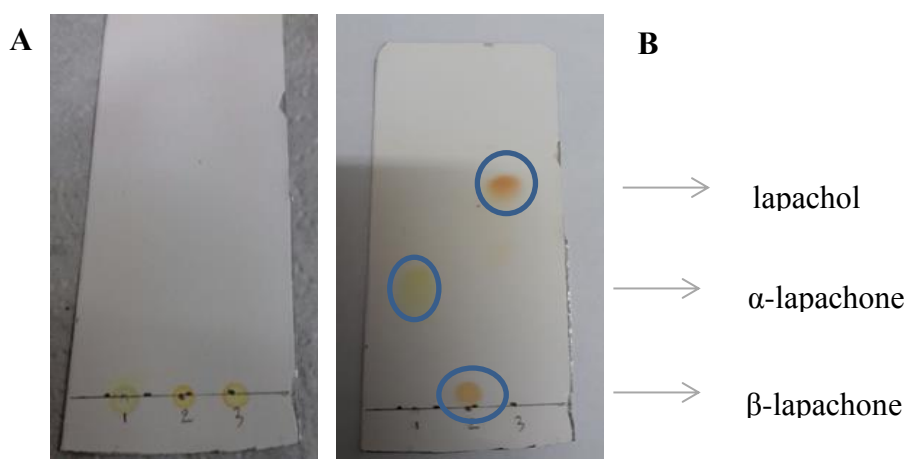


Figure 3.9. Thin-layer chromatograms of lapachones before (A) and (B) after the run.

3.11

Voltammetric measurements of trifloxystrobin, gentamicin, lapachol, α -lapachone and β -lapachone

Diagnostic studies of the redox process for determination of trifloxystrobin were made using CV with a scan rate up to 400 mV s^{-1} and a step potential of 2 mV in a potential range from +1050 to +2300 mV using BR buffer (0.04 mol L^{-1}) as the supporting electrolyte, within the pH range from 2.0 to 12.0, adjusted by adding appropriate amounts of sodium hydroxide. SWV was also used to evaluate the redox process. For the determination of trifloxystrobin by SWV, BR buffer (pH 4.0; 0.040 mol L^{-1}) was used as the supporting electrolyte. After 15 s of equilibration time, the scanning potential was made from +1400 to +2300 mV with signal measurement made at +1744 mV. A frequency of 30 Hz, step potential

of 20 mV and pulse amplitude of 40 mV completed the electroanalytical conditions. Then, 30 sequential cyclic voltammetric scans (within the +1200 to +2200 mV range at a scan rate of 100 mV s⁻¹) were made until the stabilisation of the measured current. When the cleaning procedure was not able to restore the analyte signal, the electrode activation procedure was performed. Often, when a systematic loss of sensitivity was observed, the signal response from the BDD was restored through multiple pulse amperometry by applying pulses at +1200 mV pulses (every 0.03 s) and at +1800 mV pulses (every 0.3 s) during about 1000 s, using H₂SO₄ 0.10 mol L⁻¹ as the supporting electrolyte. Quantifications were performed using the analyte addition procedure and peak height measurements.

Diagnostic studies of the redox process of gentamicin sulfate were made using CV with a 100 mV s⁻¹ scan rate and 2 mV potential step within a potential range from +1000 to +2300 mV using acetate buffer (0.2 mol L⁻¹, pH 3.0) as supporting electrolyte. To perform the determination of gentamicin sulfate using BIA-amperometry with multiple pulses, acetate buffer (0.01 mol L⁻¹; pH 4.4) was the supporting electrolyte under constant stirring (600 rpm). Aliquots of 60 µL of analyte standards or samples were added directly on the surface of BDD electrode (in triplicate) by means of the automatic micropipette. Signal, current peak height, as measured at 2000 mV. Quantification was performed using interpolation in the analytical curve.

All voltammetric experiments involving lapachol and derivatives were made after the purging solutions, in the electrochemical cell, with nitrogen gas (about 2 min) before scanning. CV experiments were made from -900 mV to +600 mV in the working electrolytic solution either containing or not CTAB. SWV measurements were made using the appropriate supporting electrolyte either to evaluate the redox process or to perform analytical determinations of lapachol. Redox diagnostic experiments were made in the range from +600 to -1000 mV. Analytical determinations were made with analyte pre-concentration at +400 mV, for 140 s (under convective transport regime and purging with nitrogen gas). After, equilibration time (1 min without agitation and purging), the scanning from +600 to -900 mV was made at 30 Hz using 20 mV potential step and 40 mV pulse amplitude. Analyte signal was measured as current peak height at -470 mV.

3.12

Study of trifloxystrobin degradation under UV exposure

The UV degradation study was conducted by placing 0.2 μmol of trifloxystrobin (200 μL of trifloxystrobin of the stock solution) in the quartz tubes. The tubes were taken to a water bath (set as 60°C) to gently evaporate the solvent. Then, the tubes were placed in the reactor to UV expose the analyte solid film deposited at the walls and bottom of the tube. One of the tubes was withdrawn from the reactor every 5 min until the last one at 20 min. A volume of 2.0 mL of acetonitrile was added to the tubes to re-dissolve the solid material adhered to the tube wall. Then, a 100 μL aliquot of the solution was added to the electrochemical cell to be analysed using the developed voltammetric method. The results were represented as a percent value related to the concentration of the analyte in a solution not exposed to the UV (100%). The experiment was repeated three times in order to get an authentic replicate for each UV exposition time. The experiment with incidence of UV was also made by exposing 0.2 μmol of trifloxystrobin dissolved in 10.00 mL acetonitrile/H₂O (40/60% v/v) solution. One of the tubes was withdrawn from the reactor every 5 min until the last one at 20 min. Then, a 100 μL aliquot of each solution was added to the electrochemical cell to be analysed using the developed voltammetric method.

3.13

Chromatographic analysis

Analyses by GC-MS system were conducted using sample volume of 1 μL with a temperature of 300°C, in the transfer line, and 230°C for the ion source. The ionization was achieved by electron impact with split injection mode. The analyses used a heating ramp (35-150°C at a rate of 2°C min⁻¹) followed by a 15°C min⁻¹ temperature ramp in the range from 150°C to 300°C.

The HPLC comparative method was adapted of Claes *et al.*, [80]. In this method was used a HPLC with fluorescent detector which the excitation was made at 380 nm (λ_{exc}) and the emission was collected at 450 nm (λ_{em}), under isocratic elution with acetonitrile/acetate of ammonium:acetic acid solution (50:50 %v/v). The mobile phase flow rate was 1 mL min⁻¹ and the injection volume was of 50 μL . Each derivatizing standard solution or derivatizing solution samples, containing gentamicin sulfate and OPA was prepared 10 min before

introduction into the chromatographic system in order to let the reaction to be processed. Under these conditions, the retention time of the different gentamicin sulfate were 13.3 min (gentamicin C_{1a}), 19.9 min (gentamicin C_{2a}), 22.1 min (gentamicin C₂) and 23.5 min (gentamicin C₁). The analyses were made in three replicates.

Sample extracts were analyzed by HPLC-UV under isocratic elution with methanol/acetic acid 5% solution (80/20% v/v) [82]. The mobile phase flow rate was 1 mL min⁻¹ and the introduced sample volume was 10 µL. Under these conditions, the retention time of lapachol was 5.7 min. Analytical curves were constructed by introducing 20 µL of the standard stock solutions of lapachol from 2.4 mg L⁻¹ to 96.9 mg L⁻¹. The analyses were made in three replicates with absorciometric detection at 278 nm.

4

Electrooxidation of trifloxystrobin at the boron-doped diamond electrode: electrochemical mechanism, quantitative determination and degradation studies

Paper published as “*Electro-oxidation of trifloxystrobin at the boron-doped diamond electrode: electrochemical mechanism, quantitative ultratrace determination and degradation studies*” Almeida JMS, Toloza CAT, Dornellas RM, da Silva AR, Aucélio RQ, Int J. Environ. Anal. Chem., 2016, 10, 959-977. DOI: 10.1080/03067319.2016.1220005 (see attachment I).

4.1

Introduction

Pesticides play a key role in agriculture and proper control of their residues is crucial to evaluate potential harm to the human population and environment [85]. The application of fungicides in fruit trees and in vegetables is made by spraying the leaves so that the active molecule is gradually and steadily absorbed, allowing prolonged and uniform plant protection [86]. Trifloxystrobin (Figure 4.1) is a synthetic strobilurin class fungicide used in the production of important commodities such as soybean and oranges. It is a mesostemic fungicide that interferes with the respiration of plant-pathogenic fungi. It is mostly used as a broad-spectrum foliar fungicide against many fungal pathogens among them *Ascomycete*, *Deuteromycete*, *Basidiomycete*, and *Oomycete* classes. Trifloxystrobin has four geometrical isomers in function of the arrangement of the groups connected to the two N=C present in the molecule structure. (E,E)-trifloxystrobin is the most biologically active fungicide among the four isomers. Trifloxystrobin degrades rapidly in water and soil by mechanisms including metabolism, photolysis, and hydrolysis [87].

In function of the high quantities of pesticide employed in large plantations, often nearby waterbodies, the level of trifloxystrobin must be monitored. According to the Brazilian National Health Surveillance Agency, that follows criteria adopted by other international health agencies, the acceptable daily intake value for trifloxystrobin is 30 $\mu\text{g kg}^{-1}$ body weight [88]. In addition, the Codex Alimentarius [89] establishes maximum residue limits for

trifloxystrobin of $40 \mu\text{g kg}^{-1}$, thus the level of this pesticide must be monitored to guarantee no harm for population nearby plantations and also to evaluate if the crop production meets adequate standards to be exported to countries with rigid sanitary regulations.

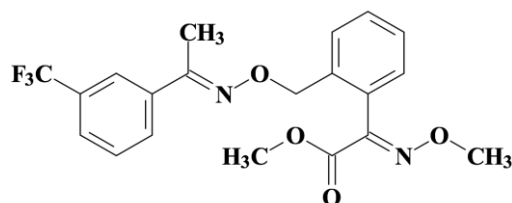


Figure 4.1. Chemical structure of trifloxystrobin

Gas chromatography (GC) and HPLC are the main techniques for the determination of strobilurins (including trifloxystrobin). GC with tandem mass spectrometry (MS/MS) was used to determine trifloxystrobin, along with other pesticides, in fruits and vegetables after liquid-liquid extraction (LLE), with recoveries from 89% to 106% [90]. The determination of strobilurin fungicides (trifloxystrobin included) in wheat, apples and grapes was made using GC with three different types of detection and previous extraction of analytes from samples using LLE and clean-up by gel permeation chromatography (GPC). The recoveries varied from 70% to 110% and LOD for trifloxystrobin in samples varied from 0.004 to 0.014 mg kg^{-1} [91]. Bo *et al.*, used GC-MS to determine eight strobilurin fungicides in fruits, vegetables, beverages, cereals, nuts, meat, eggs and milk [92]. The extraction of the analytes was performed by GPC. The LOQ for trifloxystrobin was 0.005 mg kg^{-1} with recoveries from 69% to 120%. Seven strobilurins were determined in baby food samples by GC-MS using solid-phase microextraction (SPME) on a fibre polydimethylsiloxane-divinylbenzene [93]. The LOQ for trifloxystrobin was $0.024 \mu\text{g kg}^{-1}$ with 96% of recovery. Strobilurin fungicides were also determined, in grapes and wines, using a variant of this method by using a programmed vaporization temperature of sampling, LLE and clean-up using SPE with stationary phase of a double-layer graphite/ethylenediamine-*N*-propyl [94]. The LOQ for trifloxystrobin was 0.002 and 0.003 mg kg^{-1} for white wine and red wine, respectively, with recoveries within 98-101%. GC-MS was also used for the determination of seven strobilurins

(including trifloxystrobin) along with other fungicides in fruits and fruit juices. Pretreatment of the samples was performed with liquid-liquid microextraction (LLME) assisted by ultrasound. The LOD was $0.01 \mu\text{g L}^{-1}$ for trifloxystrobin with recoveries from 101% to 117% [95].

Four strobilurin fungicides were determined in grape and wine by HPLC with absorption photometric detection (HPLC UV) at 210 nm [96]. The analytes were extracted by LLE and the clean-up/pre-concentration performed by SPE on a silica cartridge. For trifloxystrobin, the LOD was 0.150 mg kg^{-1} in grapes (about 0.150 mg L^{-1} for wines). The recoveries were from 85% to 94%. The determination of seven strobilurins in fruits using HPLC UV was made after the pretreatment of samples by adsorptive extraction on a stirring bar modified with an adsorbent layer. The LOQ was $0.9 \mu\text{g kg}^{-1}$ for trifloxystrobin (recoveries from 89% to 98%) [97]. HPLC UV was also used to determine strobilurin fungicides in fruit juice samples after LLME procedure assisted by ultrasound. LOD of $4 \mu\text{g L}^{-1}$ was obtained for trifloxystrobin (recoveries in two fortification levels ranging from 88.5% to 97.5%) [98]. Yang *et al.*, [99] combined magnetic solid-phase microextraction (MSPME) and dispersive LLME with an ionic liquid, to determine four pesticides including trifloxystrobin. The analytes were determined in water samples being extracted from the sample to the adsorbent and then desorbed in acetonitrile prior to analysis. The LOD was $0.03 \mu\text{g L}^{-1}$ for trifloxystrobin.

The efficient separation of species on a chromatographic column, the ability to determine a large number of pesticides of different classes in a single run and the consolidated maturity of GC and HPLC make these techniques obvious choices for analytical monitoring of pesticides. However, complex sample cleaning/extraction procedures are required and the detection is usually poor by photometric absorption (near 210 nm) in the case of strobilurins. In addition, both cost of instrumentation and often required maintenance, particularly for approaches in tandem, are the driving force for the development of simpler analytical methods to be used in the field and for screening of fruit and fruit extracts to be liberated for food processing and also to evaluate the effect of pesticide crop application in nearby waterbodies.

Literature reports the successful use of BDD for the voltametric determination of pesticides such as picloram [100, 101], atrazine [102],

metamitron [103], linuron [104], mehiocarb [105], triclopyr [106] and fenfuram [107]. Currently, the literature does not report any electrochemical method for the determination of trifloxystrobin although recently reported amperometric and voltammetric methods have been addressed the determination of other strobilurin class fungicides [7-9,108]. In the present chapter the following studies are presented: i) the trifloxystrobin redox behaviour on a BDD establishing a plausible mechanism; ii) the voltammetric method developed taking into advantage the intense electrochemical response and its application in the determination of trifloxystrobin in natural waters and in orange juice samples; iii) the monitoring, using the developed method, of the UV-induced degradation of the fungicide, establishing some kinetics parameters.

4.3 Results

4.3.1 Preliminary studies

As a sensing material, the nanocrystalline BDD has been used for the construction of electrodes that allow the determination of chemical species that are oxidised or reduced in aqueous medium also at potentials above ± 1000 mV, which is difficult when using other traditional materials for electrodes [109]. The qualitative assessment of the voltammetric response of trifloxystrobin using the BDD was carried out by CV and the characteristic voltammograms of the analyte in solution were observed over the entire pH range tested, presenting two oxidation peaks (through the anodic scan) with current maxima, respectively, at about +1740mV (E_{p1}) and +2010mV (E_{p2}). As the scan was reversed (cathodic scan), no reduction peaks were found as counterparts of the oxidation ones. In (Figure 4.2A), typical trifloxystrobin cyclic voltammograms (at pH 4.0) are shown in the potential range from +1200 to +2400 mV. The sequential voltammogram cycles (each cycle made within 2 s and with analyte mass transport to the electrode-solution interface minimised by nonechanical agitation of the solution) showed the continuous decreasing of the trifloxystrobin (at 8.0×10^{-4} mol L⁻¹ or 0.33 g L⁻¹) oxidation peak intensities. By performing the sequential cyclic voltammetric scans for the first peak alone (cyclic scanning from +1200 to

+1900 mV), the decreasing of peak intensity to blank level occurred at the 19th cycle (Figure 4.2B). Such behaviour indicates that the first oxidation peak does not depend upon the second oxidation process that occurs at a higher potential (which was avoided in the experiment). On the other hand, by isolating the second peak (cyclic scanning from 1800 to 2400 mV) its intensity is smaller than the one observed when scanning started from +1200 mV, showing a probable dependence of the second oxidation process upon the first oxidation process. The second oxidation peak intensity reaches the blank level already after five voltammetric cycles (Figure 4.2C). In addition, the variation of the scan velocity of the experiment did not affect the overall behaviour of the process concerning the second peak.

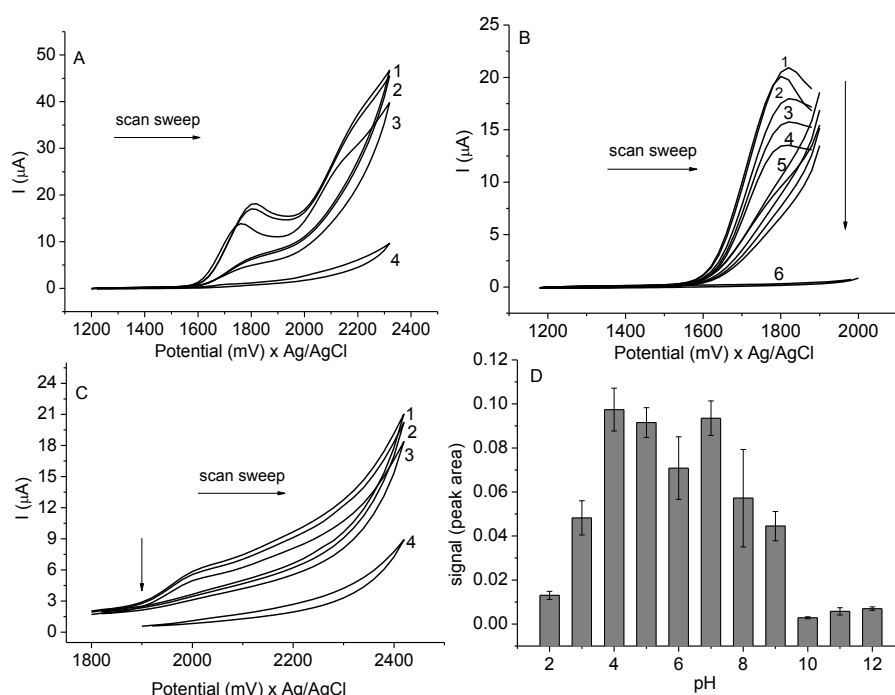


Figure 4.2. CV of trifloxystrobin ($8.0 \times 10^{-4} \text{ mol L}^{-1}$ or 0.33 g L^{-1}) on BDD electrode in BR buffer (0.040 mol L^{-1} , pH 4.0)/ACN 70/30% v/v. (A) Complete cycle from +1200 to +2300 mV potential range: (1) 1st cycle, (2) 5th cycle, (3) 11th cycle, (4) blank. (B) For the first oxidation peak: (1) 1st cycle, (2) 5th cycle, (3) 11th cycle, (4) 19th cycle and (5) blank. (C) For the second oxidation peak: (1) 1st cycle, (2) 3rd cycle, (3) 5th cycle and (4) blank. (D) Influence of pH on the first voltammetric (SWV) trifloxystrobin ($4.0 \times 10^{-5} \text{ mol L}^{-1}$ or 16 mg L^{-1}) oxidation peak area (with maximum at +1744 mV). Scan rate of 100 mV s^{-1} for CV.

4.3.2 Oxidation process

The CV study indicated the irreversibility of charge transfer and mass transfer controlled by diffusion as there was a linear relationship ($R^2 = 0.989$) between the peak intensity (I_p), measured at +1740 mV and \sqrt{v} , where v was the potential scan velocity varied between 10 and 400 mV s^{-1} (Figure 4.3A). For the second peak (measured at +2010 mV), such linear relationship also held ($R^2 = 0.990$) as seen in (Figure 4.3B). Voltammograms can be seen in (Figure 4.3C).

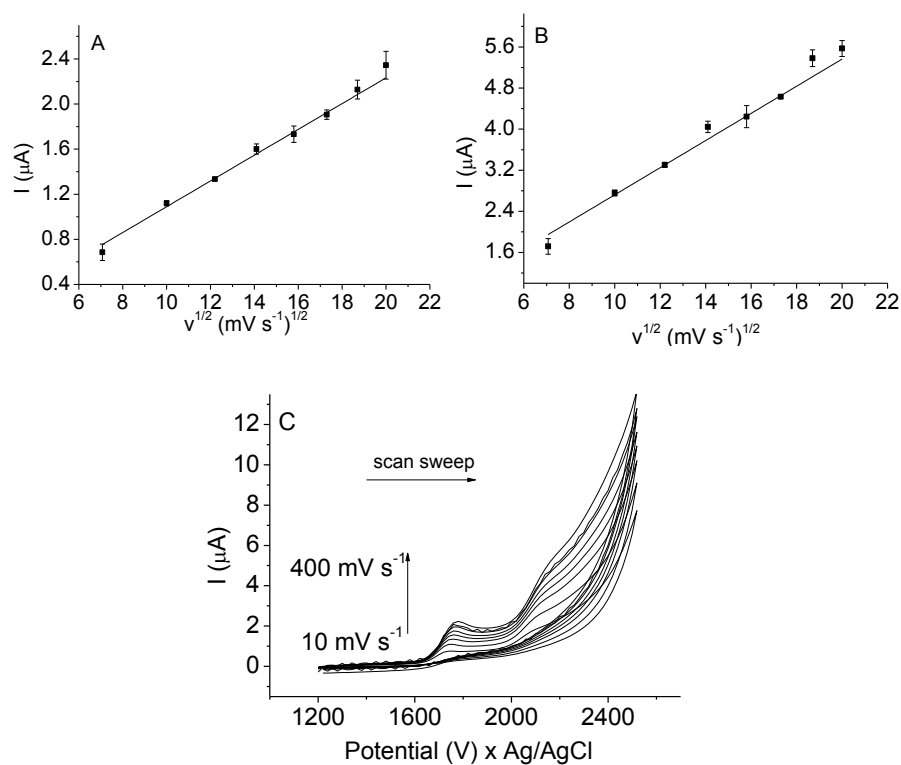


Figure 4.3. (A) and (B) CV data of a solution with $4.0 \times 10^{-4} \text{ mol L}^{-1}$ (0.16 g L^{-1}) trifloxystrobin: Peak current (I_p) versus square root of the scan rate (\sqrt{v}) representation for (A) oxidation peak with maximum at +1740 mV ($R^2 = 0.989$) and (B) oxidation peak with maximum at +2010 mV ($R^2 = 0.990$); (C) Sequence of cyclic voltammograms obtained at different scan velocities. Experimental conditions: BR buffer (pH 4.0; 0.040 mol L^{-1})/ACN (70/30% v/v) and scan rate from 10 to 400 mV s^{-1} .

The $\log(I_p)$ versus $\log(v)$ indicated adsorption-controlled processes as the slope of graphs were 0.988 for the first oxidation (Figure 4.4A) peak and 0.980 for the second oxidation (Figure 4.4B) peak. The linear increasing of I_p as the

frequency of the applied pulses (f) is increased (up to 70 Hz using SWV) confirmed the irreversibility of the first (Figure 4.4C) and second (Figure 4.4D) oxidation processes.

For irreversible systems, the SWV peak width at half height ($\Delta E_{p/2}$) is modelled by the equation $\Delta E_{p/2} = (65.5 + 0.5)/\alpha n$, where n is the number of electrons involved in the process and α is the electronics transfer coefficient [43,110]. Considering systems with α value equal to 0.5, the experimental $\Delta E_{p/2}$ can be used to calculate the number of moles of electrons involved in the redox reaction. As $\Delta E_{p/2}$ was 80 mV, the value for n is 1.6, suggesting that the oxidation process relative to the first peak involves two electrons per molecule. For the second reaction, a two electron ($n = 1.8$) process was also found.

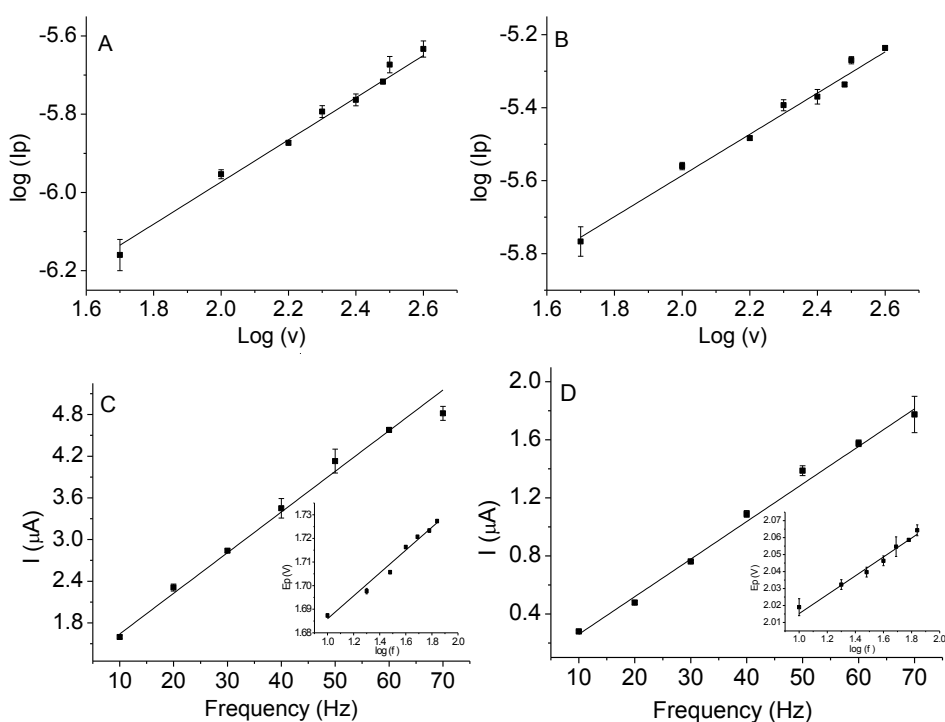


Figure 4.4. CV study (trifloxystrobin $4.0 \times 10^{-4} \text{ mol L}^{-1}$ or 0.16 g L^{-1}) of the logarithm of peak current intensity ($\log I_p$) in function of the logarithm of the scan velocity ($\log v$) for: (A) the first oxidation peak ($R^2 = 0.988$) and (B) the second oxidation peak ($R^2 = 0.980$). SWV peak current (I_p) in function of frequency for (C) first oxidation peak ($R^2 = 0.996$) and (D) second oxidation peak ($R^2 = 0.992$). Detail presents the potential (E_p) in function of the logarithm of the frequency ($\log f$) for: (C) first oxidation peak ($R^2 = 0.981$) and (D) second oxidation peak ($R^2 = 0.988$).

Irreversible reactions are characterised by the linear relationship (with slope equal to $-2,3RT/\alpha nF$) between the maximum peak potential (E_p) and the log (f) [110]. For trifloxystrobin (first oxidation peak), such a linear relationship held (see detail in (Figure 4.4C)). Through the slope of the curve, the αn product (product of the electron transfer coefficient and the number of electrons involved in the electrode reaction) was close to 1, which would lead roughly to a value of α of 0.5 for two electrons involved in the reduction. Similar results are found for the second oxidation peak (see detail in Figure 4.4D).

The dependencies of the E_p values in function of pH were studied for both peaks, in the range from pH 3.0 and 6.0. In both cases, neither a clear tendency nor significant variations for the E_p values were found as expected since trifloxystrobins and possible its first oxidation product present no relevant acid/basic characteristics.

According to the literature [111,112] and based on the information collected for each of the oxidation processes, a mechanism for the oxidation can be proposed (Figure 4.5). The first step resembles the already proposed mechanism for the strobilurin kresoxim-methyl [7], that involves the loss of an electron which gives rise to a radical cation (structure II) followed by the abstraction of a proton leading to a radical. The loss of another electron generates a carbocation, which is stabilised by resonance due to electron delocalisation in the aromatic ring. Once the process occurs in aqueous medium, it is possible that one water molecule promotes the nucleophilic attack on the deficient carbon forming the species of structure V. Finally, a cleavage might occur with the formation of two neutral molecules, one of them an acetophenone oxime (structure VI). Tallec and Tarvel demonstrated that acetophenone oximes can undergo irreversible electrochemical oxidation by the loss of two electrons leading to the formation of ketones [113] at potentials above +1800 mV and in the presence of 15% water. Therefore, it is believed that, in step 2, the acetophenone oxime (produced in the step 1) might be cleaved with the loss of two electrons and a proton (per molecule), thereby forming the aromatic ketone (structure XI). Thus, the proposed mechanisms justify the irreversible oxidation, promoted by the loss of two electrons for each of the oxidation processes.

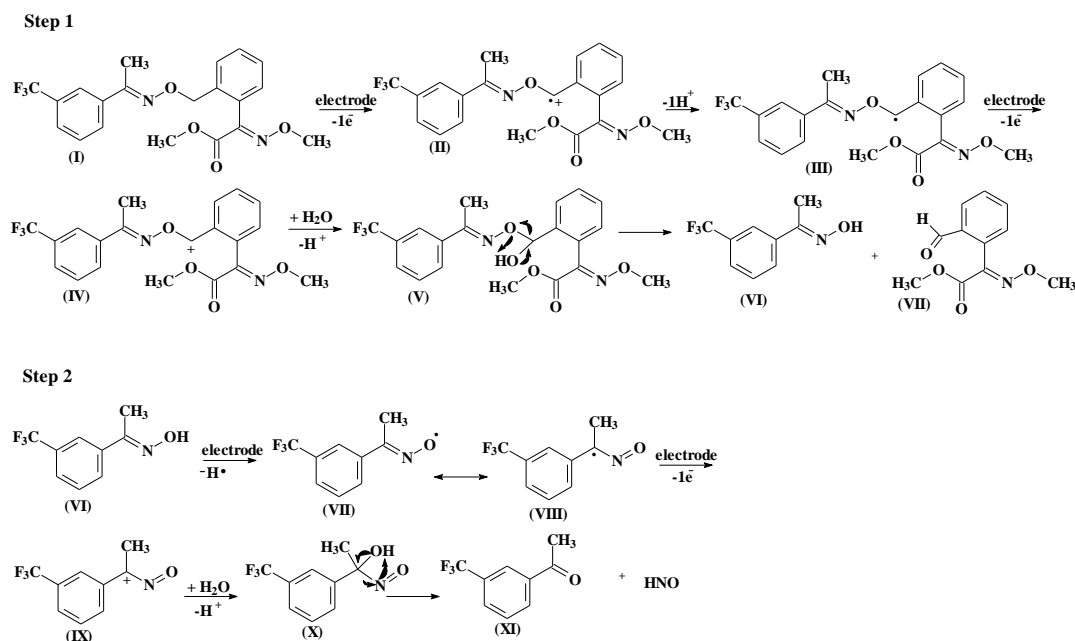


Figure 4.5. Proposed trifloxystrobin electrochemical oxidation mechanism mediated by BDD.

4.3.3

Optimization of experimental and instrumental conditions

Over the pH range tested (2.0-12.0), both oxidation peaks were more intense between pH 4.0 and 7.0. In this range, the relative intensities of each of the peaks, evaluated using SWV, were statistically similar (analysis of variance at 95% confidence limit) no matter the pH used. (In Figure 4.2D), the areas of the voltammetric peak with maximum at +1744 mV are shown over the entire studied pH range. It was observed a clear decreasing of response in the extreme acid conditions and over the range of pH values above 7.0.

The supporting electrolyte at pH 4.0 was chosen to proceed with the development of the method because it produced more reproducible results (below 2% based on 10 sequential measurements on the same solution).

In order to achieve the best experimental conditions for the determination of trifloxystrobin using SWV and BDD, a univariate optimization was performed taking into account the critical parameters affecting the intensity and signal reproducibility. The studied parameters were: (i) pulse frequency (f) and (ii) pulse amplitude (a). The monitored analytical signal was the area of the peak with

maximum at +1744 mV due to the fact that the first voltammetric peak presents better definition and higher signal, obtained at a less positive potential. The step potential was kept at 20 mV. The anodic scanning was applied without forcing any previous deposition of material onto the electrode surface as this strobilurin (or any reaction product) did not accumulate onto the surface of the BDD. All studies were performed in triplicate.

The increase of pulse amplitude, studied in the range from 10 mV to 100 mV, improved the measured signal (peak area) until the amplitude 80 mV. The selected pulse amplitude was 40 mV because of the sharpness (relationship between peak height and peak width). The peak area increased as the pulse frequency was varied from 10 to 70 Hz. The best compromise between peak area and peak width was obtained at 30 Hz. Besides, under such conditions, the scan velocity (the product of f and ΔE) is not too fast, enabling the oxidation reaction to proceed efficiently. Thus, with these parameters chosen, the scan velocity was 600 mV s^{-1} .

4.3.4

Analytical figures of merit

The analytical figures of merit were obtained using the selected experimental conditions to determine trifloxystrobin (Table 4.1). A sequence of voltammograms of a solution containing increasing concentrations of analyte is shown in (Figure 4.6A). The analytical signal (current) was directly and linearly proportional to the concentration trifloxystrobin in the electrochemical cell (Figure 4.6B). The analytical curve equation (with the standard deviations of sensitivity and linear coefficient) was $I_p (\mu\text{A}) = (1.0 \times 10^{-1} \pm 4.8 \times 10^{-6}) C (\text{mol L}^{-1}) + (8.8 \times 10^{-2} \pm 1.1 \times 10^{-3})$; ($R^2 = 0.997$) and dynamic linear range covered three decades (10^{-7} - $10^{-5} \text{ mol L}^{-1}$). The measurements were performed in triplicate and the associated errors of sensitivity and linear coefficient in the curve were calculated as the standard deviation. For quantitative purposes, integrated peak area was used as the measured signal. The instrumental LOD was $1.4 \times 10^{-7} \text{ mol L}^{-1}$ (0.058 mg L^{-1}) and the instrumental LOQ was $4.6 \times 10^{-7} \text{ mol L}^{-1}$ (0.19 mg L^{-1}). The LOD was calculated using $3s_b/m$ and the LOQ using $10s_b/m$, where s_b is the standard deviation estimated by 10 consecutive measurements of the peak of the

lower analyte concentration of the analytical addition curve and m is the slope of the analytical curve. In (Figure 4.6C), the signal produced by the analyte at the LOQ level is shown against the blank signal.

The instrumental precision was obtained as the variation coefficient of 10 consecutive measurements of the signal produced by the analyte standards. Four different concentrations: 1.0×10^{-6} (0.4 mg L^{-1}); 5.0×10^{-6} (2.0 mg L^{-1}); 1.0×10^{-5} (4.1 mg L^{-1}) and 5.0×10^{-5} (20 mg L^{-1}) were used. Each of the measurements was made after a solution agitation step to replenish the solution-electrode interface. The intermediate precision was determined by comparing the results obtained from the analysis (10 independent replicates) of a trifloxystrobin-fortified simulated potable water sample at two concentration levels in the electroanalytical cell: 1.0×10^{-6} (0.4 mg L^{-1}) and 1.0×10^{-5} (4.1 mg L^{-1}). Instrumental precision was about 3% at the 10^{-6} mol L^{-1} concentration level, decreasing to about 2% at the 10^{-5} mol L^{-1} concentration level. The intermediate precision values, estimated by the variation coefficient obtained in analyte-fortified mineral water, were about 10% (at 1.0×10^{-6} mol L^{-1}) and 7% (at 1.0×10^{-5} mol L^{-1}).

Table 4.1. Experimental conditions selected for the square-wave voltammetric determination of trifloxystrobin using the BDD.

Parameter	Value
Supporting electrolyte	Britton Robinson buffer (pH 4.0; 0.040 mol L^{-1})
Amplitude (a)	40 mV
Scan increment (ΔE_s)	20 mV
Frequency (f)	30 Hz
Monitored signal	Peak with maximum at +1734 mV
Scan potential range	of +1400 for +2300 mV

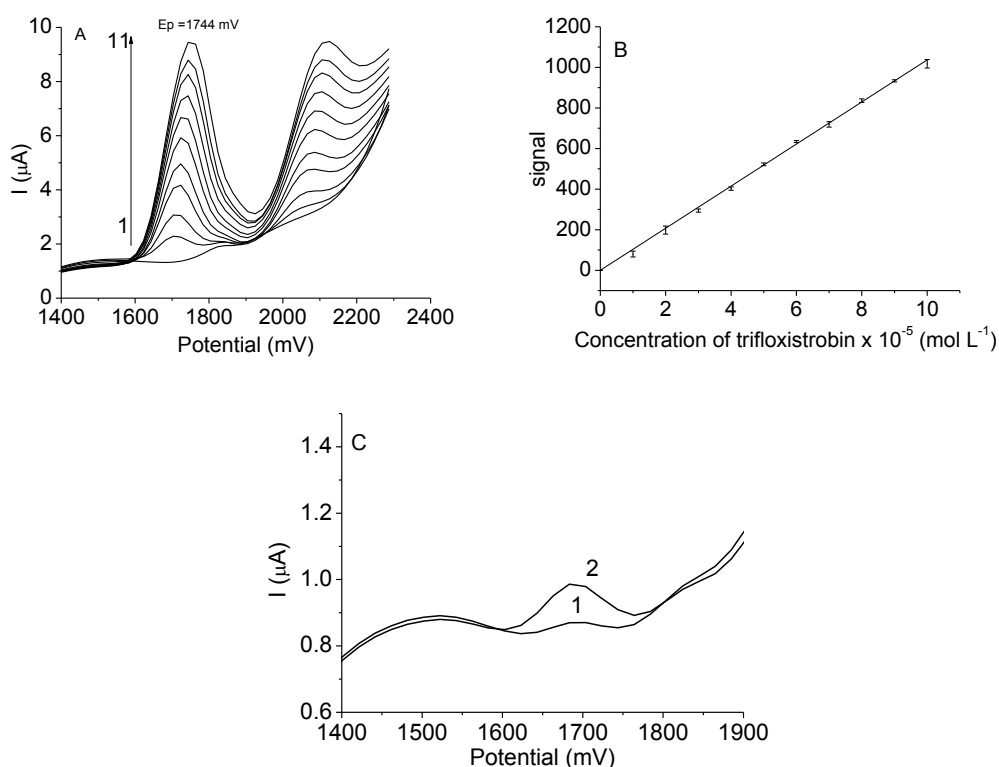


Figure 4.6. (A) SWV response with DDB as the working electrode: Concentration of trifloxystrobin: (1) blank; (2) $1.0 \times 10^{-5} \text{ mol L}^{-1}$ (4.1 mg L^{-1}); (3) $2.0 \times 10^{-5} \text{ mol L}^{-1}$ (8.2 mg L^{-1}); (4) $3.0 \times 10^{-5} \text{ mol L}^{-1}$ (12.2 mg L^{-1}); (5) $4.0 \times 10^{-5} \text{ mol L}^{-1}$ (16.3 mg L^{-1}); (6) $5.0 \times 10^{-5} \text{ mol L}^{-1}$ (20.4 mg L^{-1}); (7) $6.0 \times 10^{-5} \text{ mol L}^{-1}$ (24.5 mg L^{-1}); (8) $7.0 \times 10^{-5} \text{ mol L}^{-1}$ (28.6 mg L^{-1}); (9) $8.0 \times 10^{-5} \text{ mol L}^{-1}$ (32.7 mg L^{-1}); (10) $9.0 \times 10^{-5} \text{ mol L}^{-1}$ (36.8 mg L^{-1}); (11) $1.0 \times 10^{-4} \text{ mol L}^{-1}$ (40.8 mg L^{-1}). (B) Analytical curve ($R^2 = 0.998$) and (C) Voltammograms showing the difference between the signal produced by (1) blank and (2) trifloxystrobin at a concentration equivalent to the LOQ ($4.6 \times 10^{-7} \text{ mol L}^{-1}$ or 0.19 mg L^{-1}). Experimental conditions indicated in Table 1.

Studies were conducted to evaluate the potential interference imposed by other fungicides (other strobilurins and triazoles) in the electroanalytical signal produced by trifloxystrobin. The interference was evaluated by the ratio between the signal from a solution containing only the analyte and the signal measured from a solution containing the mixture of the analyte together with other fungicide (strobilurin or triazole), in this case, the analyte concentration is the same in both solutions ($1 \times 10^{-5} \text{ mol L}^{-1}$ or 4.1 mg L^{-1}). Interference was evaluated through the $I_{\text{analyte}}/I_{(\text{analyte} + \text{other fungicide})}$ values, which is given by the ratio between the signal measured from the solution containing only the analyte and the signal obtained from mixture containing analyte and the potential interferent (in this case, other fungicide). These $I_{\text{analyte}}/I_{(\text{analyte} + \text{other fungicide})}$ values near unity did not indicate

interference. Values greater than 1 indicate a decrease in the analyte signal due to the presence of another fungicide, while values below unity indicated increasing of the measured signal due to the contribution from the other fungicide. These tests were carried out with fixed concentration of analyte and two different analyte:other fungicide proportions (1:0; 1:1; 1:2 and, in some cases also 1:3). Measurements were performed in triplicate and the calculations were based on the integrated peak area with results shown in Table 4.2.

Picoxystrobin and kresoxim-methyl were found to interfere when they were twice the concentration of trifloxystrobin, increasing the measured signal due to the proximity of the oxidation peaks from these strobilurins with the ones of the analyte. Fluoxastrobin and tebuconazole interfere in the determination when present at the same concentration of the analyte. For tebuconazole, the interference seems to decrease the analyte signal. In this case, tebuconazole might have the preference in reacting at the electrode surface, slowing down the kinetics of oxidation of the analyte. The interference observed in the presence of cyproconazole has the effect of increasing the measured voltammetric signal to values higher than the expected one.

It is unusual the combined use of different fungicides of the strobilurin class in a specific crop, but the two evaluated triazoles (tebuconazole and cyproconazole) might be associated with trifloxystrobin in some commercial products. Thus, it is important that the analyst get previous information on what products have been used to treat a crop before performing the analysis.

Table 4.2. Evaluation the interference imposed by other strobilurin and triazole fungicides in the trifloxystrobin (1.0×10^{-5} mol L⁻¹ or 4.1 mg L⁻¹) electroanalytical signal^a (n = 3).

Fungicide	Proportion (trifloxystrobin / other fungicide)	$\frac{I_{(trif.)}}{I_{(trif. + other fungicide)}} \pm S_{ratio}^b$
Fluoxastrobin	1:0	1.00 ± 0.07
	1:1	1.22 ± 0.15
	1:2	2.27 ± 0.17
picoxystrobin	1:0	1.00 ± 0.13
	1:1	1.10 ± 0.14
	1:2	1.47 ± 0.16
	1:3	1.63 ± 0.15
kresoxim-methyl	1:0	1.00 ± 0.04
	1:1	1.15 ± 0.06
	1:2	1.26 ± 0.04
Tebuconazole	1:0	1.00 ± 0.05
	1:1	1.98 ± 0.12
	1:2	2.87 ± 0.19
cyproconazole	1:0	1.00 ± 0.01
	1:1	0.84 ± 0.11
	1:2	0.53 ± 0.07
	1:3	0.53 ± 0.01
	1:4	0.47 ± 0.19

^aFor instrumental conditions see Table 1.

^bThe standard deviation is the propagated one considering the ratio of signals and their standard deviations: $S_{ratio} = \frac{I_{trif.}}{I_{(trif. / other fungicide)}} \times \left[\left(\frac{S_{I_{(trif.)}}}{I_{(trif.)}} \right)^2 + \left(\frac{S_{I_{(trif. + other fungicide)}}}{I_{(trif. + other fungicide)}} \right)^2 \right]^{1/2}$

4.3.5

Application of method

The proposed method utilising SWV with the BDD was used to determine trifloxystrobin in water samples and in a commercial orange juice fermented with soy milk. The juice sample was chosen as trifloxystrobin is indicated to be used in

both citrus and soybean crops. The signals from the original samples were measured before they were fortified with the analyte at $7.0 \times 10^{-6} \text{ mol L}^{-1}$ (2.9 mg L^{-1}) to be quantified by analyte addition method.

In Table 4.3, the recovery results (authentic triplicates performed in two different days) are shown. Percent recoveries in water samples varied from 92.4% to 104.0%, which showed the good accuracy of the method. For orange juice samples, recoveries were in the 80% range, probably affected by the loss of analyte during SPE sample cleaning procedure. Despite this loss, the method can indicate the contamination of these samples. The accuracy in the analysis of the juice sample might be improved if analyte standard used in the analyte addition curve is also passed through the SPE cartridge to compensate the loss of analyte in the treated sample solution.

Table 4. 3. Recoveries for trifloxystrobin (n=3 in two different days) in analyte fortified samples ($7.0 \times 10^{-6} \text{ mol L}^{-1}$ or 2.9 mg L^{-1}).

Sample	Day	Recovered concentration	
		$\text{mol L}^{-1 \text{ a}}$ $\text{mg L}^{-1 \text{ b}}$	Percent recovery (%)
Queen Creek water	1	$(7.3 \pm 0.5) \times 10^{-6}$ 2.98 ± 0.2	104.0 ± 6.3
	2	$(7.0 \pm 0.1) \times 10^{-6}$ 2.86 ± 0.04	100.3 ± 0.7
Rodrigo de Freitas Lagoon water	1	$(6.8 \pm 0.4) \times 10^{-6}$ 2.78 ± 0.16	96.7 ± 6.6
	2	$(6.5 \pm 0.6) \times 10^{-6}$ 2.65 ± 0.25	93.1 ± 8.5
Mineral water	1	$(6.5 \pm 0.1) \times 10^{-6}$ 2.65 ± 0.04	92.43 ± 2.1
	2	$(6.8 \pm 0.8) \times 10^{-6}$ 2.78 ± 0.33	96.4 ± 11.5
Fermented soy orange juice	1	$(6.0 \pm 0.1) \times 10^{-6}$ 2.45 ± 0.04	85.9 ± 0.6
	2	$(5.7 \pm 0.2) \times 10^{-6}$ 2.04 ± 0.08	81.9 ± 2.9

^aThe recovered values in mol L^{-1} are associated with the standard deviations for n=3.

^bThe recovered values in mg L^{-1} are associated with their confidence intervals considering the standard deviation for n=3 and a confidence limit of 95%.

4.3.6

UV-induced trifloxystrobin degradation

The photodegradation of trifloxystrobin upon exposure to UV was evaluated by monitoring the SWV peak current at +1744 mV. The results showed a rapid degradation of trifloxystrobin upon the exposition to the UV light as only 15% of the analyte remains intact after only 5 min of exposition (Figure 4.7A).

The degradation profile indicated a second-order kinetics as the linear relationship ($R^2 = 0.987$) was found between the inverse of the determined concentration of trifloxystrobin ($1/[\text{trif}]_0$) and the UV exposition time (Figure 4.7B). The rate constant (k) was $3.7 \times 10^{-4} \text{ L mol}^{-1} \text{ min}^{-1}$ and the time of half-life ($t_{1/2}$) of 1.07 min. This second-order model of degradation indicated that after 20 min only about 1.3% of trifloxystrobin remained in its original form. For comparison purposes, Dornellas *et al.* [8] investigated the UV photoinduced degradation of pyraclostrobin, irradiating the pyraclostrobin solution (in ACN). The authors also observed a second-order kinetics of degradation but in a much slower reaction, with ($t_{1/2}$) of 9.8 min. Similarly, performing the experiment irradiating trifloxystrobin in solution ($1.0 \times 10^{-3} \text{ mol L}^{-1}$ in water/ACN 60%/40% v/v). In contrast to what was observed previously by irradiating the solid film of the fungicide, the photodegradation in solution was faster to the point that no voltammetric signal of the original analyte could be measured after 5 min of exposure (first point of the experiment).

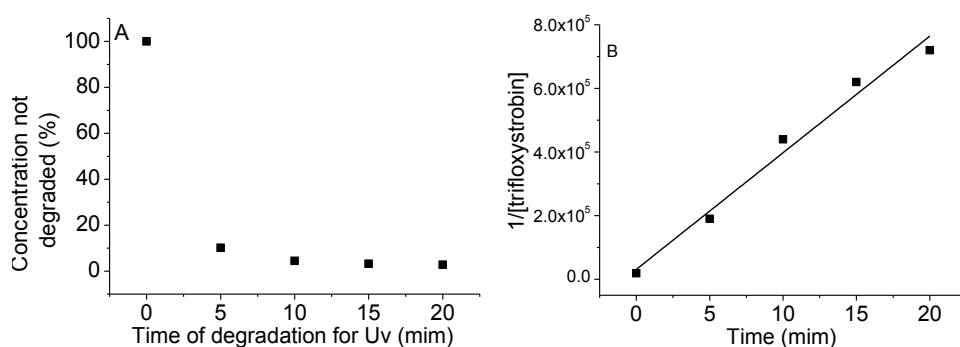


Figure 4.7. UV exposure of trifloxystrobin: (A) Analyte percent degradation in function of time; (B) The relationship between the inverse of the concentration of trifloxystrobin and time ($R^2 = 0.987$). Instrumental parameters of the analyte determination indicated in Table 1.

The solution containing the photodegraded trifloxystrobin was analysed by GC-MS. The chromatogram showed initially four peaks at retention times (RT) 14.68, 14.88, 15.66 and 15.86 min (circulated in Figure 4.8A). These peaks are characteristic of the four isomers (geometric ones) of the trifloxystrobin (EE, EZ, ZE, ZZ) as discussed by Banerjee *et al.* when investigating the exposition of a trifloxystrobin solution to the light from a xenon source [114]. In the mass

spectroscopic data, no matter the trifloxystrobin isomer, it were observed peaks at m/z 132, 145, 149 and 207 (Figure 4.8B), which are characteristics of the fragmentation mechanism of the original analyte [115]. Besides the four isomers, the chromatogram shows additional peaks, one at RT of 34.00 min and another at RT 52.07 min (Figure 4.8A).

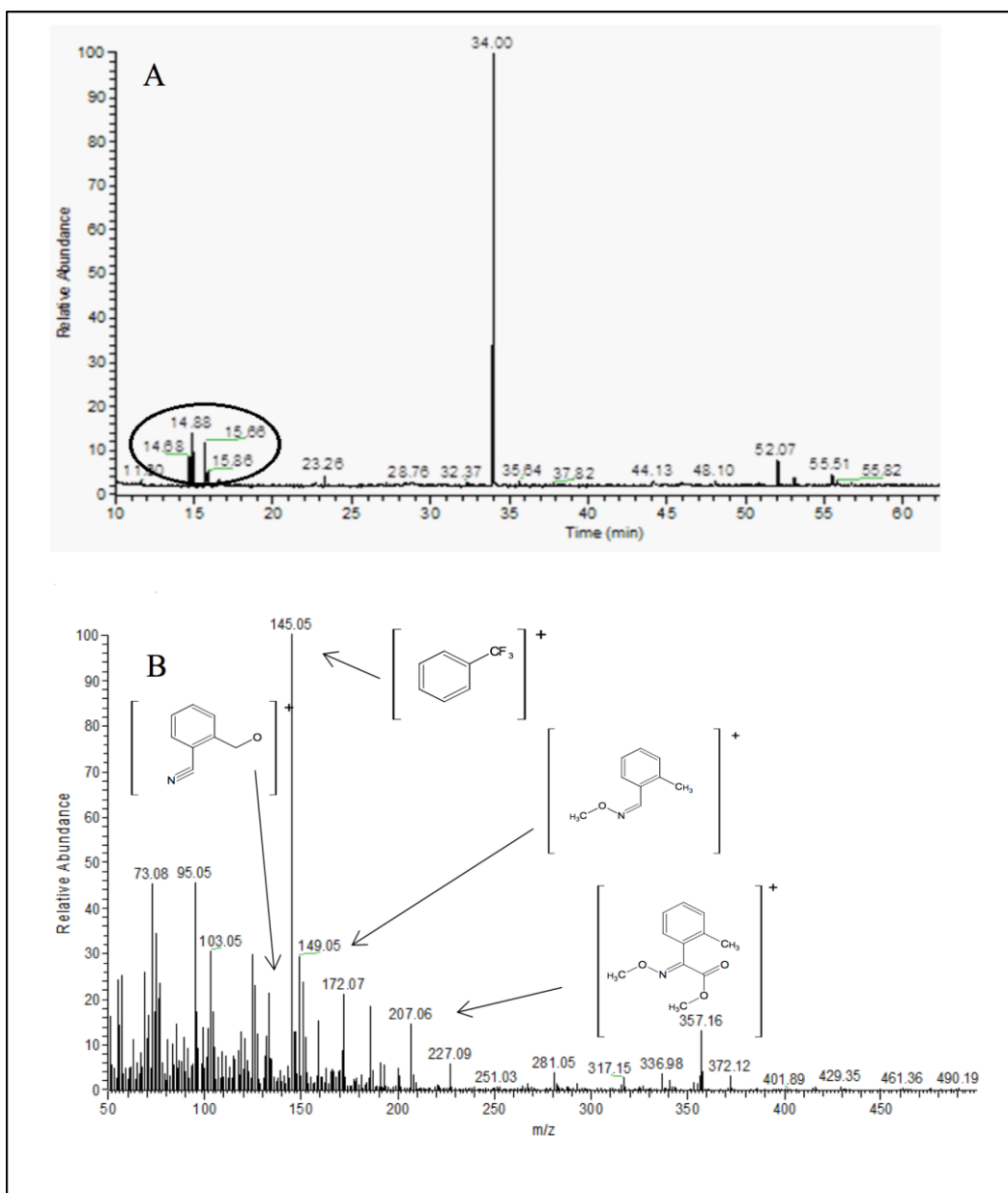


Figure 4.8. (A) GC chromatogram for the degraded solution trifloxystrobin. (B) Mass spectrum of one of the isomers of trifloxystrobin (RT = 14.64 min).

The mass spectrum of the chemical species with RT 34.00 min present a peak at m/z 207 whose fragments indicates one of the possible photodegradation

products of trifloxystrobin (Figure 4.9A). The structure of the other main possible photodegradation product of the original analyte can be predicted, as the mass spectrum of the peak at RT 52.07 min produce an intense fragment with m/z 173, compatible with the structure shown in the detail in (Figure 4.9B).

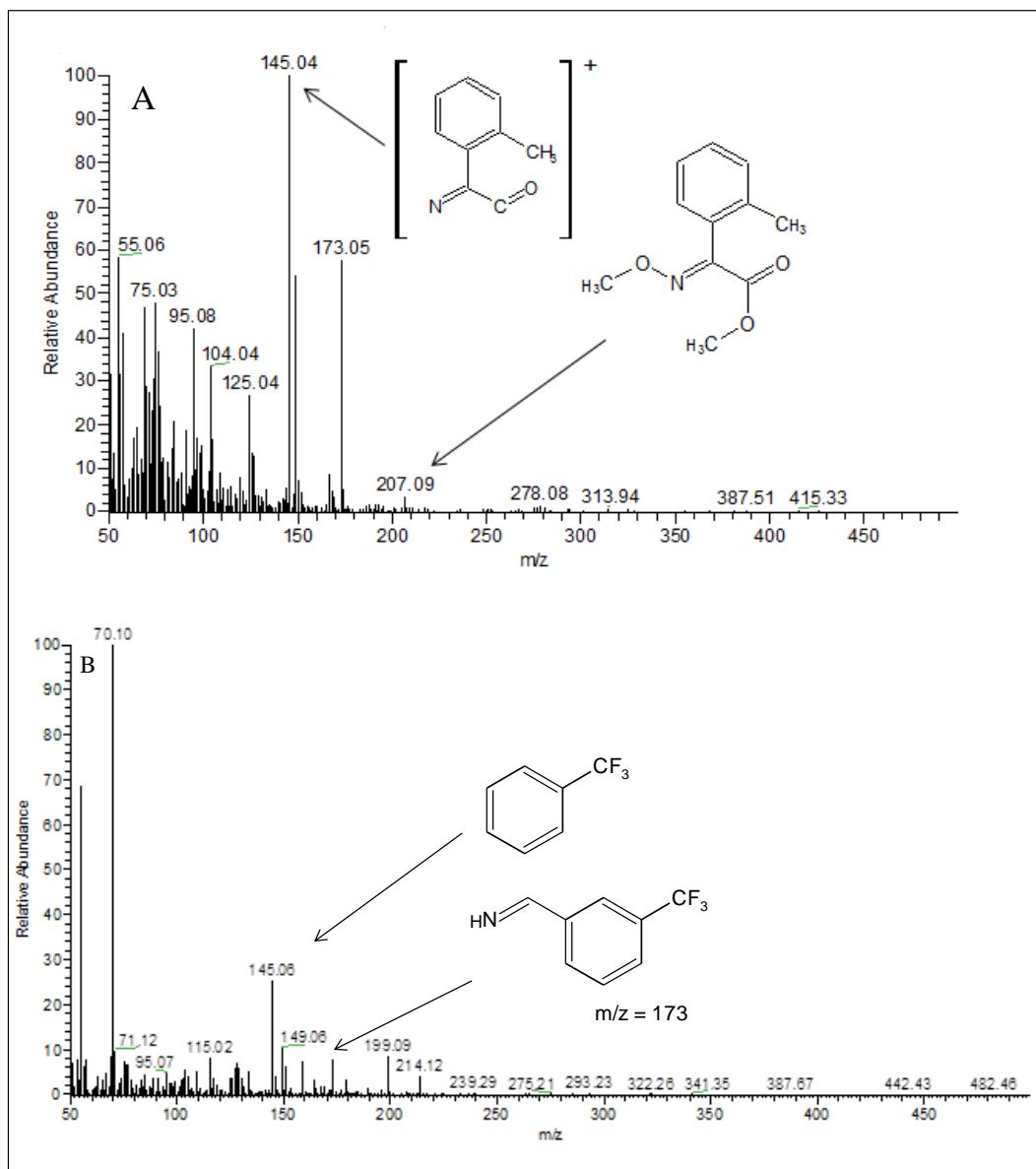


Figure 4.9. Mass spectrum for the product degradation corresponding to: (A) RT = 34.00 min and (B) RT = 52.07 min.

4.4. Partial conclusion

A simple and easy to use voltammetric method was developed for the quantification of trifloxystrobin. The choice of BDD was crucial to enable a measurable signal at a high oxidation potential. The method was sensitive enabling a LOD of $1.4 \times 10^{-7} \text{ mol L}^{-1}$ (0.058 mg L^{-1}) enough for the screening for trifloxystrobin in field applications. The procedure used to separate the analyte from orange juice sample can be also used to preconcentrate the analyte in the solid-phase extraction (C18) cartridge, improving at least 10 times the detection of analyte in the sample. Precision and accuracy achieved indicated the reliability of the voltammetric method. The method presents analytical characteristics that are competitive with other electroanalytical methods (used for the detection of strobilurins or for the separation of strobilurins before the detection of their natural absorbance) found in the literature (see Table 4.4) [8,9, 44,116-118]. The proposed method was used to establish the UV-degradation second-order kinetics for trifloxystrobin. Oxidation on the BDD occurred in two steps and a mechanism was proposed based on diagnostic experiments and literature data. The irreversible oxidation process suggests that the BDD can also be used to degrade trifloxystrobin in remediation procedures.

Table 4. 4. Some figures for electroanalytical methods for the determination of strobilurin and electrophoretic separation of strobilurins using absorbance measurement for detection

Sample	Analytes	Technique	Electrode or Detection	Range	LOD	LOQ	Ref
Potato / Grape	Dimoxystrobin Azoxystrobin	SW-ASV	HMDE ^a	0.016-0.26 mg L ⁻¹ 0.02-0.32 mg L ⁻¹	7.2×10^{-4} mg L ⁻¹ 3.6×10^{-4} mg L ⁻¹	2.4×10^{-3} mg L ⁻¹ 1.2×10^{-3} mg L ⁻¹	44
Urine / Water	Picoxystrobin	DP-ASV	BiFE	1.43 - 6.98 mg L ⁻¹	8.4×10^{-3} mg L ⁻¹	1.13×10^{-2} mg L ⁻¹	116
Grape juice	Kresoxim-methyl	SWV	BDD	0.27-11 mg L ⁻¹	0.09 mg L ⁻¹	0.27 mg L ⁻¹	7
Water / grape juice	Pyraclostrobin	SWV	BDD	1.5- 7.76 mg L ⁻¹	0.095 mg L ⁻¹	0.32 mg L ⁻¹	8
Water	Dimoxystrobin	BIA ^b	BDD	330 - 19800 mg L ⁻¹	1.24×10^{-4} mg L ⁻¹	4.09×10^{-4} mg L ⁻¹	9
Urine	Picoxystrobin Pyraclostrobin	MEKC ^{c,d}	Absorption photometry (220 nm)	0.032 - 1.84 mg L ⁻¹ 0.052 - 1.94 mg L ⁻¹	9.6×10^{-3} mg L ⁻¹ 7.0×10^{-3} mg L ⁻¹	3.2×10^{-2} mg L ⁻¹ 2.1×10^{-2} mg L ⁻¹	117
Fruits and Vegetables	Azoxystrobin Kresoxim-methyl Pyraclostrobin	MEKC ^{c,d}	Absorption photometry (220 nm)	0.01 - 5 mg L ⁻¹	2.0×10^{-3} mg kg ⁻¹ 1.0×10^{-3} mg kg ⁻¹ 2.0×10^{-3} mg kg ⁻¹	- - -	118

^aHMDE: Hanging mercury drop electrode; ^bBIA: Batch-injection amperometry; ^cMEKC: Micelar electrokinetic chromatography; ^dWith analite concentration in capillary.

5

Kanamycin-template imprinted polymer based solid-phase extraction and batch-analysis amperometry for gentamicin sulfate determination

Manuscript submitted as: “*Determination of gentamicin sulfate by batch-injection amperometry after solid-phase extraction using a kanamycin-template molecularly imprinted polymer*” to Sensors and Actuators B.

5.1

Introdução

Gentamycins are complex aminoglycoside (AMG) antibiotics consisting of three major components, called gentamicin sulfate C_1 , C_{1A} and C_2 (Figure 5.1) [119] and a number of minor components, such as sisomicin, gentamicin C_{2b} (also known as sagamycin) and dihydroxy gentamicin C_{2a} , which is a precursor of the gentamicins C_{2a} , C_2 and C_1 . It was first isolated from two species of bacteria that belong to the genus *Micromonospora* [120] and has been used to deal with infections caused by *P. aeruginosa* and *Enterobacteriaceae* and, when combined with other antibiotics, to treat endocarditis, brucellosis, otitis and dermatitis [121]. In veterinary use, it is administered to treat mastitis in dairy cattle, contaminateing milk and making it unavailable for consumption up to ten days after administration [122]. Gentamycins are marketed as sulfate in order to ensure its solubility in aqueous medium. The choice of sulfate as stabilizing counter-ions is due to the small difference between the pK_a of the sulfate and the cations of gentamycins, which contribute to the stability of the drug [123].

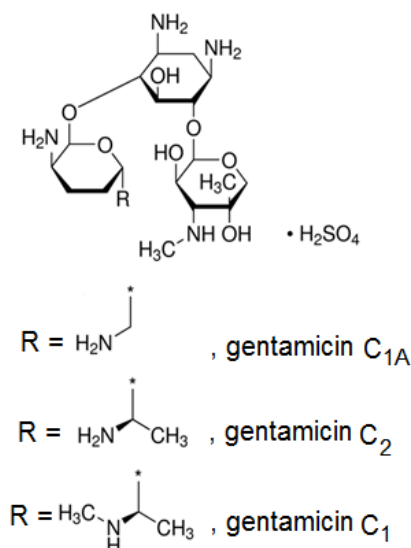


Figure 5.1. Structures of gentamicin sulfate $\text{C}_{1\text{A}}$, C_2 and C_1 .

Gentamycins lack strong chromophores but despite that it was determined, with a poor LOD of 2 mg mL^{-1} , by molecular absorption photometry (at 195) nm after separating the different gentamycins by capillary zone electrophoresis [122,124]. Electrophoretic separation of the gentamycins, using cyclodextrin as pseudostationary phase, was also made by optical absorciometry (LOD down to $0.13 \text{ } \mu\text{g mL}^{-1}$ at 330 nm) after chemical derivatization with OPA [125]. HPLC was employed to determine the different gentamycins, using absorciometric detection, after chemical derivatization with 1-fluoro-2,4-dinitrobenzene at 365 nm (LOD of $0.07 \text{ } \mu\text{g mL}^{-1}$) and applied to analyze human plasma and urine [126,127]. HPLC with absorciometric detection of gentamicin (mixture of gentamycins) as sulfate, after extraction of the analyte from milk and calf tissue samples, was mad by derivatizing the analyte with OPA (LOD down to $0.6 \text{ } \mu\text{g mL}^{-1}$) [128]. Gentamycins, derivatized with OPA, has been also detected by fluorescence (340/440 nm) in HPLC analysis (LOD down to 25 ng g^{-1}) [129]. HPLC coupled to mass spectrometry (MS) was used (electrospray ionization MS, electrospray ion trap MS, and electrospray-tandem MS, among others) [130-138]. Determinations, after different sample treatments, were made in muscle and kidney tissues, in milk, in pharmaceuticals, biological samples and in hospital residues. LOD values varying from 12.8 mg mL^{-1} (milk) [132] to 0.5 ng g^{-1} , (biological tissues) [130] have been achieved.

Gentamycins have also been determined by colorimetry or by fluorimetry after chemical derivatization of the analyte previously extracted from samples, for instance using SPE [139]. The colorimetric determination after derivatization either with 1-fluoro-2,4-dinitrobenzene (at 415 nm) [140] or after reaction with ninhydrin (at 400 nm) [141] enabled the determination of concentrations as low as 50 ng mL⁻¹ [140]. The indirect determination of gentamycins (LOD of 5.1 ng mL⁻¹) was made after its oxidation in a mixture of KMnO₄/H₂SO₄, then measuring signal from indigocarmine (at 610 nm) that has the absorbance affected by the unreacted oxidant agent [142]. The fluorimetric determination of gentamycins (465/530 nm) was made after derivation with 4-chloro-7-nitrobenzo-2-oxa-1,3-diazole with a narrow linear response range (from 0.11 µg mL⁻¹ to 4.2 µg mL⁻¹) [143]. The determination of these AMG was also achieved after formation of gentamycins-safranin charge transfer complex that fluorescence at 521/545 nm (LOD of 1.2 pg mL⁻¹). Another approach was based on the energy transfer from gentamicin to Eu³⁺ (fluorescence measured at the 616 nm Eu³⁺ line) leading to concentration measurement at 10 µg mL⁻¹ [144,145].

The need for cumbersome chemical derivatization or formation of complexes to enable either direct or indirect the optical detection of gentamycins can be avoided by measuring the analyte-induced quenching of the chemiluminescence from the reaction between luminol and hypochlorite, in alkaline medium [146]. A multicommutation system as used to automatize analysis achieving LOD of 0.023 µg mL⁻¹. Indirect determination of gentamycins were also made by using gold nanoparticles (AuNPs) and silver nanoparticles as probes. Gold and silver nanostructures, under the influence of electromagnetic radiation, generate oscillating dipoles that give rise to localized surface plasmon resonance (LSPR), which show remarkable changes when nanoparticles interact with other chemical species, in most cases leading to the decrease of the original SPR spectral bands and/or generating a new band, encompassing a red shift and broadening, caused by changes in plasmon as nanoparticles agglomerate [147,148].

The use of lipoic acid capped Eu/AuNPs was proposed based on the luminescence static quenching attributed to the binding of the amino group of gentamicin sulfate to the carboxylic group of the lipoic acid, leading to LOD of 91 ng mL⁻¹ [149]. The method was applied to pharmaceuticals and milk but no

information was given on how selectively was achieved. Wang *et al.* synthesized Ag-coated AuNPs and used as photoluminescent probes to determine gentamicin sulfate (LOD of 0.10 mg L^{-1}) in blood plasma (recovery of about 80%) [150]. Gentamicin sulfate was selective determined using optical properties of Au nanotubes, stabilized in ovalbumin and cetyltrimethylammonium bromide, leading to LOD of 0.05 ng mL^{-1} [151].

Spherical AuNPs and or gold nanorods were employed to enable the practical and reliable quantification of gentamicin in veterinary pharmaceutical formulations, leading to detection of gentamicin sulfate at concentrations down to 0.4 ng mL^{-1} [152]. A similar approach was used by Wang *et al.* to determine gentamicins as sulfate down to 3 ng mL^{-1} in pharmaceutical formulations and in milk, despite the fact that the procedure used to clean-up the sample probably did not eliminate potential interferents that deflagrate the agglomeration of AuNPs [153]. Aqueous dispersions of silver nanoparticles was used to detect gentamicin sulfate (at concentrations as low as 20 ng mL^{-1}) by monitoring the color changing of the dispersions, due to the decreasing of the LSPR spectral band at 400 nm [148].

The use of electrochemical detection of the gentamycins have been used with a gold working electrode in HPLC systems using either a C18 column or column charged with polystyrene-divinylbenzene [154]. Despite the general tendency of gold electrodes to passivate, the absolute LOD of 20 ng was reported in the analysis of pharmaceuticals. Five different selective ion electrodes made with modified polyvinyl chloride were recently for the potentiometric determination of gentamicin in pharmaceuticals and in biological fluids. The most sensitive electrode enabled LOD of 0.48 mg L^{-1} with good reproducibility and selectivity [155].

BIA has been used with BDD as the amperometric sensor operating at elevated positive potentials [9]. In such conditions, selectivity in the oxidation process of the analyte is not selective as other chemical species may be electrochemically degraded in such conditions. A previous SPE procedure improves selectivity as interferences are separated from the analyte. However, classical sorbents present selectivity based on general parameters such as polarity or charge, thus losing space for the more selective MIP, which are synthetic materials produced in the presence of template (target analyte or similar). After

removal of template, the empty sites tend to have a high analyte recognition ability due to size and conformation based compatibility [156-158]. MIP as sorbent for SPE has been also presented resistance to strongly acid and basic media and compatibility with various types of organic solvents, besides the ability to pre-concentrate analytes [159,160].

Very recently, Moreno-Gonzalez *et al.* used HPLC coupled with mass spectrometry for the determination of eleven AMG (LOD value for gentamicin sulfate of 1.3 -14.7 $\mu\text{g kg}^{-1}$) in different types of milk after SPE using a commercial molecular imprinted polymer (SupeIMIP[®] SPE - AMG) [158]. The commercial MIP promoted a sample clean-up so that matrix effect accounted to less than 15% in recovery. Khan *et al.* developed a photoluminescent probe constituted by CdTe quantum dots modified with thioglycolic acid for the determination of kanamycin sulfate. Selectivity was achieved by SPE using a synthesized MIP (using kanamycin sulfate as template), which promoted successful sample (milk and yellow fever vaccine) clean-up, quantitative recoveries [83] and LOQ of 8.1 ng mL^{-1} .

In this chapter, the amperometric determination of gentamicin sulfate components was made using a BIA system with a BDD electrode, aiming high sensitivity, ultra-trace detection capability and high analytical frequency. Laboratory-made SPE cartridges containing kanamycin-MIP were used to promote sample clean-up, ensuring selectivity for the amperometric detection. The synthesized kanamycin-MIP was characterized and its retention capability studied.

5.3

Results

5.3.1 Preliminary studies

5.3.2

Electrochemical qualitative study

A qualitative study, using CV, was made to evaluate the electrochemical behavior of gentamicin sulfate on the BDD using acetate buffer (0.2 mol L^{-1}) at pH 4.0. Under such conditions, it is expected that gentamicin sulfate is

predominantly protonated since it presents primary and secondary amines in their chemical structure and pK_a values in the 6.2-9.9 range [79]. A peak oxidation (anodic scan) appeared at around +2000 mV after addition of gentamicin sulfate (338 mg L^{-1} cell concentration) with no counterpart reduction peak when scan was reversed to the cathodic direction (Figure 5.2A). A sequence of cyclic scans (Figure 5.2B), under no forced convection transport, indicated the continuous decreasing of the gentamicin peak until no oxidation peak was observed after the 20th cycle, which indicated the irreversibility of the process.

The study of the peak intensity (I_p) in function of the square root of scan velocity (\sqrt{v}), as seen in (Figure 5.2C), present a tendency to linear relationship ($R^2 = 0.928$), indicating a probable irreversibility of the charge transfer process and mass transfer controlled by diffusion. The linear relationship ($R^2 = 0.984$) between I_p and the frequency (f) applied in square-wave voltammetry (SWV) confirmed irreversibility of the process (Figure 5.2D).

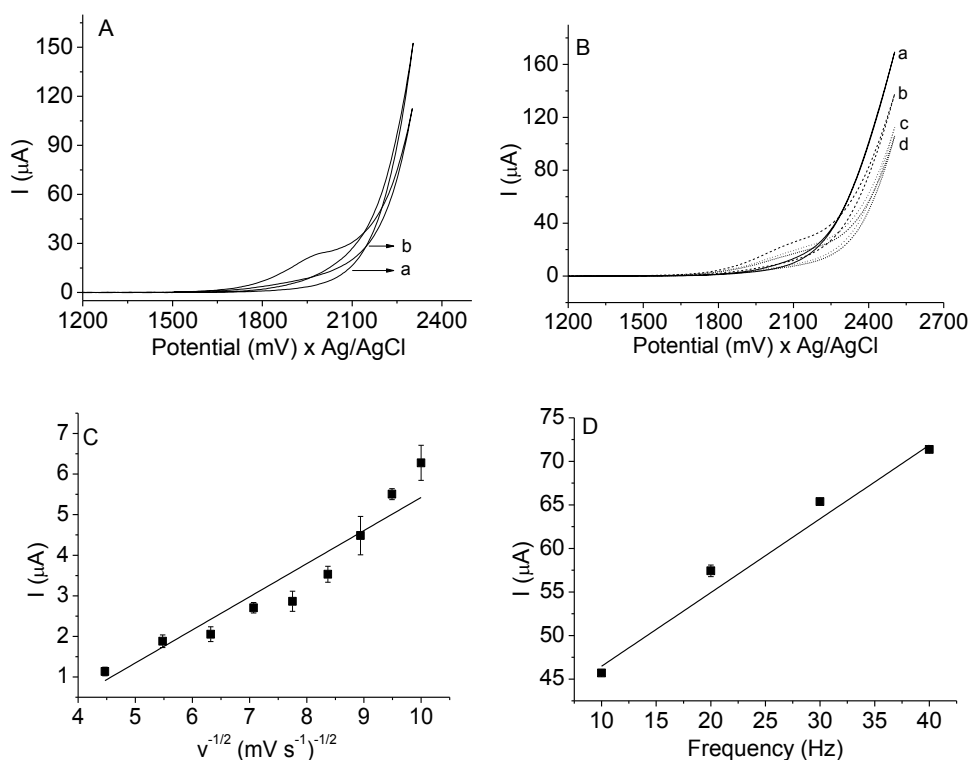


Figure 5.2. (A) Gentamicin sulfate cyclic voltammetry on BDD electrode: (a) supporting electrolyte and (b) gentamicin sulfate. (B) Sequence of cyclic voltammograms (1200 to 2100 mV) under no forced convective transport: (a) supporting electrolyte; (b) 1st cycle; (c) 20th cycle and (d) 40th cycle. (C) Square root of scan rate (\sqrt{v}) in function of analyte peak current (I_p). (D) Analyte peak current measured by SWV in function of applied frequency (f). Experimental conditions: Electrolyte support: acetate buffer (0.2 mol L^{-1} ,

pH 4.0). SWV parameters: amplitude = 40 mV; frequency = 30 Hz; step potential = 2 mV; Cyclic voltammetry parameters: $\nu = 100 \text{ mV s}^{-1}$; amplitude = 40 mV; gentamicin sulfate (338 mg L^{-1}).

5.2

Optimization of parameters for measurements using batch injection amperometry

The SWV measurement, at acidic conditions (from 3.5 to 6.0), using the BDD working electrode, produced a single oxidation peak for gentamicin sulfate with maximum at around +2000 mV (see Figure 5.3A for the voltammogram at pH 4.0). Based on this response, a systematic pulse amperometry experiment was made to evaluate both the best potential and pH used to promote the most effective oxidation of gentamicin sulfate leading to the most intense amperometric response. For this study, acetate buffer solution 0.01 mol L^{-1} (in the pH range between 3.8 and 5.4) was used because of the more stable amperograms. The hydrodynamic voltammograms were achieved in the potential range between +1400 to +2200 mV (Figure 5.3B) in the BIA system by introducing $80 \mu\text{L}$ of a gentamicin sulfate solution (5.1 mg L^{-1}) measured in triplicate. It was observed that larger current signals were obtained at pH 4.4 at applied potentials of +2200 mV. The background signal was also monitored by introducing blank aliquots onto the electrode. It was found a small current that increased as the applied potential was increased. Therefore, the potential chosen to detect gentamicin sulfate was +2000 mV instead of the +2200 mV.

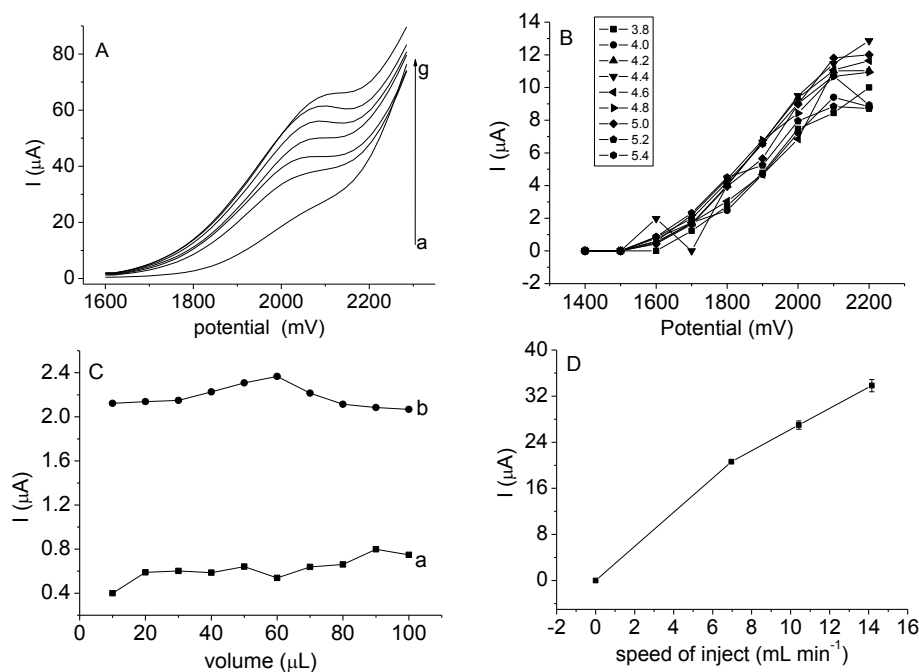


Figure 5.3. (A) Gentamicin sulfate SWV voltammograms in acetate buffer 0.01 in the pH 4.0; a-blank, (b-g) 56.4 - 338.1 mg L^{-1} in the range additions. (B) Gentamicin sulfate hydrodynamic voltammograms in acetate buffer 0.01 mol L^{-1} in the pH range from 3.8 to 5.4 obtained from the peak current as a function of the applied potential pulses (1400 - 2200 mV). Stirring speed: 600 rpm; injection volume: 80 μL gentamicin sulfate 5.07 mg L^{-1} . (C) The effect of sample volume on the peak current for gentamicin (from 10 to 100 μL): (a) Blank and (b) Gentamicin sulfate 9.0×10^{-8} mmol. (D) Effect of variation in the injection rate of the peak current. Supporting electrolyte: acetate buffer 0.01 mol L^{-1} pH = 4.4 and work potential 2000 mV.

The need to maintain the stirring of the electrolyte solution during the BIA analysis was evaluated using five replicates. Under no stirring, a steady decrease in peak current after successive injections was observed. This result indicated the adsorption of the analyte (or of its oxidation products) on the surface of BDD electrode, thereby reducing the contact surface for the analyte oxidation in subsequent additions. It was observed that signal stability and good repeatability were achieved under stirring no matter the applied rate (from 100 to 900 rpm) since analyte and oxidation products were efficiently removed (fast convective removal forcing the infinite dilution) from the proximity of the electrode surface before the next addition. All analyzes were performed at 600 rpm because of the better current peak profile achieved from this velocity on. The sample introduction speed (adjusted in the electronic micropipette) was also studied. As the tested injected volumes (Figure 5.3C) increased from 10 to 100 μL the concentration of the injected standard was decreased in order to get a fixed

quantity of gentamicin sulfate of 9.0×10^{-8} mmol. It was found that the peak current increased with the increase in the gentamicin injection volume up until 60 μL . It was also observed that, in terms of signal intensity, the response obtained with the other volumes evaluated remains practically constant, reflecting some robustness for this parameter.

The study of injection of sample (60 μL volume) was conducted using the electronic micropipette with variable injection volume rates adjusted to four different values from 7 to 14 mL min^{-1} (Figure 5.3D). The maximum sample volume introduction rate was chosen as it enabled the most intense measured current and the sharpest time profile (in the base of the profile) as the sampling rate was increased allowing better reproducibility to measure peak height as the analytical signal. The experimental parameters chosen for for the determination of gentamicin sulfate by BIA-amperometry are described in Table 5.1.

Table 5.1. BIA-amperometry chosen experimental conditions to determine gentamicin.

Parameter	Value
Supporting electrolyte	Acetate buffer 0.01 mol L^{-1} pH 4.4
Work potential	2000 mV
Agitation speed	600 rpm
Sample introduction rate	14 mL min^{-1}
Injection volume	60 μL

5.3

Analytical determination of gentamicin sulfate and figures of merit for the BIA-amperometric method

The diagram in Figure 5.4A indicates alternate samplings (triplicate) of gentamicin sulfate standard solutions at two concentrations (2.8 mg L^{-1} and 11.3 mg L^{-1}) and there were no residual effects on the subsequent signal measurement arising from memory effect of previous analyte introduction. The amperometric responses (Figure 5.4B) obtained under the chosen conditions (for increasing analyte concentrations) and the respective analytical curve (Figure 5.4C) are also shown. The analytical response, showing signal saturation and loss of linearity, is

shown in Figure 5.4D. A linear response was observed with analyte curve equation of $(6.2 \times 10^{-1} \pm 2.9 \times 10^{-2} \text{ mg L}^{-1} \mu\text{A}) X + (1.6 \times 10^{-6} \pm 3.3 \times 10^{-7})$ and the analytical frequency was estimated in 90 sample introductions per hour. The instrumental LOD of 0.5 mg L^{-1} ($8.1 \times 10^{-7} \text{ mol L}^{-1}$) and the instrumental LOQ of 1.5 mg L^{-1} ($2.7 \times 10^{-6} \text{ mol L}^{-1}$) were calculated using respectively $3s_b/m$ and $10s_b/m$, where s_b is the standard deviation of ten consecutive signal measurements of the lowest analyte concentration in the analytical addition curve and m is the sensitivity of this curve.

The precision of the method was evaluated as the instrumental precision by varying ten consecutive measurements of the signal produced by the analyte standard at two different concentration levels. At 2.8 mg L^{-1} ($5.0 \times 10^{-6} \text{ mol L}^{-1}$) the precision was 3.0% and at 11.3 mg L^{-1} ($2.0 \times 10^{-5} \text{ mol L}^{-1}$) was 2.3%. 3.0% in the level of concentration $5.0 \times 10^{-6} \text{ mol L}^{-1}$ (2.8 mg L^{-1}), decreasing to about 2.3% in the concentration level of $2.0 \times 10^{-5} \text{ mol L}^{-1}$ (11.3 mg L^{-1}).

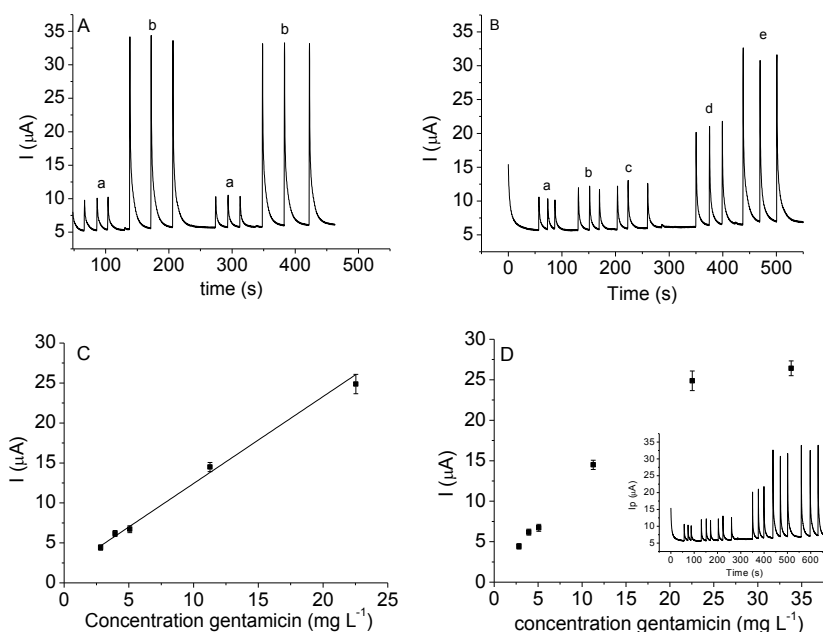


Figure 5.4. (A) Successive sample introductions of a solution containing (a) 2.8 mg L^{-1} and (b) 11.3 mg L^{-1} of gentamicin sulfate. Electrolyte: 0.01 mol L^{-1} acetate buffer solution pH 4.40; injected volume: $60 \mu\text{L}$; stirring rate: 600 rpm . (B) Response BIA-amperometry system with BDD electrode for injections in triplicate (a) 2.8 ; (b) 3.9 ; (c) 5.1 ; (d) 11.3 , and (e) 22.5 mg L^{-1} solution of gentamycin standard. (C) Analytical curve with equation of $Y = (1.1 \times 10^{-6} \pm 5.1 \times 10^{-8} \text{ mg L}^{-1} \mu\text{A}) X + (1.6 \times 10^{-6} \pm 3.3 \times 10^{-7})$ and $R^2 = 0.988$ for increasing concentrations of gentamicin. (D) Analytical responses for gentamicin showing signal saturation. Instrumental parameters: see Table 1.

5.4

Interference study

5.4.1

Substances commonly found in gentamicin veterinary formulations

A study to evaluate interferences imposed from organic and inorganic substances commonly found in gentamicin sulfate veterinary formulations was made. Interference was measured as the $I_{\text{analyte}}/I_{(\text{analyte}+\text{interferent})}$ values, which is the ratio between the signal obtained from a solution containing only the analyte and the signal measured from a solution containing the mixture of the analyte and one potential interferent. The analyte concentration was kept the same for both solutions (5.1 mg L^{-1} or $9 \times 10^{-6} \text{ mol L}^{-1}$). Ratio values close to 1 indicated interference imposed by the tested substance while ratio values smaller than 1 indicated that the tested substance also reacted under the influence of the applied potential on the surface of the BDD electrode, producing a measurable current. Tests were made using various analyte/potential interferent molar ratios: 1/1; 1/0.5; 1/0.1; 1/0.05; 1/0.01 and 1/0.005. Measurements were made in triplicate and the calculations were based on peak current.

Di-sodium EDTA interfered only in the 1/1 proportion, increasing the intensity of the measured signal. Sodium metabisulfite imposed interference at all of the ratios studied. Methylparaben did not caused interference in the gentamicin sulfate signal while propylparaben increased the measured signal at the 1/1 proportion. In contrast, the presence of bromhexine hydrochloride, at all of the tested proportions, produced $I_{\text{analyte}}/I_{(\text{analyte}+\text{interferent})}$ values above unity, indicating that this substance interfered decreasing measured signals perhaps by adsorbing onto the surface of the electrode affecting the interaction of the analyte with the BDD.

5.4.2

Solid-phase extraction studies using the cartridge packed with the aminoglycoside-selective molecularly imprinted polymer

The interference from some of the substances tested and from the complex matrix can only be minimized by separating gentamicin sulfate from samples, which can be made in an efficient, rapid and costly effective way using SPE. The initial test was made to evaluate the efficiency of the kanamycin-MIP based

cartridge in retaining gentamicin sulfate and to select conditions to elute the retained analyte after clean-up. In order to do that, the kanamycin-MIP was compared to the non-imprinted polymer (NIP) using syringe barrels packed with 70.0 mg of either polymer. These cartridges were loaded with 40 μL of a 225.4 mg L^{-1} gentamicin sulfate standard (absolute amount of 9 ng). The cartridge was then washed with 10 aliquots of 1 mL of ultrapure water (using a flow system to semi-automatize the SPE procedure) before final elution was made using HCl aqueous solution ($1.0 \times 10^{-3} \text{ mol L}^{-1}$) as in acidic conditions gentamicin is protonated, disfavoring its interaction with the polymer. The signal measurements made by BIA-amperometry of the eluted solution showed that the percent recovery of the gentamicin loaded into the SPE cartridge was 95.8% while the one achieved using NIP was only 9.7%, showing the capability of the kanamycin-MIP for selective retention. In order to select more appropriate elution conditions to compatibilize the sample extract with the conditions adjusted for the BIA-amperometric determination, the experiment was made again by replacing the hydrochloride acid solution to acetate buffer (0.01 mol L^{-1} ; pH 3.5), which is the electrolyte support for the developed amperometric method. The experimental recovery results indicated a similar efficiency of elution. Therefore, the analyte elution was made using acetate buffer.

Similar SPE (with kanamycin-MIP solid phase) tests were made with three other aminoglycosides (kanamycin, neomycin and streptomycin) besides one macrolide (erythromycin). The recovery results (after elution of the retained substances with acetate buffer) for all of them were similar to those obtained with gentamicin: kanamycin (97.3%), neomycin (91.2%), streptomycin (91.5%), all of them in the form of salt, and erythromycin (90.5%) as neutral molecule. Such retention efficiency is probably due to the similarity of the tested substances with the chemical structure (the same in the case of kanamycin) proving the possibility to use the kanamycin-MIP for the determination of aminoglycoside and macrolide antibiotics.

A study was made to evaluate the MIP retaining capacity for the same substances tested as potential interferents in the BIA-amperometric analysis. The excipients evaluated were anhydrous disodium EDTA, sodium metabisulfite, methylparaben and propylparaben. They were tested at an equivalent amount of gentamicin (225.4 mg L^{-1}). Differently from that with gentamicin sulfate, these

four excipients were readily eluted from the kanamycin-MIP during the washing step with water, because they do not have any structural similarity with the polymer template. Therefore, these substances are not efficiently retained in the solid phase. Results showed that the SPE with kanamycin-MIP is efficient to separate interferences commonly found in pharmaceutical formulations enabling the selective determination of gentamicin sulfate.

The saturation capacity of the kanamycin-MIP SPE cartridge (packed with 70 mg of the polymer) was performed in order to find the maximum quantity of gentamicin sulfate the cartridge may hold. A solution of gentamicin (225.4 mg L^{-1} or $4.0 \times 10^{-4} \text{ mol L}^{-1}$) was passed through the cartridge in a continuous way (1 mL min^{-1}) using the flow system. Aliquots of 1 mL of the solution passing through the cartridge were collected and stored. From each of these aliquots, 60 μL was collected and diluted with acetate buffer (0.01 mol L^{-1} ; pH 3.5) to form a 1 mL solution to be monitored using the BIA-amperometric method. Initially no signal characteristic of the presence of gentamicin was observed (only the signal characteristic of the blank), indicating that the analyte was being properly retained in the cartridge. As the collected volume increased (Figure 5.5) the signal sharply increased only after the eighth aliquot of the eluted solution, suggesting that the retention of the analyte in the polymer was no longer effective, because all the cavities of the polymer were saturated with the analyte and the excess analyte could no longer interact with the printed polymer.

As the amount of analyte, in mol, increased, the efficiency in the analyte retention is reduced because the excess of analyte cannot interact with the already filled template cavities in the polymer. Therefore, for 70 mg of polymer, the loading analyte limit was 3.2 μmol .

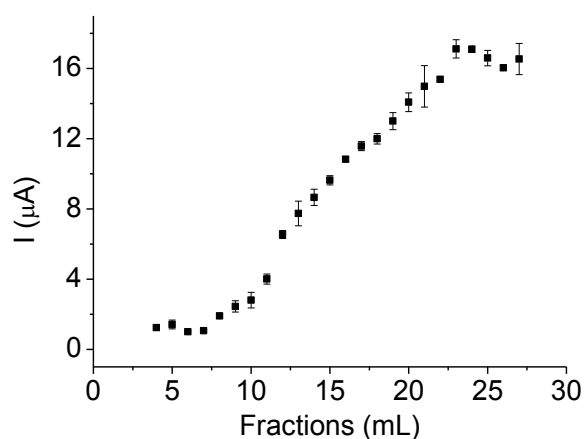


Figure 5.5. Study of the saturation capacity (225.4 mg L^{-1} or $4.0 \times 10^{-4} \text{ mol L}^{-1}$) of the SPE cartridge packed with kanamycin-MIP in the retention of gentamicin sulfate. Fractions of 1 mL analyzed in the BIA-amperometry system.

5.5

Application of the BIA-amperometric method

The determination of gentamicin sulfate was performed in pharmaceutical formulations (for veterinary use) using the BIA-amperometric method after SPE using a cartridge packed with the kanamycin-MIP. A control sample, prepared, at concentration level of 6.9 mg L^{-1} of the gentamicin sulfate standard in water, was also analyzed. The goal of this control sample was to evaluate the recovery, taking into consideration the total gentamicin signal (gentamycins C_1 , C_{1a} or C_2) in the standard. For pharmaceutical formulation, such information on the relative proportions for each type of gentamicin is not available.

The recovery achieved for the control sample was adequate, providing an experimental result close to the expected value for the fortification. For the pharmaceutical formulations, recoveries tended to be about 12 to 15% higher than the values expected, based on the information given in formulations instructions. These results may indicate some interference imposed by a matrix component that eventually could have been eluted along with the analyte during SPE. However, it is possible that the concentration of gentamicin sulfate in these samples were slightly higher than the expected values as it is common in commercial samples that must necessarily provide a minimum content of active principle to be

approved in quality control assays. In Table 5.2 the results for the determination of gentamicin sulfate are presented.

Table 5.2. Recoveries for the gentamicin sulfate determination in simulated samples and in pharmaceutical formulation using BIA-amperometry (n = 3).

Samples	Expected concentration (mg L ⁻¹)	Found concentration (mg L ⁻¹)	Recovery (%)
Simulated sample	16.9	17.6 ± 0.31	104.1 ± 1.8
Pharmaceutical formulation A	4.4 × 10 ⁴ ^a	4.95 ± 0.08 (× 10 ⁴)	112.5 ± 1.9
Pharmaceutical formulation B	4.0 × 10 ⁴ ^a	4.46 ± 0.12 (× 10 ⁴)	115.1 ± 1.5
Pharmaceutical formulation C	8.0 × 10 ⁴ ^a	9.07 ± 0.12 (× 10 ⁴)	113.4 ± 1.6

^a According to the label of the pharmaceutical formulation.

In order to evaluate the systematic higher result obtained for the veterinary formulations, these three pharmaceutical samples were also analyzed by HPLC with molecular absorption detection. The results obtained (three authentic samples prepared in three replicates) are shown in Table 5.3. When compared to the results obtained with the proposed BIA-amperometric method, using a comparative statistical test (two-tailed *t*-student test), no significant difference between the results achieved was found by using the proposed and the comparative chromatographic method ($t_{\text{experimental}} = 1.9$ for formulation A, $t_{\text{experimental}} = 1.1$ for formulation B and $t_{\text{experimental}} = 1.1$ for formulation C with $t_{\text{critical}} = 2.2$, with a confidence limit of 95% for $n_1 = n_2 = 3$). The experimental results for the pharmaceutical formulations were also compared using analysis of variance (single-factor ANOVA with 95% confidence level and $n_1 = n_2 = 3$). These two sets of samples were similar as $F_{\text{experimental}} < F_{\text{critical}}$ ($F_{\text{experimental}} = 3.70$ and $F_{\text{critical}} = 5.00$).

Table 5.3. Comparative results for gentamicin sulfate determination in pharmaceutical formulation samples using the proposed method and the one based on the use of HPLC.

Samples	Concentration found using BIA-amperometry method (mg L ⁻¹)	Concentration found using HPLC method (mg L ⁻¹)
Pharmaceutical formulation A	4.95 ± 0.08 (× 10 ⁴)	4.78 ± 0.07 (× 10 ⁴)
Pharmaceutical formulation B	4.46 ± 0.12 (× 10 ⁴)	4.52 ± 0.10 (× 10 ⁴)
Pharmaceutical formulation C	9.07 ± 0.12 (× 10 ⁴)	9.10 ± 0.09 (× 10 ⁴)

5.6

Partial conclusion

Gentamicin sulfate was successfully determined in the mg L⁻¹ range in pharmaceutical formulations ensuring selectivity by using SPE using a kanamycin-MIP solid packed cartridge, selective for the aminoglycoside antibiotics. The quantification was made using a simple BIA-amperometric method leading to LOD and LOQ values of respectively 0.5 mg L⁻¹ (8.1×10^{-7} mol L⁻¹) and 1.5 mg L⁻¹ (2.7×10^{-6} mol L⁻¹). Recoveries in samples were up to 15% higher than the ones expected, according to the pharmaceutical formulation instructions, but comparison with results achieved using HPLC with molecular absorption detection showed that the formulations actually presented an excess of drug, thus indicating that the proposed method produced an accurate result. BIA-amperometry allowed a high frequency in analysis using a relatively simple and robust instrumentation and a simple experimental procedure.

6

Voltammetric determination of lapachol in the presence of lapachones and in ethanolic extract of *Tabebuia impetiginosa* using an epoxygraphite composite electrode

Manuscript published as: “*Voltammetric determination of lapachol in the presence of lapachones and in ethanolic extract of Tabebuia impetiginosa using an epoxy-graphite composite electrode*” Almeida JMS, Balbin-Tamayo AI, Toloza CAT, Figueira IDO, Pérez-Gramatges A, da Silva AR, Aucélio RQ. *Microchem. J.*, 2017, 133, 629-637. DOI: 10.1016/j.microc.2017.04.036.

6.1

Introduction

The tropical flora is an abundant source of different classes of bioactive substances, among them naphthoquinones, which are commonly found in the *Bignoniaceae* family of plants [161]. Lapachol (Figure 6.1) is a *para*-naphthoquinone that presents many biologic activities against different bacteria [162], HIV-1 virus [163], mollusk-host parasites [164] and protozoa such as the *Trypanosoma cruzi* [165]. Oliveira and co-authors demonstrated that lapachol also has activity against *Aedes aegypti* that is the vector of the Dengue virus and Zika virus [166]. Their isomers α -lapachone and β -lapachone (Figure 6.1) are also present in species of the *Bignoniaceae* family, however in significantly less quantities when compared to lapachol, which may comprise up to 7% of the heartwood of the plant [161,167].

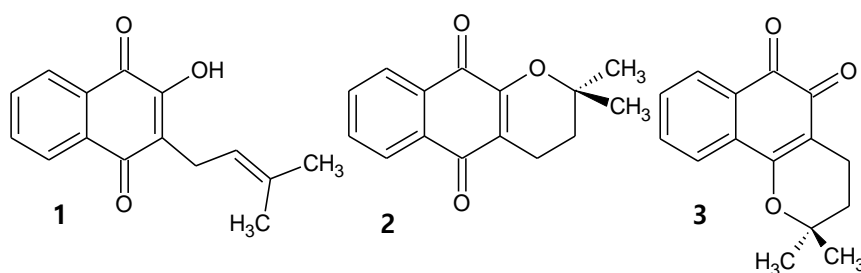


Figure 6.1. Chemical structures of (1) lapachol, (2) α -lapachone and (3) β -lapachone.

The main approach for the determination of lapachol and other naphthoquinones in plant extracts is based on high performance liquid

chromatography (HPLC) with UV photometric absorption (UV) detection [168,169]. Steinert *et al.*, proposed a HPLC-UV to separate and determine naphthoquinones in extracts of *Tabebuia avellanae* (Bignoniaceae). However, authors failed to detect lapachol in the aqueous extracts analyzed [168]. Lapachol and other naphthoquinones were isolated from the ethanolic extract of *Zeyheria montana* roots (genus *Tabebuia*) and successfully quantified by HPLC-UV, indicating the presence of 0.001% w/w of lapachol in the sample [169].

Indirect determination based on the photoluminescence quenching of quantum dots (QDs) in the presence of lapachol have recently been reported [82,170]. It was demonstrated the use of 3-mercaptopropionic acid CdTe QDs, used as a probe for lapachol enabled LOD of 1.9 mg L^{-1} and the analysis of urine samples (with a previous cleaned-up using an acrylic polymer packed cartridge). The 3-mercaptopropionic acid-CdTe QDs photoluminescence quenching promoted by lapachol, β -lapachone, α -lapachone or β -lapachone-3-sulfonic acid was improved in aqueous dispersions containing hexadecyltrimethylammonium bromide (CTAB). The presence of CTAB promoted rapid stabilization of the quantum dots (QDs) after interaction with naphthoquinones and improved the magnitude of quenching effect. This enabled instrumental LOD of 0.04 mg L^{-1} for lapachol and its successful determination in heartwood ethanolic extract of *T. impetiginosa* [82]. Other luminescence based methods rely on the signal generated after the reduction of naphthoquinones, using sodium hydrosulfite, to generate a fluorescent derivative of lapachol that is unstable in the presence of oxygen [171]. The reduction with sodium dithionite or sodium borohydride enabled the fluorimetric determination of lapachol (LOD in the $\mu\text{g L}^{-1}$ range) and other quinones in pharmaceutical formulations. However, the generation of different derivatization products may affect precision of the method [172].

Voltammetry has been employed for redox studies and for the determination of naphthoquinones [173-176]. Studies using CV made by Goulart *et al.*, using GCE, showed that the lapachol anion-radical interacts with oxygen producing deprotonated lapachol and peroxy radicals [175]. The electrochemical reduction of lapachones was studied by Oliveira-Brett *et al.* using CV, SWV and differential pulse voltammetry in a hydroalcoholic medium. The reduction processes, on the GCE, for β -lapachone, β -lapachone-3-sulfonic acid and β -lapachone 3-bromo- β -lapachone were reversible and pH-dependent. In contrast,

for α -lapachone the process was irreversible at pH 4.5 and *quasi*-reversible at pH 7.0. Another study on the electrochemical reduction of β -lapachone and its 3-sulfonic acid derivative in aqueous medium was also made using GCE. Results indicated a reversible and pH-dependent reduction process and evidence of interaction between β -lapachone and topoisomerase [176]. Differential pulse voltammetry was applied for the determination of β -lapachone-3-sulfonic acid with LOD of 0.41 mg L^{-1} [174].

In this chapter, the development of a sensitive SWV method to determine lapachol using a graphite-epoxy composite electrode is described. Analytical response was improved in the medium containing the cationic surfactant CTAB. A simple previous thin-layer chromatographic separation allowed the selective determination of lapachol in the heartwood ethanolic extract of *T. impetiginosa*.

6.2 Results

6.2.1 Preliminary studies

6.2.1.1 Electroactive area

The amounts of epoxy resin and graphite used to prepare the epoxy-graphite composite was adjusted by Tamayo-Balbin *et al.* [41] as the chosen proportion (97% graphite and 3% resin, m/m) presented excellent mechanical properties and produced sharp diffusional peak currents from guanine with low current baseline signal. Lapachol diffusional currents were also found to be well shaped and intense. The characterization of the electroactive area was made using CV (from -250 to +650 mV) with a electrochemical cell containing $[\text{Fe}(\text{CN})_6]^{3-}$ ($1.0 \times 10^{-3} \text{ mol L}^{-1}$) in KNO_3 (0.5 mol L^{-1}). Sequential scans generated peak current (I_p) magnitudes that linearly increased in function of scan rate (ν), from 20 to 100 mV s^{-1} . As the electroactive species concentration (C) was $1.00 \times 10^{-6} \text{ mol cm}^{-3}$, the electroactive area could be estimated as 0.0078 cm^2 from the simplified Randles-Sevcik equation: $A = I_p / (2.686 \times 10^5 \nu^{1/2} n^{3/2} C D^{1/2})$, where D is $6.32 \times 10^{-6} \text{ cm}^2 \text{ s}^{-1}$ and $n = 1$. For the GCE, the electroactive area was 0.019 cm^2 .

6.2.1.2

Influence of CTAB on the electroanalytical process at different pH values

Surfactants might play important roles in electrochemical processes since they can mediate the interaction between electroactive species and electrode [177,178]. Surfactants might influence redox processes and minimize the passivation of the electrode surface caused by adsorption of electrogenerated products or by sample matrix components [179,180]. In addition, they improve the solubility of more hydrophobic analytes and facilitate mass transport [181,182].

Guin *et al.* have reviewed the electrochemical reduction of quinones in different media [183]. In buffered aqueous medium the quinone-hydroquinone redox pair involves the transferring of two-electrons, at potentials that vary with pH, with steps involving different reduced and oxidized species with different pK_a values. At acidic pH, due to the fast kinetics and availability of protons, the two-step protonation process affect both carbonyl groups and can be viewed as a single step two electron and two proton process. At basic pH the reduction process is due to electrons only while at neutral pH, reduction involves either one proton and two electrons or two electrons only [183]. For lapachol, Ngameni *et al.* [173] have shown that the increasing of pH causes broadening of both anodic (in more extent due to the difficulty in re-oxidation of hydrolapachol) and cathodic CV peaks, which is a reflection of the kinetics of the different processes taking place. At basic conditions, the more hydrophilic non-protonated species (due to the proton loss in the hydroxyl group of the enol system) is dominant over the protonated one.

The behavior in aqueous basic medium (pH 9 using Tris-HCl) was confirmed in the present work as the reduction process is not favored, due to the lack of protons, but with oxidation process still occurring, probably involving only electrons (voltammogram b of Figure 6.2A). In the presence of CTAB (near CMC), the reduction peak is restored probably because of the stabilization provided, reducing the energy to produce radicals. An improvement in oxidation is clearly observed, probably occurring in different steps as the cyclic voltammogram shows, besides the main oxidation peak, a shoulder at more positive potentials (voltammogram a of Figure 6.2A).

In the voltammogram obtained at pH 6 (phosphate buffer) aqueous medium, the oxidation peak was smaller than the reduction one, indicating a *quasi*-reversible process (voltammogram *a* of Figure 6.2B). In such conditions, lapachol has a pK_a value of about 6 (which refers to the enol ionization [184]), therefore, the ratio between protonated and non-protonated species is about 1. In contrast, when the cationic surfactant CTAB was included into the pH 6 solution, a reversible behavior seems to be taking place with more intense peak currents (voltammogram *b* of Figure 6.2B). In medium containing CTAB, the pK_a of acid solutes such as lapachol is decreased to about two units [185,186], making the non-protonated and hydrophilic species predominant at pH 6.0. In aqueous medium at pH 4.0 (acetate buffer), the *quasi*-reversible behavior was also observed and the intensity of both redox peak currents was smaller than the ones at pH 6.0 (voltammogram *a* of Figure 6.3C). At pH 4.0 non-protonated species is predominant, however as CTAB is included, the non-protonated/protonated ratio of these species becomes close to 1 and the oxidation peak increases to the point that the electrochemical process seems to be reversible (voltammogram *b* of Figure 6.2C). CTAB also shifted the oxidation peak to a more anodic potential and the reduction peak to a more cathodic potential. Despite that, the peak current intensities were significantly smaller than the ones observed at pH 6.0.

The presence of CTAB seems to improve the diffusion of lapachol towards the electrode providing better transport and more effective redox reaction. Micelles and pre-micellar aggregates confine reagents and products involved in the reaction mechanism steps (especially the oxidation one) making their local concentration (inside the normal micelle or in between monomers that form the micellar structure) very high, thus improving reaction kinetics. The formation of radicals is also favored as they are stabilized in the micelle-organized system. It is also important to point out that reversible and intense redox processes tend to lead to very intense SWV peaks (that account signal contributions for both reduction and oxidation diffusion currents), leading to higher detection power in quantitative analysis. Thus, the medium buffered at pH 6.0 containing CTAB was chosen to establish the quantitative voltammetric method.

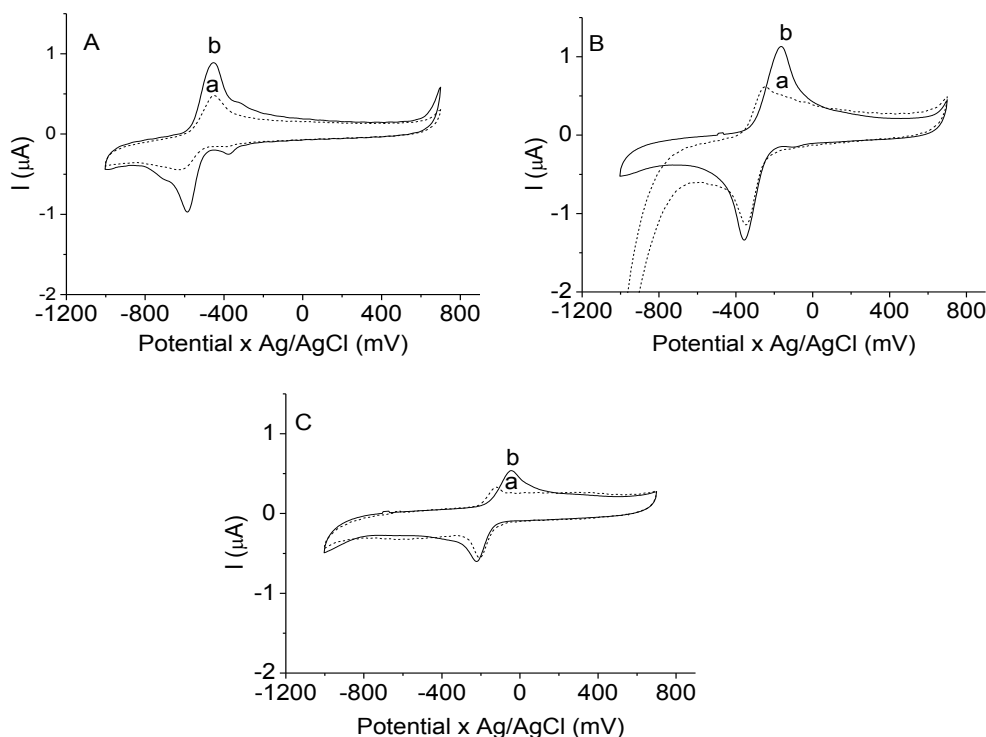


Figure 6.2. Cyclic voltammetry of the redox process of lapachol in aqueous media at different pH in the (a) absence and (b) presence of CTAB. (A) Tris-HCl buffer (4.0×10^{-2} mol L⁻¹, pH 9.0); (B) phosphate buffer (4.0×10^{-2} mol L⁻¹, pH 6.0) and (C) acetate buffer (4.0×10^{-2} mol L⁻¹, pH 4.0). $\nu = 100$ mV s⁻¹

6.2.1.3

Mechanistic studies in aqueous medium containing CTAB

As mentioned in the previous section, the qualitative study of the electrochemical process of lapachol (24 mg L^{-1}), in the presence of CTAB, by CV produced a single reduction peak (maximum at -450 mV) in the cathodic direction and the single counterpart oxidation peak (maximum at -154 mV) in the anodic direction. A further addition of lapachol (to enable final concentration of 72.7 mg L^{-1}) produced a similar result but more intense peaks. Such a behavior is typical of reversible processes (high charge transfer rates and mass transfer controlled by diffusion) enabling dynamic equilibrium at the electrode interface [187]. Sequential CV scans were made in order to check the process stability (at the scan rate of 100 mV s^{-1} , from -900 mV to 700 mV and without forced convective mass transport). Even after the tenth cycle (Figure 6.3A) there was no evidence of decreasing of peak magnitude, indicating that the species in the solution-electrode interface are readily and repeatedly interconverted into the oxidized and reduced forms. Furthermore, the calculated ratio between the anodic peak current (I_{pa}) and

the cathodic peak current (I_{pc}) at 100 mV s^{-1} scan rate was equal to 0.83. Literature reports that in simpler redox systems, this ratio tends to get closer to 1 as the pH becomes more acid and the prompt availability of H^+ ions guarantee fast reoxidation [173]. Ratio values close or equal to the unity, independently of the scan rate, are typical of reversible systems as it was observed for lapachol in the presence of CTAB (Figure 6.3B) [14,188]. The difference between anodic and cathodic peak potentials ($\Delta E_p = E_{pa} - E_{pc}$) remained constant with the changing the scan rate (from 10 to 100 mV s^{-1}), which is an indication of reversibility. The reversibility of the process was confirmed as the square root of the scan rate ($\sqrt{\nu}$), from 10 to 1000 mV s^{-1} , produced a linear response ($R^2 = 0.982$) in function of I_p (cathodic). Linearity ($R^2 = 0.990$) was also found regarding $\log \nu$ in function of $\log I_p$, producing a slope value of 0.6 that suggest that the process involved is mostly diffusional rather than adsorptive (Figure 6.3C) [43].

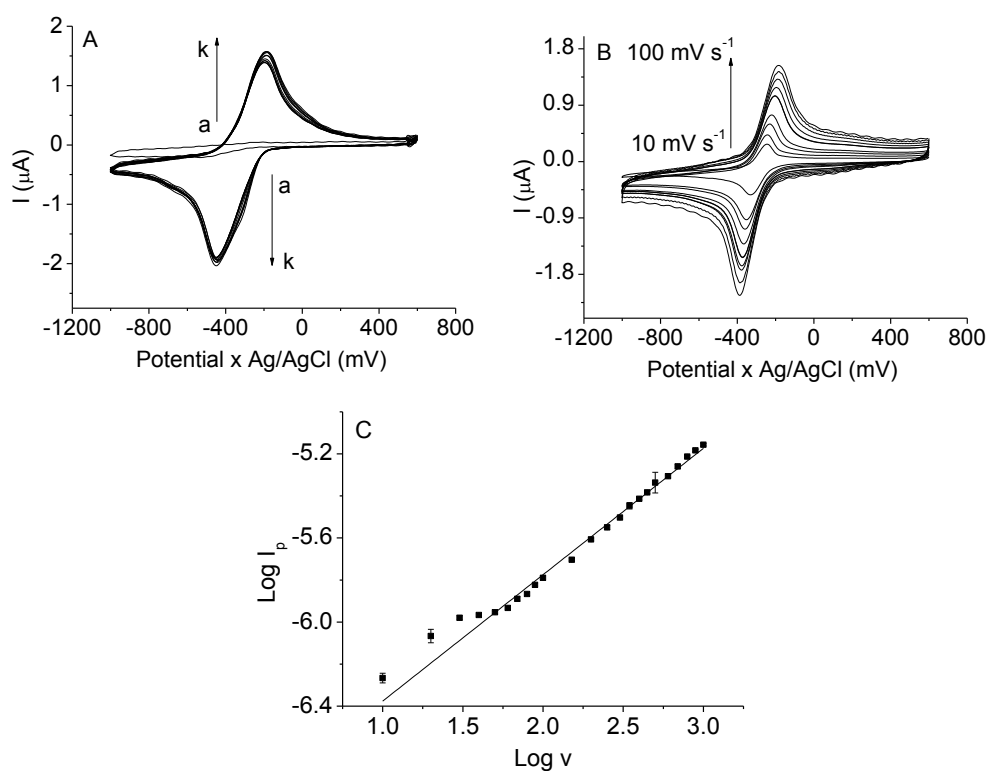


Figure 6.3. (A) Sequential cyclic scans (line a-k) for lapachol at 100 mV s^{-1} at 72.7 mg L^{-1} of lapachol. (B) Cyclic scans at rate of $10\text{-}100 \text{ mV s}^{-1}$ for lapachol in presence of CTAB $1.2 \times 10^{-4} \text{ mol L}^{-1}$ by check the reversibility of the redox process. (C) Study of the $\log \nu \times \log I_p$ (29.1 mg L^{-1}) of lapachol; $\nu = 10$ to 1000 mV s^{-1} . Experimental conditions: phosphate buffer ($4.0 \times 10^{-2} \text{ mol L}^{-1}$; pH 6), $1.2 \times 10^{-4} \text{ mol L}^{-1}$ CTAB, KNO_3 (1 mol L^{-1}) in aqueous medium at $\nu = 100 \text{ mV s}^{-1}$.

SWV also provided important insights on the process. The frequency (in fact $\log f$, with f from 10 to 90 Hz) dependence upon peak potential (E_p) was linear ($R^2 = 0.994$), as shown in (Figure 6.4A). In addition, the increase in I_p in function of \sqrt{f} (Figure 6.4B) was directly proportional and linear ($R^2 = 0.964$), which is an indication that the process is controlled by reagent diffusion [188].

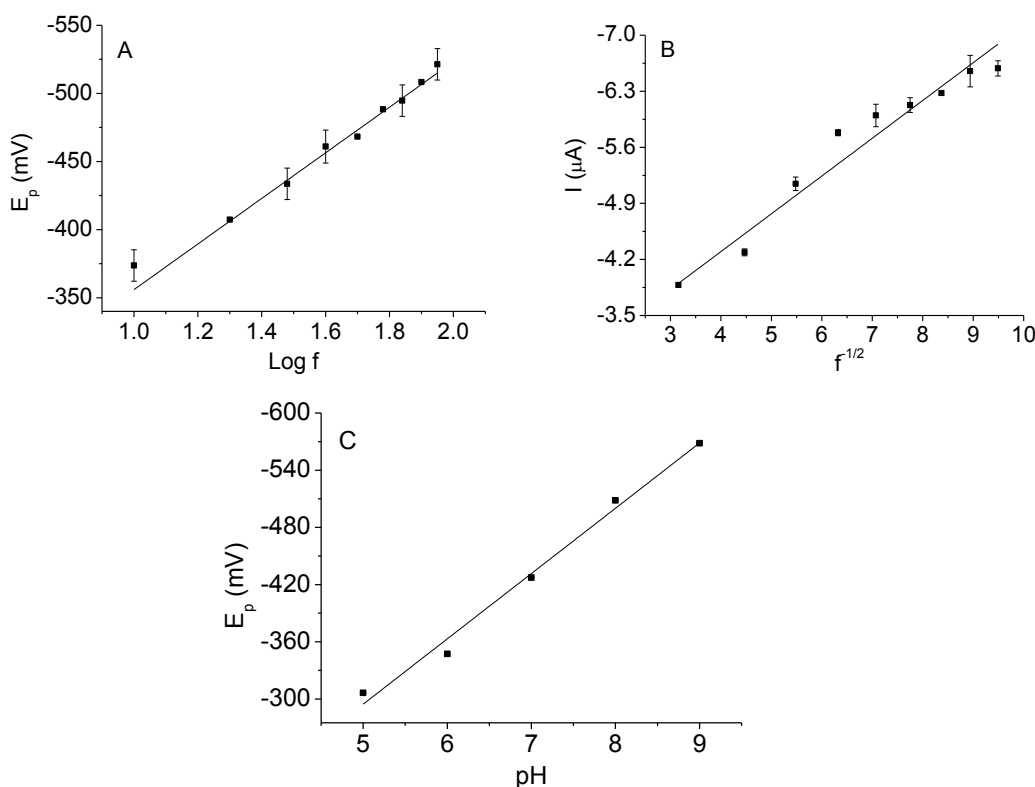


Figure 6.4. (A) Study of $\log f \times E_p$ in the range from 10 - 90 Hz; (B) Study of $\sqrt{f} \times I_p$ in the range from 10 to 90 Hz; (C) Study of $\text{pH} \times E_p$ in the pH range from 5 to 9, using SWV using 29.1 mg L^{-1} of lapachol.

In the presence of CTAB, the E_p shifted to more negative values as the pH of the supporting electrolyte was increased (Figure 6.4C). This is typical processes that are influenced by the hydrogenionic concentration of the medium, which was confirmed by the linear relationship given by E_p (mV) = $(48.0 \pm 1.3) + (-68.5 \pm 0.18) \text{ pH}$, that relates to the Nernst equation and transfer of two electrons [188,189]. This is compatible with the reduction of the two carbonyl groups, one of them next to the hydroxyl group, that might promote the hydrogenbonding-aided stabilization of the radicals generated during reduction [174]. The concentration of CTAB ($8.1 \times 10^{-4} \text{ mol L}^{-1}$) in the supporting electrolyte was

slightly below the theoretical critical micellar concentration (CMC of $1.0 \times 10^{-3} \text{ mol L}^{-1}$) and chosen based on preliminary tests shown in Figure 6.5.

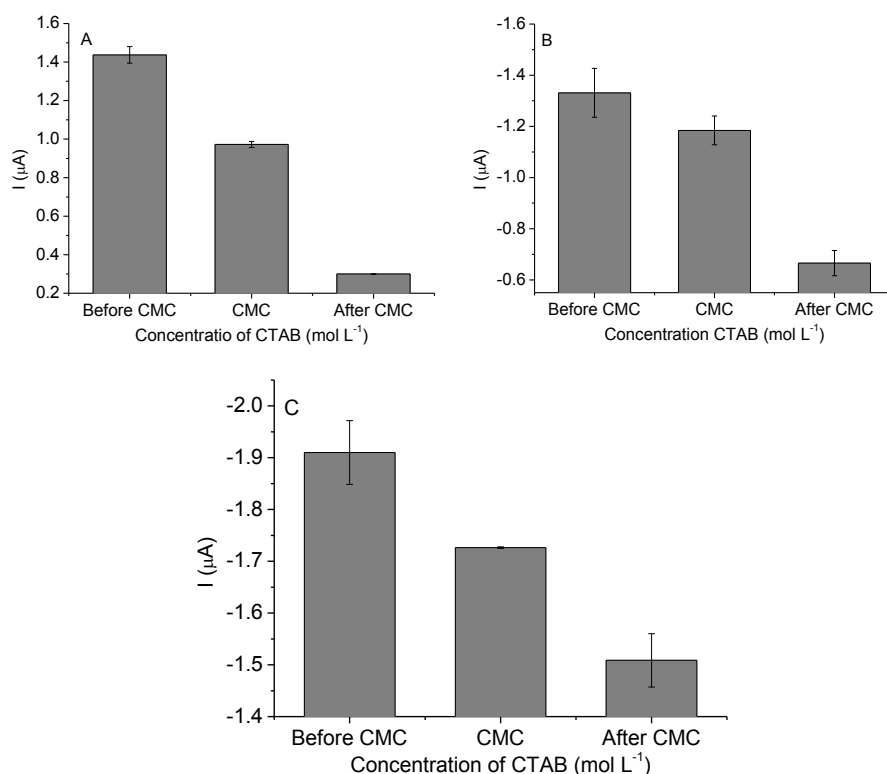


Figure 6.5. Voltammetric responses from 72.7 mg L^{-1} of lapachol in aqueous media in presence of CTAB before CMC ($8.1 \times 10^{-4} \text{ mol L}^{-1}$), at CMC ($1.0 \times 10^{-3} \text{ mol L}^{-1}$) and after CMC ($1.5 \times 10^{-3} \text{ mol L}^{-1}$). (A) Cyclic voltammetry (anodic peak); (B) cyclic voltammetry (cathodic peak) and (C) square-wave cathodic voltammetry. Experimental conditions: phosphate buffer ($4.0 \times 10^{-2} \text{ mol L}^{-1}$; pH 6), KNO_3 (1 mol L^{-1}) in aqueous medium at $\nu = 100 \text{ mV s}^{-1}$.

6.3.2

Optimization of experimental and instrumental conditions for analysis using SWV

It was found that lapachol accumulates on the surface of the electrode (under forced convective transport and purging with N_2) at the same rate no matter the applied potential (in the range of +600 to -100 mV), which enables the pre-concentration of the analyte prior to quantification. The re-dissolution current measured after different preconcentration times can be seen in (Figure 6.6A),

where saturation is achieved after 140 s. For quantitative purposes, 160 s of analyte accumulation, at +400 mV, was set to measure the SWV re-dissolution analyte current.

Square-wave voltammetric instrumental parameters (pulse amplitude from 10 to 100 mV, and frequency from 10 to 60 Hz) were adjusted using a 20 mV potential step. Despite the fact that the magnitude of the measured re-dissolution current was directly proportional to either frequency or pulse amplitude, the distortions in the shape of the voltammetric peaks had also been considered in the final choice of values: 40 mV pulse amplitude and frequency of 30 Hz (Figure 6.6B and 6.6C).

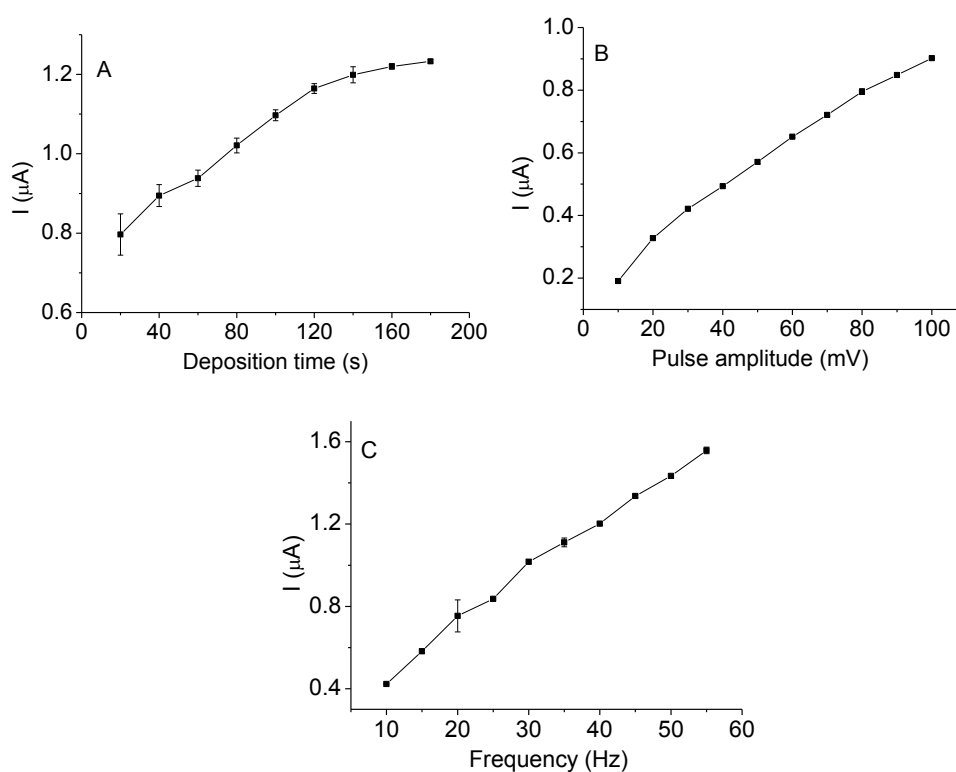


Figure 6.6. SWV signal (measured using graphite-epoxy electrode) dependence upon: (A) deposition time; (B) pulse amplitude (a) and (C) pulse frequency (f). Electrolyte support: CTAB ($1.2 \times 10^{-4} \text{ mol L}^{-1}$), phosphate buffer ($4.0 \times 10^{-2} \text{ mol L}^{-1}$; pH 6) and KNO_3 (1.0 mol L^{-1}) in aqueous medium. Lapachol concentration of 0.388 mg L^{-1} .

6.3.3

Analytical determination of lapachol

6.3.3.1

Analytical characteristics

Analytical figures of merit were obtained using the selected experimental conditions to determine lapachol (Table 6.1).

Table 6.1. Conditions for the SWV determination of lapachol.

Parameter	Value
Electrolytic mixture	CTAB (1.2×10^{-4} mol L ⁻¹) / phosphate buffer (4.0×10^{-2} mol L ⁻¹ ; pH 6) / KNO ₃ (1 mol L ⁻¹)
Deposition Potential	400 mV
Time deposition	140 s
Amplitude	40 mV
Step potential	20 mV
Frequency	30 Hz
Monitored signal	in 447 mV
Sweep potential range	600 to -900 mV

The analytical signal (peak current) was directly and linearly proportional to the concentration lapachol in the electrochemical cell ($R^2 = 0.996$). The standard addition curve equation was I_p (μA) = $(2.5 \times 10^{-7} \pm 7.0 \times 10^{-9}) C_{\text{lapachol}}$ (mg L^{-1}) + $(3.8 \times 10^{-6} \pm 3.4 \times 10^{-8})$ ($R^2 = 0.999$), covering the range up to 0.49 mg L⁻¹ of analyte (Figure 6.7A). Measurements were performed in triplicate and the associated errors of sensitivity and linear coefficient were calculated as standard deviations. The instrumental LOD of 0.029 mg L⁻¹ and the instrumental LOQ of 0.097 mg L⁻¹ were calculated using respectively $3s_b/m$ and $10s_b/m$, where s_b is the standard deviation of ten consecutive signal measurements of the lowest

analyte concentration in the analytical addition curve and m is the sensitivity of this curve. The instrumental precision of 2% was obtained from ten consecutive measurements of the signal (measured after pre-concentration step) produced by the analyte standards at two different concentrations (0.097 mg L^{-1} and 0.580 mg L^{-1}).

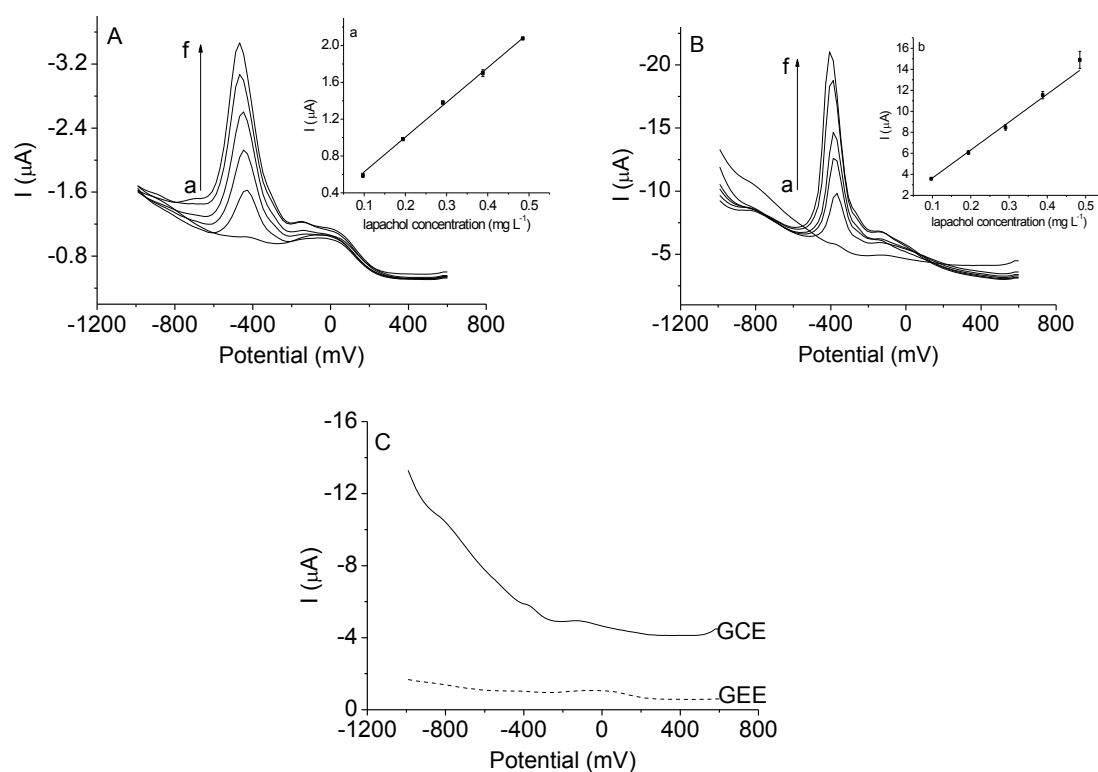


Figure 6.7. SWV analytical addition curves of lapachol covering the concentration range from 0.097 mg L^{-1} to 0.485 mg L^{-1} and using: (A) graphite-epoxy electrode and (B) glassy carbon electrode (GCE). Experimental conditions of Table 1. (C) Background signal measured using the graphite-epoxy electrode (GEE) and the glass carbon electrode (GCE).

In order to establish a comparison, the analytical addition curve was also made using the GCE electrode (electroactive area of about 0.019 cm^2) using SWV and the same conditions established in this work. The standard addition curve ($R^2 = 0.996$) was $I_p (\mu\text{A}) = (9.9 \times 10^{-7} \pm 9.2 \times 10^{-8}) C_{\text{lapachol}} (\text{mg L}^{-1}) + (2.7 \times 10^{-5} \pm 7.7 \times 10^{-7})$ covering about the same concentration range with almost the same sensitivity despite the electroactive area of about three times larger the one of the graphite-epoxy composite electrode (Figure 6.7B). It can be also noticed that the background signal generated using the graphite-epoxy electrode was significantly

less intense than the one associated with the GCE electrode, which reflects in the signal-background ratio, that in turn affect the ability to detect low concentrations of lapachol (Figure 6.7C).

6.3.3.2

Interference from other naphthoquinones and determination of lapachol in ethanolic extract of *T. impetiginosa*

The interference from α -lapachone and β -lapachone (both isomers of lapachol) were evaluated. SWV voltammogram peak from the isomer α -lapachone completely overlaps the one of lapachol (Figure 6.8A). In contrast, a partial overlap of the SWV voltammetric peaks of lapachol and β -lapachone occurred (Figure 6.8B). Therefore, a first-order derivative was applied to resolve these voltammetry peaks (Figure 6.8C), allowing the selective determination of lapachol in the presence of β -lapachone or even the determination of both.

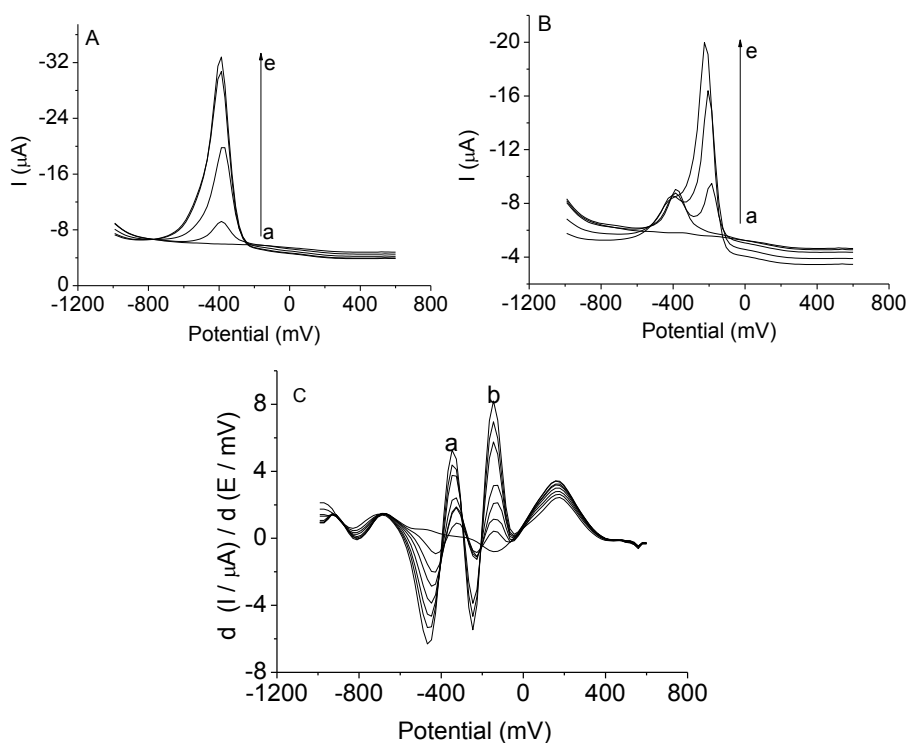


Figure 6.8. Voltammograms of mixtures containing lapachol (4.8 mg L^{-1}) and its isomers: (A) mixture with α -lapachone and (B) mixture with β -lapachone. Concentrations indicated for the isomer: a) blank; b) 0 mg L^{-1} ; c) 4.8 mg L^{-1} ; d) 7.3 mg L^{-1} and e) 9.7 mg L^{-1} . (C) First derivative of the voltammetric response for a) lapachol from $97 \text{ } \mu\text{g L}^{-1}$ to $775 \text{ } \mu\text{g L}^{-1}$ and b) β -lapachone from $97 \text{ } \mu\text{g L}^{-1}$ to $388 \text{ } \mu\text{g L}^{-1}$. Optimized experimental conditions (Table 6.1).

Analyte addition curves of both lapachol and β -lapachone were constructed under the optimized conditions and using the first-order derivative of the voltammogram. The standard addition curves produced linear analytical response ($R^2 = 0.996$) for lapachol from $4.0 \times 10^{-7} \text{ mol L}^{-1}$ ($97 \mu\text{g L}^{-1}$) to $3.2 \times 10^{-6} \text{ mol L}^{-1}$ ($760 \mu\text{g L}^{-1}$) modelled by the equation: $dI_p/dE = (-6.6 \times 10^{-7} \pm 8.5 \times 10^{-8}) C_{\text{lapachol}} (\text{mol L}^{-1}) + (-3.5 \pm 0.04)$. For β -lapachone, the linear response ($R^2 = 0.943$) covered the concentration range from $4.0 \times 10^{-7} \text{ mol L}^{-1}$ ($97 \mu\text{g L}^{-1}$) to $1.6 \times 10^{-6} \text{ mol L}^{-1}$ ($390 \mu\text{g L}^{-1}$) with analyte addition curve equation of $dI_p/dE = (-7.7 \times 10^{-7} \pm 1.1 \times 10^{-7}) C_{\text{lapachol}} (\text{mol L}^{-1}) + (-2.0 \pm 0.09)$.

The addition of an aliquot of the alcoholic extract of the heartwood of *T. impetiginosa* directly into the electrochemical cell produced a large and wide signal that indicates that the matrix imposes interference in the analysis. The separation of lapachol from matrix components of the sample was made by thin-layer chromatography (TLC) in order to eliminate any potential interference during analysis. The separation by TLC was very simple and relatively rapid, leading to percent recoveries of lapachol higher than 95% on the spot of lapachol at the RF 0.78. This was verified by two different analysts, each one using three authentic replicas of a standard solution of lapachol. By spotting a lapachol mass of $97 \mu\text{g}$, the average loss of analyte during the separation procedure was of $3.3 \pm 0.3\%$ (for the analyst 1) and $3.5 \pm 0.4\%$ (for the analyst 2), which enabled a recovery of $93.7 \mu\text{g}$, taking into account the 3.4% average percent loss of analyte. This result can be considered satisfactory but, when required, the percent loss can be used to correct the final analysis result from plant extract.

The intermediate precision of the SWV method was also calculated taking into consideration the analysis results of samples obtained by both analysts. The intermediate precision considered the variability of the TLC procedure. Two levels of analyte were used in the evaluation using $40 \mu\text{L}$ of a sample extract. The results (in absolute mass) obtained by the analyst 1 were $3.10 \pm 0.05 \mu\text{g}$ while analyst 2 obtained $3.05 \pm 0.04 \mu\text{g}$. The combined standard deviation (analyst 1 and analyst 2) produced the intermediary precision of $0.06 \mu\text{g}$ or 2% of the grand average.

Samples of heartwood extract of *T. impetiginosa* were successfully analysed aiming the determination of lapachol. Analyses of different aliquots of the extract (diluted 500 times because of the sensitivity of the method) were made in three different days and the results (average of three replicates) are shown in Table 6.2. The average lapachol concentration (with a confidence limit of 95% and $n=9$) in the heartwood extract of *T. impetiginosa* was $340 \pm 10 \text{ mg L}^{-1}$.

Table 6.2. Lapachol concentration (analysed in three days, $n=3$ replicates) in wood *T. impetiginosa* (Pink Ipê) and in commercial extracts after separation by TLC.

Sample	Day	Concentration (mg L^{-1})
<i>T. impetiginosa</i> extract (Pink Ipê)	1	^a (0.34 ± 0.016)
	2	^a (0.32 ± 0.009)
	3	^a (0.36 ± 0.02)
Commercial extract	1	< LOD
	2	< LOD
	3	< LOD

^a Results from sample extracts diluted 500 times.

The same extract samples were also analysed by HPLC and the results (three samples made in three replicates) are shown in Table 6.3 along the ones obtained by the SWV proposed method. The results are in statistical agreement as the Student's t-test produced (using the *grand* average value) a $t_{\text{calculated}} = 1.2$ for a t_{critical} of 2.0, at a 95% confidence limit ($n_1 = n_2 = 24$). Analysis of variance (single factor) using each average value as an independent result produced a $F_{\text{calculated}}$ of 1.3 for a F_{critical} of 4.3, at a 95% confidence limit an $n_1 = n_2 = 24$.

Table 6. 3. Determination of lapachol in samples of heartwood of Pink Ipê.

Sample	Method	Concentration in extract (mg L^{-1})	Content of lapachol in the wood (%)
1	SWV	^{a,b} (0.1696 ± 0.0121)	1.36 ± 0.10
2	HPLC-UV	^c (0.17686 ± 0.00848)	1.41 ± 0.07

^a Concentration corrected by the 500 dilution factor.

^b TLC procedure to separate analyte.

^c Sample solution not diluted.

The proposed voltammetric method was used to determine lapachol in a commercial formulation of vegetal powder (Pau d'arco), supposedly containing *T. impetiginosa*. Lapachol could not be detected by the method and no indication of the analyte was found in the characteristic RF of the TLC plate.

6.3.4

Preliminary studies aiming the selective determination of α -lapachone and β -lapachone

Redox processes involving naphthoquinones at carbon-based substrates, especially in the case of GCE, are well known and they have been extensively covered in the literature [174,183]. However, these studies are almost always performed using only one naphthoquinone, as different ones tend to have very close redox potentials, and evaluating mixtures makes the conduction of such studies very challenging because of significant interferences. Therefore, it is desirable to achieve selective conditions to enable the simultaneous observation of the behavior of different naphthoquinones, also allowing their detection.

In the specific case of this section, two naphthoquinone isomers (α -lapachone and β -lapachone) were chosen. Studies indicated that mutual interference imposed by this pair of isomers can be minimized by a combination of proper electrolytic medium and properly chosen instrumental/experimental conditions (ionic strength, pH, proportion and type of electrolytic mixture, applied potential and deposition time, frequency, pulse amplitude and potential step), which were the ones used for the determination of lapachol.

A study using CV (Figure 6.9A) showed that for α -lapachone, peaks 1 and 4 are respectively related to the oxidation (at -442 mV) and the reduction (at -503 mV), while for β -lapachone, the peaks 2 and 3 are respectively related to the oxidation (at -190 mV) and reduction (-344 mV) using 100 mV s^{-1} in the potential range from -1000 mV to 1000 mV and without forced convective mass transport. Several CV cycles were made to check the stability of the process and even after 15 cycles (Figure 6.9A) there was no evidence of a decreasing in peaks magnitudes, indicating that the species at the solution-electrode interface are readily and repeatedly converted into the oxidized and reduced forms.

The plots of the square root of the ν (with ν ranging from 40 to 100 mV s^{-1}) as a function of the I_p for the reduction of both lapachonas were linear, with $R^2 = 0.989$ for α -lapachone (peak 4) and $R^2 = 0.997$ for β -lapachone (peak 3). From this same study (Figure 6.9B) it was observed that the β -lapachone redox process (peaks 2 and 3) is clearly reversible, since both oxidation and reduction present close intensities. Moreover, the literature [183] states that electrochemical processes involving this type of naphthoquinone are reversible because of the rapid kinetics and availability of protons with the two-phase protonation process affecting both carboxylic groups leading it to be seen as a one-step process involving two electrons and two protons. For the α -lapachone, a similar result to that described by Abreu *et al.* [174] was observed, with a behavior different from what is generally expected from naphthoquinones in aqueous media [174] with the CV presenting an intense cathodic peak and a less intense anodic one. According to Abreu *et al.*, the electrochemical behavior of α -lapachone is more dependent upon pH than that of β -lapachone, since α -lapachone reduction, at pH 4.5, is considered irreversible, involving the transfer of two electrons. Moreover at pH 7, a semi-reduced intermediate species formed from α -lapachone undergo cleavage favoring a resonance that will result in a more stable intermediate species (semi-reduced species) that is stabilized by hydrogen bonding canonical form that prevails during CV [174] resulting in a *quasi*-reversible process. The increase of I_p as a function of \sqrt{f} (Figure 6.9D) was directly proportional and linear ($R^2 = 0.974$ and 0.997 for α -lapachone and β -lapachone, respectively), which is an indication that the process was controlled by the diffusion of reagents [188].

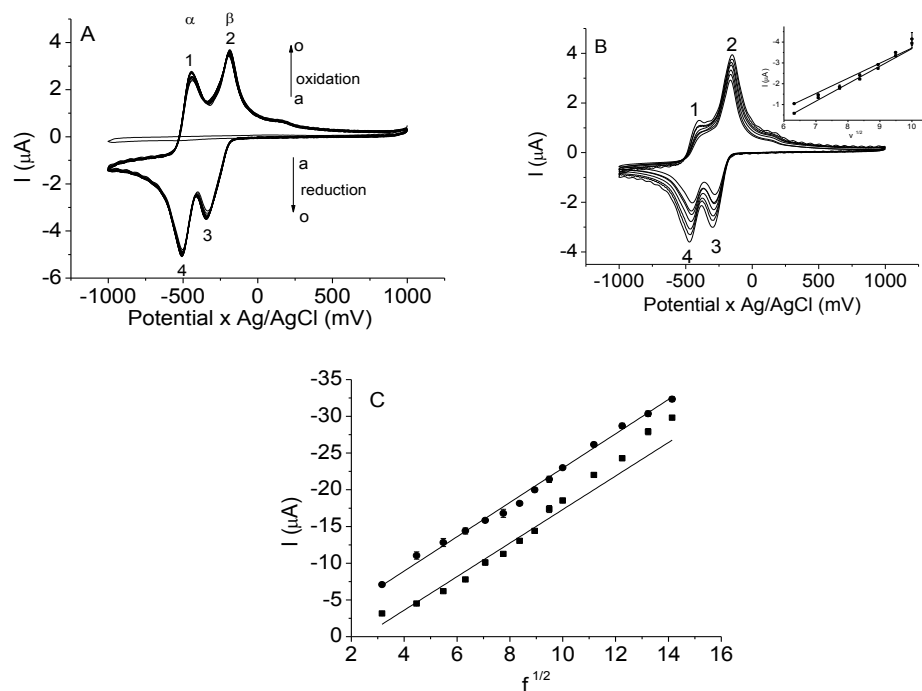


Figure 6.9. (A) Sequential cyclic voltammograms (line a-o) for α -lapachone and β -lapachone (both at $4.0 \times 10^{-4} \text{ mol L}^{-1}$) at 100 mV s^{-1} . (B) The cyclic voltammetry using ν from 40-100 mV s^{-1} for α -lapachona and β -lapachona in the presence of CTAB $1.2 \times 10^{-4} \text{ mol L}^{-1}$. (C) Study concerning $\sqrt{f} \times I_p$ in the f range from 10 to 200 Hz using phosphate buffer ($4.0 \times 10^{-2} \text{ mol L}^{-1}$ and pH 6), CTAB ($1.2 \times 10^{-4} \text{ mol L}^{-1}$), KNO_3 (1 mol L^{-1}) at $\nu = 100 \text{ mV s}^{-1}$.

The SWV was used to attempt the simultaneous quantification of these isomers. The conditions employed are the same as those used for lapachol (see Table 6.1). Voltammograms corresponding to the signals of α -lapachone (-370 mV; peak 1) and β -lapachone (-190 mV; peak 2) are shown in Figure 6.10A. The concentration of the lapachones was varied from $1.0 \times 10^{-6} \text{ mol L}^{-1}$ to $1.3 \times 10^{-5} \text{ mol L}^{-1}$ to construct response curves (insertion in Figure 6.10A) that confirms that the analytical signal (peak current) was directly and linearly proportional to the concentration of both lapachones in the electrochemical cell ($R^2 = 0.997$ for peak 1 and $R^2 = 0.995$ for peak 2). The standard addition curve equations were I_p (μA) = $(9.0 \times 10^{-2} \pm 6.0 \times 10^{-4}) C_{\alpha\text{-lapachona}} (\text{mol L}^{-1}) + (3.1 \times 10^{-8} \pm 4.5 \times 10^{-9})$ based on peak 1 and I_p (μA) = $(4.8 \times 10^{-2} \pm 2.3 \times 10^{-4}) C_{\beta\text{-lapachona}} (\text{mol L}^{-1}) + (5.0 \times 10^{-8} \pm 1.5 \times 10^{-9})$ based on peak 2. Measurements were performed in three replicates and errors associated with sensitivity and linear coefficient were calculated as standard deviations. Despite the fact that lapachones concentration down to $10^{-7} \text{ mol L}^{-1}$

order could be readily detected, the range below 10^{-6} mol L⁻¹ were not explored here because of mutual interferences occur. However, in solutions containing only one of the isomers indicated that LOD values could reach the 10^{-8} mol L⁻¹ range.

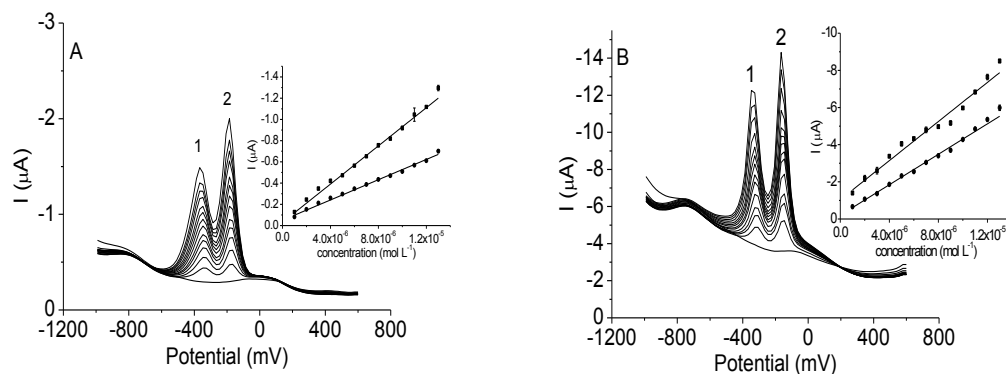


Figure 6.10. SWV analytical addition curves of α -lapachone and β -lapachone covering the concentration range from 1.0×10^{-6} mol L⁻¹ to 1.3×10^{-6} mol L⁻¹ using: (A) graphite-epoxy electrode and (B) glassy carbon electrode (GCE).

Studies using either the epoxy-graphite electrode or the GCE were made in order to compare the signals and the behavior of these naphtoquinone isomers in these substrates. The experiment using GCE was carried out under the same conditions employed for the graphite-poxy electrode. The standard addition curves using the GCE were I_p (μA) = $(5.3 \times 10^{-1} \pm 7.3 \times 10^{-3}) C_{\alpha\text{-lapachone}}$ (mol L⁻¹) + $(1.0 \times 10^{-6} \pm 5.9 \times 10^{-8})$ ($R^2 = 0.969$) using peak 1 and I_p (μA) = $(4.1 \times 10^{-1} \pm 3.8 \times 10^{-3}) C_{\beta\text{-lapachone}}$ (mol L⁻¹) + $(2.0 \times 10^{-7} \pm 2.4 \times 10^{-8})$ ($R^2 = 0.994$) using peak 2. Although covering roughly the same concentration range and enabling similar sensitivities, the electrode area of the glassy carbon is approximately three times larger than the area of the epoxy-graphite electrode. It was also observed that the baseline signal (background signal) produced by the epoxy-graphite electrode was significantly lower than the one produced by the GCE, which enabled better detection power. However, apparently the resolution achieved by either electrode allows selective determinations at relatively higher concentration range of the isomers (above 10^{-6} mol L⁻¹).

6.3.5 Partial conclusion

A simple voltammetric method was developed for the quantification of lapachol and applied in the analysis of extracts heartwood of *T. impetiginosa*. The laboratory-made graphite-epoxy electrode enabled good linear response and low background when compared to GCE. The use of CTAB in the supporting electrolyte (at pH 6) enabled intense and reversible redox peaks for lapachol that produced an intense SWV signal. The instrumental LOD of 0.029 mg L⁻¹ was achieved with linear range covering two orders of magnitude. Determination of lapachol in the presence of β -lapachone was successful made by using first order derivative in the signal and a TLC procedure allowed to separation of lapachol from components in the plant extracts, thus allowing accurate determinations. The studies performed with the pair of naphtoquinone isomers seem to indicate the possibility for the simultaneous determination of α -lapachone and β -lapachone by SWV. Further studies are required.

7 Conclusion

Electrochemical methods using carbon-based electrodes (BDD and graphite-epoxy electrodes) were developed, aiming to improve analytical performance in either voltammetry or amperometry and to investigate electrochemical mechanisms using SWV and CV. Electrochemical based methods, in many cases, present advantages over expensive and sophisticated analytical methods, many times allowing determinations directly in samples without any treatment or after the application of simple separation procedures. In addition, carbon based electrodes tend to be robust and produce reliable reproducible results.

Studies to achieve proper experimental and instrumental conditions were carried out aiming the quantitative analysis (ultra trace in sense) of trifloxystrobin, lapachol and gentamicin sulfate. In these cases, there were either a lack of electrochemical methods described in the literature or there was no study concerning the use of the BDD or the graphite-epoxy electrodes. The use of BDD electrode favored the development of a voltametric method for trifloxystrobin and an amperometric method for gentamicin sulfate as their electrochemical signal were observed at high positive potentials favoring their irreversible oxidation. In both cases, a low detection power was achieved (10^{-7} mol L⁻¹ for trifloxystrobin and gentamicin sulfate) with high precision and accuracy. The developed methods present analytical characteristics that are competitive with other methods found in the literature. Besides, for gentamicin sulfate, high analytical frequency was achieved by using BIA and selectivity was favored by using solid phase extraction using a laboratory-made kanamycin-MIP whose capacity and selectivity towards other selected substances were carefully evaluated. In the case of trifloxystrobin, an irreversible two-steps oxidation mechanism was proposed based on data provided by SWV and CV. The method was sensitive enough to allow investigation of this pesticide stability under heat and UV exposure. Although very resilient to heat (up to 60°C) trifloxystrobin was degraded by UV in a second order kinetic reaction for which $t_{1/2}$ and kinetic constant were calculated.

The use of a laboratory made epoxy-graphite electrode clearly improved the detection limit for lapachol when compared to the use of GCE. The use of CTAB in the supporting electrolyte (at pH 6) promoted better analyte mass transport to the surface of the electrode, leading to a reversible redox process that produce an intense SWV signal. Lapachol redox mechanism under such conditions was proposed based on SWV and CV data. Although selective towards β -lapachone, the other isomer (α -lapachone) imposed interferences that were circumvented by using a simple TLC separation. Preliminary studies were made to check the viability of the simultaneous detection of two naphthoquinone isomers (α -lapachone and β -lapachone).

8 Future works

Important points may still be addressed to complement or as a continuation of the project, such as:

For the strobilurin class of pesticides:

- ✓ As the sensors are also sensitive to the presence of other strobilurins, it is also possible to evaluate the photodegradation mechanism of other strobilurin class fungicides using the developed electroanalytical method, also trying to characterize their degradation products by NMR, HPLC-MS and other techniques.
- ✓ Evaluate the use of the graphite-epoxy electrode for the determination of trifloxystrobin establishing a performance comparison with the BDD electrode and use chemical modifiers in the composition of the graphite-epoxy electrode aiming the selective determination of trifloxystrobin.

For gentamicin sulfate:

- ✓ Determine gentamicin sulfate in milk samples by using the developed electrochemical method and SPE with cartridges packed with the aminoglycoside selective MIP.
- ✓ Identify, by NMR, possible gentamicin electrochemical products generated during the electrolysis cycles on the DBB electrode.

For naphthoquinones:

- ✓ Apply the developed method in the determination of α -lapachone and β -lapachone simulating real samples and validate the method using the HPLC technique;
- ✓ Further explore the dependence of pH on the electrochemical behavior of α -lapachone and β -lapachone to investigate, in more detail, the mechanism of interaction between the electrodes studied in this work;
- ✓ To evaluate new strategies for modifying the carbon-based electrodes used in this work, using new types of nanomaterials that may yield promising electrochemical studies.

References

- [1] ADAMS, R. N. Carbon paste electrodes. **Anal. Chem**, v. 30, n. 9, p. 1576 – 1576, Sept 1958.
- [2] PACHECO, W. F.; SEMAAN, F. S.; ALMEIDA, V. G. K.; RITTA, A. G. S. L.; AUCÉLIO, R. Q. Voltametrias: Uma Breve Revisão Sobre os Conceitos. **Rev. Virtual Quim**, v. 5, n. 4, p. 516-537, Aug 2013.
- [3] TERASHIMA, C.; RAO, T. N.; SARADA, B.V.; KUBOTA, Y.; FUJISHIMA, A. Direct electrochemical oxidation of disulfides at anodically pretreated boron-doped diamond electrodes. **Anal. Chem**, v. 75, n. 7, p. 1564-1572, Apr 2003.
- [4] RABAAOUI, N.; ALLAGUI, M. S. Anodic oxidation of salicylic acid on BDD electrode: Variable effects and mechanisms of degradation. **J. Hazar Mater**, v. 243, p. 187-192, Dec 2012.
- [5] DRAGOE, D.; SPĂȚARU, N.; KAWASAKI, R.; MANIVANNAN, A.; SPĂȚARU, T.; TRYK, D. A.; FUJISHIMA, A. Detection of trace levels of Pb²⁺ in tap water at boron-doped diamond electrodes with anodic stripping voltammetry. **Electrochim. Acta**, v. 51, n. 12, p. 2437-2441, Jan 2006.
- [6] PEDROSA, V. A.; CODOGNOTO, L.; AVACA, L. A. Determinação voltamétrica de 4-clorofenol sobre o eletrodo de diamante dopado com boro utilizando a voltametria de onda quadrada. **Quim. Nova**, v. 26, n. 6, p.844-849, May 2003.
- [7] DORNELLAS, R. M.; FRANCHINI, R. A. A.; DA SILVA, A. R.; MATOS, R. C.; AUCÉLIO, R. Q. Determination of the fungicide kresoximmethyl in grape juices using square-wave voltammetry and a boron-doped diamond electrode. **J. Electroanal. Chem**, v. 708, n. 1, p. 46-53, Nov 2013.
- [8] DORNELLAS, R. M.; NOGUEIRA, D. B.; AUCÉLIO, R. Q. The boron-doped diamond electrode voltammetric method for ultra-trace determination of the fungicide pyraclostrobin and evaluation of its photodegradation and thermal degradation. **Anal. Methods**, v. 6, p. 944-950, Nov 2014.
- [9] DORNELLAS, R. M.; TORMIN, T. F.; RICHTER, E. M.; AUCÉLIO, R. Q.; MUÑOZ, R. A. A. Electrochemical Oxidation of the Fungicide Dimoxystrobin and Its Amperometric Determination by Batch-Injection Analysis. **Anal. Letters**, v. 47, n. 3, p. 492-503, Oct 2014.
- [10] DEROCO, P. B.; MEDEIROS, R. A.; ROCHA-FILHO, R. C.; FATIBELLO-FILHO, O. Selective and simultaneous determination of indigo carmine and allura red in candy samples at the nano-concentration range by flow injection analysis with multiple pulse

- amperometric detection. **Food. Chem**, v. 247, n. 1, p. 66–72, May 2018.
- [11] ALPAR, N.; YARDIM, Y.; SENTÜRK, Z. Selective and simultaneous determination of total chlorogenic acids, vanillin and caffeine in foods and beverages by adsorptive stripping voltammetry using a cathodically pretreated boron-doped diamond electrode. **Sens. Actuator B-Chem**, v. 257, p. 398–408, Mar 2018.
- [12] LUKÁČOVÁ-CHOMISTEKOVÁ, Z.; CULKOVÁ, E.; BELLOVÁ, R.; MELICHERČÍKOVÁ, D.; DURDIK, J.; BEINROHR, E.; RIEVAJ, M.; TOMČÍK, P. Voltammetric detection of antimony in natural water on cathodically pretreated microcrystalline boron doped diamond electrode: A possibility how to eliminate interference of arsenic without surface modification. **Talanta**, v. 178, n. 1, p. 943–948, Feb 2018.
- [13] WANG, J. Analytical electrochemistry, third ed., John Wiley e Sons, Hoboken, 2006, pp 154.
- [14] BRETT, C. M. A.; BRETT, A. M. O. Electrochemistry: principles, methods and applications, first ed., Oxford University Press, Oxford, 1993, pp133.
- [15] MILTON, G. W. The Theory of Composites, first ed., Cambridge University Press, Cambridge, 2002, chapter 1.
- [16] MILTON, G. W. The Theory of Composites, first ed., Cambridge University Press. May 2002, pp 2.
- [17] KALCHER K. Chemically modified carbon paste electrodes in voltammetric analysis. **Electroanalysis**, v. 2, n. 6, p. 419-433, Aug 1990.
- [18] MATSON, W. R. Electrode for anodic stripping voltammetry. **Environmental Sciences Ass Inc**, n. US3855099A, Dez 1974.
- [19] GENO, P. W.; RAVICHANDRAN, K.; BALDWIN, R. P. Chemically modified carbon paste electrodes: Part IV. Electrostatic binding and electrocatalysis at poly(4-vinylpyridine)-containing electrodes. **Jour of Elect. Chem. and Inter. Elect**, v. 183, n. (1–2), p. 155-166, Feb 1985.
- [20] ALEGRET, S.; BARTROLÍ, J. JIMÉNEZ, C.; MARTÍNEZ-FÀBREGAS, E.; MARTORELL, D.; VALDÉS-PEREZGASGA, F. ISFET-based urea biosensor. **Sens. Actuator B-Chem**, v. 16, n. (1–3), p. 453-457, Oct 1993.
- [21] TOLEDO, R. A.; SANTOS, M. C.; CAVALHEIRO, E. T. G.; MAZO, L. H. Determination of dopamine in synthetic cerebrospinal fluid by SWV with a graphite–polyurethane composite electrode. **Anal. Bioanal. Chem**, v. 381, n. 6, p. 1161-1166, Feb 2005.
- [22] ANDERSON, J. E.; TALLMAN, D. E. Graphite-epoxy mercury thin film working electrode for anodic stripping voltammetry. **Anal. Chem**, v. 48, n. 1, p. 209-, Jan 1976.

- [23] DIEWALD, W.; KALCHER, K.; NEUHOLD, C.; ŠVANCARA, I.; CAI, X. Voltammetric behaviour of thallium (III) at a solid heterogeneous carbon electrode using ion-pair formation. **Analyst**, v. 119, n. 2, p. 299-304, 1994.
- [24] TALLMAN, D. E.; PETERSEN, S. L. Composite electrodes for electroanalysis: Principles and applications. **Electroanalysis**, v. 2, n. 7, p. 499- 510, Oct 1990.
- [25] SEMAAN, F. S.; PINTO, E. M.; CAVALHEIRO, E. T. G.; BRETT, C. M. A. A graphite polyurethane composite electrode for the analysis of furosemide. **Electroanalysis**, v. 20, n. 21, p. 2287- 2293, Nov 2008.
- [26] MASCINI, M.; PALLOZZI, F.; LIBERTI, A. A polythene grafite electrode for voltammetry. **Anal. Chim. Acta**, v. 43, n. 1, p. 126-131, Mar 1973.
- [27] KLATT, L. N.; CONNELL, D. R.; ADAMS, R. E.; HONIGBERG, I. L.; PRICE, J. C. Voltammetric characterization of a graphite-teflon electrode. **Anal. Chem**, v. 47, n. 14, p. 2470-2472, Dec1975.
- [28] SWOFFORD, H. S.; CARMAN, R. L. Voltammetric applications of rotating and stationary varbon-epoxy electrode. **Anal. Chem**, v. 38, n. 8, p. 966-969, Jul 1966.
- [29] WANG, J.; NASCER, N. Modified carbon-wax composite electrodes. **Anal. Chim. Acta**, v. 316, n. 2, p. 253-259, Nov 1995.
- [30] STULÍK, K.; PACÁKOVÁ, V.; STÁRKOVÁ, B. Carbon paste for voltammetric detectors in high-performance liquid chromatography. **J. Chromatogr. A**, v. 213, n. 1, p. 41-46, Aug 1981.
- [31] MANO, E. B. *Introdução a Polímeros*. São Paulo: Edgard Blucher, 1985. 111p.
- [32] LY, S. Y.; JUNG, Y. S.; KIM, S. K.; LEE, H. K. Trace Analysis of Lead and Copper Ions in Fish Tissue Using Paste Electrodes. **Anal. Letters**, v. 40, n. 14, p. 2683-2692, Nov 2007.
- [33] ILINOIU E. C.; MANEA, F.; SERRA, P. A.; PODE, R. Simultaneous/Selective Detection of Dopamine and Ascorbic Acid at Synthetic Zeolite-Modified/Graphite-Epoxy Composite Macro/Quasi-Microelectrodes. **Sensors**, v. 13, n. 6, p. 7296-7307, Jun 2013.
- [34] ZHU, Y.; ZHANG, Y.; LI, J.; HAN, Y.; DONG, G.; ZHANG, H.; AL, E. T. Determination of melamine in fresh milk by electrochemistry with solid phase microextraction at bismuthyl chloride modified graphite epoxy composite electrode. **Am. J. Anal. Chem.** v. 2, n. 5, p. 612-618, Sep 2011.
- [35] CALIXTO, C. M. F.; CERVINI, P.; CAVALHEIRO, E. T. G. Determination of atenolol in environmental water samples and pharmaceutical formulations at a graphite-epoxy composite electrode. **Int. Jour Env. Anal. Chem**, v. 92, n. 5, p. 561-570, Oct 2011.

- [36] CETÓ, X.; GONZÁLEZ-CALABUIG, A.; CAPDEVILA, J.; PUIG-PUJOL, A.; VALLE, M. D. Instrumental measurement of wine sensory descriptors using a voltammetric electronic tongue. **Sens. Actuator B-Chem**, v. 207, p. 1053-1059, Feb 2015.
- [37] ALEGRET, S.; ALONSO, J.; BARTROLI, J.; MARTINEZ-FABREGAS, E.; VALDES-PEREZGASGA, F. Applications of graphite-epoxy composites in the construction of electrochemical sensors and biosensors. **NATO ASI series, Series E: Applied Sciences**, v. 252, p.67-79, 1993.
- [38] CERVINI, P. Aplicação de eletrodos compósitos a base de poliuretana-grafite. Tese de doutorado (Universidade de São Paulo - USP), 2006.
- [39] CALIXTO, C. M. F.; CERVINI, P.; CAVALHEIRO, E. T. G. Eletrodo compósito à basede grafite-araldite®: aplicações didáticas. **Quím. Nova**, v. 31, n. 8, p. 2194-2198, Oct 2008.
- [40] AZEVEDO, A. L. M.; OLIVEIRA, R. S.; PONZIO, E. A.; SEMAAN, F. S. Sensor development exploiting graphite-epoxy composite as electrode material. **IOP Conf. Ser. Mater. Sci. Eng**, v. 97, n. 012008, p. 1-4, 2015.
- [41] BALBÍN-TAMAYO, A. I.; RISO, L. S.; PÉREZ-GRAMATGES, A.; FARIAS, P. A. M.; ESTEVA-GUAS, A. M.; YAMANAKA, H. Electrochemical Characterization a New Epoxy Graphite Composite Electrode as Transducer for Biosensor. **Sensors & Transducers**, v. 202, n. 7, p. 59-65, Jul 2016.
- [42] WANG, J.; **Analytical Electrochemistry**, 2a. ed., Wiley-VCH: New Jersey, 2000.
- [43] GOSSER, D. K.; **Cyclic Voltammetry: Simulation and Analysis of Reaction Mechanisms**, first ed. **John Wiley-VCH**, New York, 1993, pp 43-60.
- [44] PACHECO, W. F.; DOYLE, A.; DUARTE, D. R. A.; FERRAZ, C. S.; FARIAS, P. A. M.; AUCELIO, R. Q. Square-wave adsorptive stripping voltammetry for trace determination of dimoxystrobin and azoxystrobin in potatoes and grapes. **Food Anal. Methods**, v. 3, n. 3, p. 205-210, Sep 2010.
- [45] SOUZA, D.; MACHADO, S. A. S.; AVACA, L. A. Voltametria de onda quadrada. Primeira parte: Aspectos teóricos. **Quim. Nova**, v. 26, n. 1, p. 81-89, Jul 2003.
- [46] MIRCESKI, V.; KOMORSKY-LOVRIĆ, S.; LOVRIĆ, M.; **Square-wave voltammetry: Theory and Application**, Berlin: Springer-Verlag, 2007.
- [47] LOVRIĆ, M.; BRANICA, M. Square-wave voltammetric peak current enhancements by adsorption and reversibility of the redox reaction. **J Electroanal. Chem. Inter. Electrochem**, v. 226, n. (1-2), p. 239-251, Jul 1987.

- [48] LOVRIĆ, M.; KOMORSKY-LOVRIĆ, S. Square-wave voltammetry of an adsorbed reactant. **J. Electroanal. Chem. Inter. Electrochem**, v. 248, n. 2, p. 239-253, Jul 1988.
- [49] TORMIN, T. F.; CUNHA, R. R.; RICHTER, E. M.; MUNOZ, R. A. A. Fast simultaneous determination of BHA and TBHQ antioxidants in biodiesel by batch injection analysis using pulsed-amperometric detection. **Talanta**, v. 99, p. 527-531, Sep 2012.
- [50] TORMIN, T. F.; GIMENES, D. T.; CUNHA, R. R.; RICHTER, E. M.; MUNOZ, R. A. A. Fast and direct determination of butylated hydroxyanisole in biodiesel by batch injection analysis with amperometric detection. **Talanta**, v. 85, n. 3 p. 1274-1278, Sep 2011.
- [51] PEREIRA, P. F.; MARRA, M. C.; MUNOZ, R. A. A.; RICHTER, E. M. Fast batch injection analysis system for on-site determination of ethanol in gasohol and fuel ethanol. **Talanta**, v. 90, p. 99-102, Feb 2012.
- [52] da SILVA, R. A. B.; MONTES, R. H. O.; RICHTER, E. M.; MUNOZ, R. A. A. Rapid and selective determination of hydrogen peroxide residues in milk by batch injection analysis with amperometric detection. **Food Chem**, v. 133, n. 1, p. 200-204, Jul 2012.
- [53] WANG, J.; ANGNES, L. Batch injection spectroscopy. **Anal. Letters**, v. 26, n. 11, p. 2329-2339, Sep 1993.
- [54] THAVARUNGKUL, P.; SUPPAPITNARM, P.; KANATHARANA, P.; MATTIASSON, B. Batch injection analysis for the determination of sucrose in sugar cane juice using immobilized invertase and thermometric detection. **Biosens. Bioelectron**, v. 14, p.19-25, Jan 1999.
- [55] WANG, J.; RAYSON, G. D.; TAHA, Z. Batch injection analysis using fiber-optic fluorometric detection. **Appl. Spectrosc**, v. 46, n. 1, p. 107-110, Jan 1992.
- [56] AMORNTHAMMARONG, N.; ZHANG, J. Z.; ORTNER, P. B. An autonomous batch analyzer for the determination of trace ammonium in natural waters using fluorometric detection. **Anal. Methods**, v. 3, n. 7, p. 1501-1506, Jun 2011.
- [57] FERNANDES, J. C. B.; GARCIA, C. A. B.; GRANDIN, L. A.; NETO, G. O.; GODINHO, O. E. S. Determination of Acetylsalicylic Acid in Tablets with Salicylate Ion Selective Electrode in a Batch Injection Analysis System. **J. Braz. Chem. Soc**, v. 9, n. 3, p. 249-251, May 1998.
- [58] LU, J.; CHEN, Q.; DIAMOND, D.; WANG, J. Inverted poly (vinyl chloride)-liquid membrane ion-selective electrodes for high-speed batch injection potentiometric analysis. **Analyst**, v. 118, n. 9, p.1131-1135, Sep 1993.
- [59] BRETT, C. M. A.; FUNGARO, D. A. Poly(ester sulphonic acid) coated mercury thin film electrodes: characterization and

- application in batch injection analysis stripping voltammetry of heavy metal ions. **Talanta**, v. 50, n. 6, p. 1223-1231, Jan 2000.
- [60] BRETT, C. M. A.; FUNGARO, D. A.; MORGADO, J. M.; GIL, M. H. Novel polymer-modified electrodes for batch injection sensors and application to environmental analysis. **J. Electroanal. Chem**, v. 468, n. 1, p. 26-33, Jun 1999.
- [61] WANG, J.; TAHA, Z. Batch injection analysis. **Anal. Chemistry**, v. 63, n. 10, p.1053-1056, May 1991.
- [62] QUINTINO, M. S. M.; ANGNES, L. Batch Injection Analysis: An Almost Unexplored Powerful Tool. **Electroanalysis**, v. 16, n.7, p. 513-523, Apr 2004.
- [63] GIMENES, D. T.; PEREIRA, P. F.; CUNHA, R. R.; DA SILVA, R. A. B.; MUNOZ, R. A. A.; RICHTER, E. M. A simple strategy to improve the accuracy of the injection step in batch injection analysis systems with amperometric detection. **Electroanalysis**, v. 24, n. 9, p. 1805-1810, Sep 2012.
- [64] FERREIRA, L. M. C.; FELIX, F. S.; ANGNES, L. Fast determination of ciclopirox in pharmaceutical products by amperometry in flow and batch injection systems. **Electroanalysis**, v. 24, n. 4, p. 961-966, Abr 2012.
- [65] LIMA, A. P.; STEFANO, J. S.; MONTES, R. H. O.; RICHTER, E. M.; MUNOZ, R. A. A. Fast determination of naproxen in pharmaceutical formulations by batch injection analysis with pulsed amperometric detection. **J. Braz. Chem. Soc**, v. 23, n.10, p.1834-1838, Oct 2012.
- [66] STEFANO, J. S.; TORMIN, T. F.; DA SILVA, J. P.; RICHTER, E. M.; MUNOZ, R. A. A. Amperometric determination of omeprazole on screen-printed electrodes using batch injection analysis. **Microchem. Journal**, v. 133, p. 398–403, Apr 2017.
- [67] CARDOZO, C. G.; CARDOSO, R. M.; SELVA, T. M. G.; DE CARVALHO, A. E.; DOS SANTOS, W. T. P.; PAIXÃO, T. R. L. C.; DA SILVA, R. A. B. Batch Injection Analysis-Multiple Pulse Amperometric Fingerprint: A Simple Approach for Fast On-site Screening of Drugs. **Electroanalysis**, v. 29, p. 2847 – 2854, Oct 2017.
- [68] SILVA, W. P.; SILVA, L. A. J.; MUÑOZ, R. A. A.; RICHTER, E. M. Determinação rápida e simultânea de propifenazona, paracetamol e cafeína utilizando análise por injeção em batelada com detecção amperométrica. **Quim. Nova**, v. 40, n.10, p. 1180-1185, Oct 2017.
- [69] ROCHA, D. P.; CARDOSO, R. M.; MENDONÇA, D. M. H.; RICHTER, E. M.; DA SILVA, S. G.; BATISTA, A. D.; MUNOZ, R. A. A. Solenoid Micro-pumps: A New Tool for Sample Introduction in Batch Injection Analysis Systems with Electrochemical Detection. **Electroanalysis**, v. 30, p. 180 –186, Nov 2018.
- [70] CARDOSO, C. E.; MARTINS, R. O. R.; TELLES, C. A. S.; AUCELIO, R. Q. Sequential Determination of Hydrocortisone and

- Epinephrine in Pharmaceutical Formulations via Photochemically Enhanced Fluorescence. **Microchim. Acta**, v.146, n. 1, p.79-84, May 2004.
- [71] MARQUES, F. F. C.; DA CUNHA, A. L. M. C.; AUCÉLIO, R. Q. Laser induced fluorescence and photochemical derivatization for trace determination of camptothecin. **Talanta**, v. 83, n. 1, p. 256-261, Nov 2010.
- [72] PATERNÒ, E. Ricerche sull'acido lapacico. **Gazz. Chim. Ital**, v. 12, p. 337-392, Jan 1882.
- [73] HOOKER, S. C. The constitution of lapachol and its derivatives. Part V. The structure of Paternò's "isolapachone"^{1,2}. **J. Am. Chem. Soc**, v. 58, n. 7, p. 1190-1197, Jul 1936.
- [74] FIESER, L. F. Naphthoquinone antimalarials. XVI. Water-soluble derivatives of alcoholic and unsaturated compounds. **J. Am. Chem. Soc**, v. 70, n. 10, p. 3232-3237, Oct 1948.
- [75] FERREIRA, C. A. C.; FERREIRA, V. F.; PINTO, A. V.; LOPES, R. S. C.; PINTO, M. C. R.; DA SILVA, A. J. R. ¹³CNMR Spectra of natural products Part 5 - Naphthopyrandiones and naphthofurandiones. **An. Acad. Bras. Cienc**, v. 59, p. 5-8, Mar 1987.
- [76] PINTO, A. V.; PINTO, M. C. F. R.; DE OLIVEIRA, C. G. T. Síntese das α - e β -norlapachonas, propriedades em meio ácido e reações com N-bromosuccinimida. **An. Acad. Bras. Cienc**, v. 54, p.107-114, 1982.
- [77] DE ANDRADE-NETO, V. F.; GOULART, M. O. F.; DA SILVA FILHO, J. F.; DA SILVA, M. J.; PINTO, M. C. F. R.; PINTO, A. V.; ZALIS, M. G.; CARVALHO, L. H.; KRETTLI, A. U. Antimalarial activity of phenazines from lapachol, beta-lapachone and its derivatives against Plasmodium falciparum in vitro and Plasmodium berghei in vivo. **Bioorg. Med. Chem. Lett**, v. 4, n. 5, p. 1145-1149, Mar 2004.
- [78] https://www.sasrx.com/documents/pdf/PI_APP_gentamicin_Injectio_n_Jul_2008.pdf (Access in 30/10/17).
- [79] <http://www.drugs.com/pro/gentamicin-sulfate.html> (Access in 30/10/17).
- [80] CLAES, P.; BUSSON, R.; VANDERHAEGHE, H. Determination of the component ratio of commercial gentamicins by high-performance liquid chromatography using pre-column derivatization. **J. Chromatogr**, v. 298, p. 445-457, Mar 1984.
- [81] FRUTOS, P.; TORRADO, S.; PEREZ-LORENZO, M. E.; FRUTOS, G. A validated quantitative colorimetric assay for gentamicin. **J. Pharm. Biomed. Anal**, v. 21, n.6, p. 1149-1159, Jan 2000b.
- [82] LIMA, J. L. X.; PERÉZ-GRAMATGES, A.; AUCÉLIO, R. Q.; DA SILVA, A. R. Improved quantum dots fluorescence quenching using organized medium: A study of the effect of naphthoquinones aiming

- the analysis of plant extracts. **Microchem. Journal**, v. 110, p. 775–782, Sep 2013.
- [83] KHAN, S.; MIGUEL, E. M.; DE SOUZA, C. F.; DA SILVA, A. R.; AUCÉLIO, R. Q. Thioglycolic acid-CdTe quantum dots sensing and molecularly imprinted polymer based solid phase extraction for the determination of kanamycin in milk, vaccine and stream water samples. **Sens. Actuator B-Chem**, v. 246, p. 444-454, Jul 2017.
- [84] B BLANCO, E.; BLANCO, G.; GONZALEZ-LEAL, J. M.; BARRERA, M. C.; DOMINGUEZ, M.; RAMIREZ-DEL-SOLAR, M. Green and fast synthesis of amino-functionalized graphene quantum dots with deep blue photoluminescence. **J. Nanopart. Res**, v.17, n. 214, p. 1-13, May 2015.
- [85] FRANK, A. L.; MCKNIGHT, R.; KIRKHORN, S. R.; GUNDERSON, P. Issues of agricultural safety and health. **Annu. Rev. Publ. Health**, v. 25, p. 225-245, Apr 2004.
- [86] BALBA, H. Review of strobilurin fungicide chemicals. **J. Environ. Sci. Health B**, v. 42, n. 4, p. 441-451, May 2007.
- [87] CHEN, J.; LOO, B.; RAY, C. Determination of Trifloxystrobin and Its Metabolites in Hawaii Soils by ASE-LC-MS/MS. **J. Agric. Food Chem**, v. 56, p.1829–1837, Feb 2008.
- [88] BRASIL, Ministério da Saúde. Agência Nacional de Vigilância Sanitária – ANVISA. D.O.U. (8September 2009), p. 50.
- [89] CODEX ALIMENTARIUS, Pesticide Residues in Food and Feed. Base.
<<http://www.codexalimentarius.net/pestres/data/pesticides/details.html?id=229>>.
<<http://www.codexalimentarius.net/pestres/data/pesticides/details.html?id=199>>.
- [90] SANINO, A.; BOLZONI L.; BANDINI, M. Application of liquid chromatography with electrospray tandem mass spectrometry to the determination of a new generation of pesticides in processed fruits and vegetables. **J. Chromatogr. A**, v. 1036, n. 2, p.161-169, May 2004.
- [91] CHRISTENSEN H. B.; GRANBY, K. Method validation for strobilurin fungicides in cereals and fruit. **Food Addit. Contam**, v. 18, n. 10, p.866-, Oct 2001.
- [92] BO, H. B.; WANG, J. H.; GUO, C. H.; QIN R.; LU, X. Y. Determination of strobilurin fungicide residues in food by gas chromatography–mass spectrometry. **Chinese J. Anal. Chem**, v. 36, p. 1471-1475, Nov 2008.
- [93] VIÑAS, P.; CAMPILLO, N.; CASTILLO, N. M.; CÓRDOBA, M. H. Method Development and Validation for Strobilurin Fungicides in Baby Foods by Solid-Phase Microextraction Gas Chromatography-Mass Spectrometry. **J. Chromatogr. A**, v. 1216, n. 1, p.140-146, Jan 2009.

- [94] GONZALEZ-RODRIGUEZ, R. M.; CANCHOGRANDE, B.; SIMAL-GANDARA, J. Multiresidue determination of 11 new fungicides in grapes and wines by liquid-liquid extraction/cleanup and programmable temperature vaporization injection with analyte protectants/gas chromatography/ion trap mass spectrometry. **J. Chromatogr. A**, v. 1216, n. 32, p. 6033-6042, Aug 2009.
- [95] VIÑAS, P.; MARTÍNEZ-CASTILLO, N.; CAMPILLO, N.; HERNÁNDEZ-CÓRDOBA, M. Liquid-liquid microextraction methods based on ultrasound-assisted emulsification and single-drop coupled to gas chromatography-mass spectrometry for determining strobilurin and oxazole fungicides in juices and fruits. **J. Chromatogr. A**, v. 1217, n. 42, p. 6569-6577, Aug 2010.
- [96] ABREU, S. M.; CORREIA, M.; HERBERT, P.; SANTOS L.; ALVES, A. Screening of grapes and wine for azoxystrobin, kresoxim-methyl and trifloxystrobin fungicides by HPLC with diode array detection. **Food Addit. Contam.**, v. 22, n. 6, p. 549-556, Feb 2005.
- [97] CAMPILLO, N.; VIÑAS, P.; AGUINAGA, N.; FÉREZ, G.; CÓRDOBA, M. H. Stir bar sorptive extraction coupled to liquid chromatography for the analysis of strobilurin fungicides in fruit samples. **J. Chromatogr. A**, v.1217, n. 27, p. 4529-4534, Jul 2010.
- [98] LIANG, P.; LIU, G.; WANG, F.; WANG, W. Ultrasound-assisted surfactant-enhanced emulsification microextraction with solidification of floating organic droplet followed by high performance liquid chromatography for the determination of strobilurin fungicides in fruit juice samples. **J. Chromatogr. B**, v. 926, p. 62-67, May 2013.
- [99] YANG, M.; XI, X.; WU, X.; LU, R.; ZHOU, W.; ZHANG, S.; GAO, H. Vortex-assisted magnetic β -cyclodextrin/attapulgite-linked ionic liquid dispersive liquid-liquid microextraction coupled with high-performance liquid chromatography for the fast determination of four fungicides in water samples. **J. Chromatogr. A**, v. 1381, p. 37-47, Jan 2015.
- [100] BANDZUCHOVÁ, L.; SVORC, L.; SOCHR, J.; SVÍTKOVÁ, J.; CHYLKOVÁ, J. Voltammetric method for sensitive determination of herbicide picloram in environmental and biological samples using boron-doped diamond film electrode. **Electrochim. Acta**, v. 111, 242-249, Nov 2013.
- [101] BANDŽUCHOVÁ, L.; ŠVORC, L.; VOJS, M.; MARTON, M.; MICHNIAK, P.; CHÝLKOVA, J. Self-assembled sensor based on boron-doped diamond and its application in voltammetric analysis of picloram. **Int. J. Environ. Anal. Chem**, v. 94, n. 9, p. 943-953, Abr 2014.
- [102] SVORC, L.; RIEVAJ, M.; BUSTIN, D. Green electrochemical sensor for environmental monitoring of pesticides: Determination of atrazine in river waters using a boron-doped diamond electrode. **Sens. Actuator B-Chem**, v. 181, p. 294-300, May 2013.

- [103] SELESOVSKA, R.; JANIKOVA, L.; CHYLKOVA, J. Green electrochemical sensors based on boron-doped diamond and silver amalgam for sensitive voltammetric determination of herbicide metamitron. **Monatsh. Chem**, v. 146, n. 5, p. 795-805, May 2015.
- [104] FIGUEIREDO-FILHO, L. C. S.; SARTORI, E. R.; FATIBELLO-FILHO, O. Electroanalytical determination of the linuron herbicide using a cathodically pretreated boron-doped diamond electrode: comparison with a boron-doped diamond electrode modified with platinum nanoparticles. **Anal. Methods**, v. 7, n. 2, p. 643-649, Nov 2015.
- [105] CHÝLKOVÁ, J.; TOMÁŠKOVÁ, M.; ŠVANCARA, I.; JANÍKOVÁ L.; ŠELEŠOVSKÁ, R. Determination of methiocarb pesticide using differential pulse voltammetry with a boron-doped diamond electrode. **Anal. Methods**, v. 7, p. 4671-4677, Apr 2015.
- [106] JANIKOVA-BANDZUCHOVA, L.; ŠELEŠOVSKÁ, R.; SCHWARZOVÁ-PECKOVÁ K.; CHÝLKOVÁ, J. Sensitive voltammetric method for rapid determination of pyridine herbicide triclopyr on bare boron-doped diamond electrode. **Electrochim. Acta**, v.154, p. 421-429, Feb 2015.
- [107] BRYCHT, M.; SKRZYPEK, S.; KACZMARSKA, K.; BURNAT, B.; LENIART, A.; GUTOWSKA, N. Square-wave voltammetric determination of fungicide fenfuram in real samples on bare boron-doped diamond electrode, and its corrosion properties on stainless steels used to produce agricultural tools. **Electrochim. Acta**, v. 169, p. 117-125, Jul 2015.
- [108] DORNELLAS, R. M.; MUÑOZ, R. A. A.; AUCÉLIO, R. Q. Electrochemical determination of picoxystrobin on boron-doped diamond electrode: Square-wave voltammetry versus BIA-multiple pulse amperometry. **Microchem. Journal**, v. 123, p. 1-8, Nov 2015.
- [109] WANG, Y.; ZHI, J.; LIU, Y.; ZHANG, J. Electrochemical detection of surfactant cetylpyridinium bromide using boron-doped diamond as electrode. **Electrochem. Commun**, v. 13, n. 1, p. 82-83, Jan 2011.
- [110] SOUZA, D.; MACHADO, S. A. S.; AVACA, L. A. voltametria de onda quadrada. primeira parte: aspectos teóricos. **Quim. Nova**, v. 26, p. 81-89, Jul 2003.
- [111] HAMMERICH, O.; LUND, H. Organic Electrochemistry (Marcel Dekker, New York, 2001), p. 471.
- [112] BUSSY, U.; FERCHAUD-ROUCHER, V. F.; TEA, I.; KREMPF, M.; SILVESTRE, V.; BOUJTITA, M. Electrochemical oxidation behavior of acebutolol and identification of intermediate species by liquid chromatography and mass spectrometry. **Electrochim. Acta**, v. 69, p. 351-357, May 2012.
- [113] BENCHARIF, L.; TALLEC, A.; TARDIVEL, R. Anodic behaviour of aromatic oximes: an electrochemical deoximation reaction. **Electrochim. Acta**, v. 42, n. (23-24), p. 3509-3512, Jan 1997.

- [114] BANERJEE, K.; LIGON, A. P.; SPITELLER, M. Photoisomerization kinetics of trifloxystrobin. **Anal. Bioanal. Chem**, v. 382, n. 7, p. 1527-1533, Jul 2005.
- [115] BANERJEE, K.; LIGON, A. P.; SPITELLER, M. **Anal. Bioanal. Chem**, v. 388, n. 8, p. 1831-1838, Aug 2007.
- [116] DORNELLAS, R. M.; FRANCHINI, R. A. A.; AUCÉLIO, R. Q. Determination of the fungicide picoxystrobin using anodic stripping voltammetry on a metal film modified glassy carbon electrode. **Electrochimica. Acta**, v. 97, p. 202-209, May 2013.
- [117] DE SOUZA, C. F.; CUNHA, A. L. M. C.; AUCÉLIO, R. Q. Determination of Picoxystrobin and Pyraclostrobin by MEKC with On-Line Analyte Concentration. **Chromatographia**, v. 70, n. 9, p.1461-1466, Nov 2009.
- [118] WANG, K.; CHEN, G.; WU, X.; SHI, J.; GUO, D. Determination of Strobilurin Fungicide Residues in Fruits and Vegetables by Micellar Electrokinetic Capillary Chromatography with Sweeping. **J. Chromatogr. Sci**, v. 52, n. 2, p. 157-161, Feb 2014.
- [119] FLURER, C. L.; WOLNIK, K. A. Quantification of getamicin sulfate in injectable solutions by capillary electrophoresis. **J. Chromatogr. A**, v. 663, n. 2, p. 259-263, Mar 1994.
- [120] WEINSTEIN, M. J.; LUEDEMANN, G. M.; ODEN, E. M.; WAGMAN, G. H.; ROSSELET, J. P.; MARQUEZ, J. A.; CONIGLIO, C. T.; CHARNEY, W.; HERZOG, H. L.; BLACK, J. Gentamicin, a new antibiotic complex from micromonspora. **J. Med. Chem**, v. 6, n. 4, p. 463-464, Jul 1963.
- [121] EDSON, R. S.; TERRELL, C. L. The Aminoglycosides. **Mayo Clin. Proc**, v. 74, n. 5, p. 519-528, May 1999.
- [122] TAN, X.; JIANG, Y. W.; HUANG, Y. J.; HU, S. H. Persistence of gentamicin residues in milk after the intramammary treatment of lactating cows for mastitis. **J. Zhejiang. Univ. Sci. B**, v. 10, n. 4, p. 280-284, Apr 2009.
- [123] SIKARRA, D.; SHUKLA, V.; KHARIA, A. A.; CHATTERJEE D. P. Thechniques for solubility enhancement of poorly soluble drugs: an overview. **J. Med. Pharm. and allied sciences**, v.1, p. 1-22, Dec 2012.
- [124] FLURER, C. L. The analysis of aminoglycoside antibiotics by capillary electrophoresis. **J. Pharm. Biomed. Anal**, v. 13, n. 7, p. 809-816, Jun 1995.
- [125] KAALE, E.; LEONARD, S.; VAN SCHEPDAEL, A.; ROETS, E.; HOOGMARTENS, J. Capillary electrophoresis analysis of gentamicin sulphate with UV detection after pre-capillary derivatization with 1.2-phthalic dicarboxaldehyde and mercaptoacetic acid. **J. Chromatogr. A**, v. 895, n. (1-2), p. 67-79, Nov 2000.

- [126] ARCELLONI, C.; COMUZZI, B.; VAIANI, R.; PARONI, R. Quantification of gentamicina in Mueller-Hinton agar by high-performance liquid chromatography. **J. Chromatogr. B**, v. 753, n. 1, p. 151-156, Mar 2001.
- [127] ISOHERRANEN, N.; SOBACK, S. Determination of Gentamicins C1, C1a and C2 in Plasma and Urine by HPLC. **Clin. Chem**, v. 46, n. 6, p. 837-842, Jun 2000.
- [128] FENNEL, M. A.; UBOH, C. E.; SWEENEY, R.W.; SOMA, L. R. Gentamicin in tissue and whole milk: an improved method for extraction and cleanup of samples for quantification on HPLC. **J. Agric. Food Chem**, v 43, n. 7, p. 1849-1852, Jul 1995.
- [129] SAR, F.; LEROY, P.; NICOLAS, A. Development and optimization of a liquid chromatographic method for the determination of gentamicin in calf tissues. **Anal. Chim. Acta**, v. 275, n. (1-2), p. 285-293, Apr 1993.
- [130] CHERLET, M.; DE BAERE, S.; DE BACKER, P. Determination of gentamicin in swine and calf tissues by high-performance liquid chromatography combined with electrospray ionization mass spectrometry. **J. Mass. Spectrom**, v. 35, n. 11, p. 1342-1350, Nov 2000.
- [131] HELLER, D. N.; PEGGINS, J. O.; NOCHETTO, C. B.; SMITH, M. L.; CHIESA, O. A.; MOULTON, K. LC/ MS/ MS measurement of gentamicin in bovine plasma, urine, milk, and biopsy samples taken from kidneys of standing animals. **J. Chromatogr. B**, v. 821, n. 1, p. 22-30, Jul 2005.
- [132] TURNIPSEED, S. B.; CLARK, S. B.; KARBIWNYK, C. M.; ANDERSEN, W. C.; MILLER, K. E.; MADSON, M. R. Analysis of aminoglycoside residues in bovine milk by liquid chromatography electrospray ion trap mass spectrometry after derivatization with phenyl isocyanate. **J. Chromatogr. B**, v. 877, n. (14-15), p. 1487-1493, May 2009.
- [133] BAIETTO, L.; D'AVOLIO, A.; DE ROSA, F. G.; GARAZZINO, S.; MICHELAZZO, M.; VENTIMIGLIA, G.; SICCARDI, M.; SIMIELE, M.; SCIANDRA, M.; DI PERRI, G. Development and validation of a simultaneous extraction procedure for HPLC-MS quantification of daptomycin, amikacin, gentamicin, and rifampicin in human plasma. **Anal. Bioanal. Chem**, v. 396, n. 2, p.791-798, Nov 2010.
- [134] LÖFFLER, D.; TERNES, T. A. Analytical method for the determination of the aminoglycoside gentamicin in hospital wastewater via liquid chromatography-electrospray-tandem mass spectrometry. **J. Chromatogr. A**, v. 1000, n. (1-2), p. 583-588, Jun 2003.
- [135] VUCICEVIC-PRCETIC, K.; CSERVENAK, R.; RADULOCIC, N. Development and validation of liquid chromatography tandem mass spectrometry methods for the determination of gentamicin, lincomycin, and spectinomycin in the presence of their impurities in

- pharmaceutical formulations. **J. Pharm. Biomed. Anal.**, v. 56, n. 4, p. 736-742, Jul 2011.
- [136] LEHOTAY, S. J.; MASTOVSKA, K.; LIGHTFIELD, A. R.; NUNEZ, A.; DUTKO, T.; BLUHM, C. N. G. L. Rapid analysis of aminoglycoside antibiotics in bovine tissues using disposable pipette extraction and ultrahigh performance liquid chromatography-tandem mass spectrometry. **J. Chromatogr. A**, v. 1313, p. 103-112, Oct 2013.
- [137] BIJLEVELD, Y.; DE HAAN, T.; TOERSCHKE, J.; JORJANI, S.; VAN DER LEE, J.; GROENENDAAL, F.; DIJK, P.; VAN HEIJST, A.; GAVILANES, A. W. D.; DE JONGE, R.; DIJKMAN, K. P.; VAN STRAATEN, H.; RIJKEN, M.; ZONNENBERG, I.; COOLS, F.; NUYTEMANS, D.; MATHÔT, R. A simple quantitative method analyzing amikacin, gentamicin, and vancomycin levels in human newborn plasma using ion-pair liquid chromatography/tandem mass spectrometry and its applicability to a clinical study. **J. Chromatogr. B**, v. 951-952, p.110-118, Mar 2014.
- [138] STYPULKOWSKA, K.; BLAZEWICZ, A.; FIJALEK, Z.; SARNA, K. Determination of gentamicin sulphate composition and related substances in pharmaceutical preparations by LC with charged aerosol detection. **Chromatography**, v. 72, n. (11-12), p. 1225-1229, Dec 2010.
- [139] STEAD, D. A.; RICHARDS, R. M. E. Sensitive fluorimetric determination of gentamicin sulfate in biological matrices using solid-phase extraction, pre-column derivatization with 9-fluorenylmethyl chloroformate and reversed phase high-performance liquid chromatography. **J. Chromatogr. B**, v. 675, n. 2, p. 295-302, Jan 1996.
- [140] RYAN, J. A. Colorimetric determination of gentamicin, kanamycin, tobramycin, and amikacin aminoglycosides with 2,4-dinitrofluorobenzene. **J. Pharm. Sci**, v. 73, n. 9, p. 1301-1302, Sep 1984.
- [141] FRUTOS, P.; TORRADO, S.; PEREZ-LORENZO, M. E.; FRUTOS, G. A validated quantitative colorimetric assay for gentamicin. **J. Pharm. Biomed. Anal.**, v. 21, n. 6, p. 1149-1159, Jan 2000a.
- [142] EL-DIDAMONY, A. M.; AMIN, A. S.; GHONEIM, A. K.; TELEBANY, A. M. Indirect spectrophotometric determination of gentamicin and vancomycin antibiotics on their oxidation by potassium permanganate. **J. Chem**, v. 4, p. 708-722, Dec 2006.
- [143] AL-MAJED, A. A.; BELAL, F.; ABOUNASSIF, M. A.; KHALIL, N. Y. Fluorimetric determination of gentamicin in dosage forms and biological fluids through derivatization with 4-chloro-7-nitrobenzo-2-oxa-1.3-diazole (NBD-Cl). **Microchim. Acta**, v. 141, p. 1-6, Jun 2003.
- [144] RIZK, M.; EL-SHABRAWY, Y.; ZAKHARI, N. A.; TOUBAR, S. S.; CARREIRA, L. A. Fluorimetric determination of aminoglycoside

- antibiotics using lanthanide probe ion spectroscopy. **Talanta**, v. 42, n. 12, p. 1849-1856, Dec 1995.
- [145] GILMARTIN, M. R.; MCLAREN, J.; SCHACHT, J. Confounding factors in lanthanide ion probe spectrofluorometric assay of aminoglycoside antibiotics. **Anal. Biochem**, v. 283, n. 1, p. 116-119, Jul 2000.
- [146] SANTOS, L. H. M. L. M.; ARAÚJO, A. N.; REIS, B.; MONTENEGRO, M. C. B. S. M. Development of a Multicommutated Flow System with Chemiluminometric Detection for Quantification of gentamicin in Pharmaceuticals. **J. Autom. Methods Manag. Chem**, v. 913207, p.1-7, Oct 2010.
- [147] TOMA, H. E.; ZAMARION, V. M.; TOMA, S. H.; ARAKI, K. The coordination chemistry at gold nanoparticles. **J. Braz. Chem. Soc**, v. 21, n. 7, p. 1158-1176, Apr 2010.
- [148] CAGLAYAN, M. G.; ONUR, F. Silver nanoparticle based analysis of aminoglycosides. **Spectrosc. Lett**, v. 47, n. 10, p. 771-780, Oct 2014.
- [149] CAGLAYAN, M. G.; ONUR, F. A metal-enhanced fluorescence study of primary amines: determination of aminoglycosides with europium and gold nanoparticles. **Anal. Methods**, v. 7, n. 4, p. 1407-1414, Dec 2015.
- [150] WANG, M. T.; LIU, M. H.; WANG, C. R. C.; CHANG, S. Y. Silver-Coated gold nanoparticles as concentrating probes and matrices for surface-assisted laser desorption/ionization mass spectrometric analysis of aminoglycosides. **J. Am. Soc. Mass. Spectrom**, v. 20, n. 10, p. 1925-1932, Oct 2009.
- [151] ZHU, Y.; QU, C.; KUANG, H.; XU, L.; LIU, L.; HUA, Y.; WAN, L.; XU, C. Simple, rapid and sensitive detection of antibiotics based on the side-by-side assembly of gold nanorod probes. **Biosens. Bioelectron**, v. 26, n. 11, p. 4387-4392, May 2011.
- [152] MIRANDA-ANDRADES, J. R.; PÉREZ-GRAMATGES, A.; PANDOLI, O.; ROMANI, E. C.; AUCÉLIO, R. Q.; DA SILVA, A. R. Spherical gold nanoparticles and gold nanorods for the determination of gentamicin. **Spectrochim. Acta Part A: Mol. Biomol. Spectrosc**, v. 172, p. 126-134, Apr 2017.
- [153] WANG, R.; FAN, S.; WANG, R.; WANG, R.; DOU, H.; WANG, L. Determination of aminoglycoside by a colorimetric method based on the aggregation of gold nanoparticles. **Nano: Brief. Reports and Reviews**, v. 4, p. 13500037-13500045, Aug 2013.
- [154] ADAMS, E.; ROELANTS, W.; DE PAEPE, R.; ROETS, E.; HOOGMARTENS, J. Analysis of gentamicin by liquid chromatography with pulsed electrochemical detection. **J. Pharm. Biomed. Anal**, v. 18, n. (4-5), p. 689-698, Dec 1998.
- [155] KHALIL, M. M.; ABED EL AZIZ, G. M. New in situ modified PVC membrane electrodes for potentiometric determination of

- gentamicin sulphate in its pharmaceutical formulation and biological fluids. **Int. J. Adv. Res**, v. 2, p. 426-437, Marc 2014.
- [156] WHITCOMBE, M. J.; KIRSCH, N.; NICHOLLS, I. A. Molecular imprinting science and technology: a survey of the literature for the years 2004-2011. **J. Mol. Recognit**, v. 27, n. 6, p. 297-401, Jun 2014.
- [157] YEH, W. M.; HO, K. C. Amperometric morphine sensing using a molecularly imprinted polymer-modified electrode. **Anal. Chim. Acta**, v. 542, n. 1, p. 76-82, Jun 2005.
- [158] MORENO-GONZÁLEZ, D.; HAMED, A. M.; GARCÍA-CAMPAÑA, A. M.; GÁMIZ-GRACIA, L. Evaluation of hydrophilic interaction liquid chromatography-tandem mass spectrometry and extraction with molecularly imprinted polymers for determination of aminoglycosides in milk and milk-based functional foods. **Talanta**, v. 171, p. 74-80, Apr 2017.
- [159] SCHIRHAG, R. Bioapplications for molecularly imprinted polymer. **Anal. Chem**, v. 86, n. 1, p. 250-261, Aug 2014.
- [160] CHEONG, W. J.; YANG, S. H.; ALI, F. Molecular imprinted polymers for separation science: A review of reviews. **J. Sep. Sci**, v. 36, n. 3, p. 609-628, Dec 2013.
- [161] HUSSAIN, H.; KROHN, K.; AHMAD, V. G.; MIANA, G. A.; GREEND, I. R. Lapachol: an overview, **ARKIVOC ii**, p. 145-171, Jun 2007.
- [162] GUIRAUD, P.; STEIMAN, R.; CAMPOS-TAKAKI, G. M.; SEIGLE-MURANDI, F.; DE BUOCHBERG, M. S. Comparison of antibacterial and antifungal activities of lapachol and betalapachone. **Planta. Med**, v. 60, n. 4, p. 373-374, Aug 1994.
- [163] LI, C. J.; ZHANG, L. J.; DEZUBE, B. J.; CRUMPACKER, C. S.; PARDEE, A. B. Three inhibitors of type 1 human immunodeficiency virus long terminal repeat-directed gene expression and virus replication. **Proc. Natl. Acad. Sci. U. S. A**, v. 9, n. 5, p. 1839-1842, Mar 1993.
- [164] LIMA, N. M. F.; CORREIA, C. S.; FERRAZ, P. A. L.; PINTO, A.V.; PINTO, M. C. R. F.; SANTANA, A. E. G.; GOULART, M. O. F. Molluscicidal Hydroxynaphthoquinones and Derivatives: Correlation Between their Redox Potential and Activity Against *Biomphalaria glabrata*. **J. Braz. Chem. Soc**, v.13, n. 6, p. 822-829, Oct 2002.
- [165] SALAS, C. O.; FAÚNDEZ, M.; MORELLO, A.; MAYA, J. D.; TAPIA, R. A. Natural and synthetic naphthoquinones active against *Trypanosoma cruzi*: an initial step towards new drugs for Chagas disease. **Curr. Med. Chem**, v.18, n. 1, p.144–161, Jan 2011.
- [166] OLIVEIRA, M. F.; LEMOS, T. L. G.; DE MATTOS, M. C.; SEGUNDO, T. A.; SANTIAGO, G. M. P.; BRAZ-FILHO, R. New enamine derivatives of lapachol and biological activity. **An. Acad. Bras. Cienc**, v. 74, n. 2, p. 211-221, Jun 2002.

- [167] HOFFMAN, E. J. *Cancer and the Search for Selective Biochemical Inhibitors*, second ed., CRC Press, New York, EUA, 2007, pp 308.
- [168] STEINERT, J.; KHANLAF, H.; RIMPLER, M. HPLC separation and determination of naphtho[2,3-b]furan-4,9-diones and related compounds in extracts of *Tabebuia avellanedae* (Bignoniaceae). **J. Chromatogr. A**, v. 693, n. 2, p. 281–287, Feb 1995.
- [169] JÁCOME, R. L. R. P.; DE OLIVEIRA, A. B.; RASLAN, D. S.; MÜLLER, A.; WAGNER, H. Análise de naftoquinonas em extratos brutos de raízes de *Zeyheria montana* M. (bolsa-de-pastor). **Quim. Nova**, v. 22, n. 2, p. 175-177, Apr 1999.
- [170] AUCÉLIO, R. Q.; PERÉZ-CORDOVÉS, A. I.; LIMA, J. L. X.; FERREIRA, A. B. B.; GUAS, A. M. E.; DA SILVA, A. R. Determination of lapachol in the presence of other naphthoquinones using 3MPA-CdTe quantum dots fluorescent probe. **Spectrochim Acta Part A: Mol. and Biomol. Spectroscopy**, v. 100, p. 155–160, Jan 2013.
- [171] FINKEL, J. M.; HARRISON JR., S. D. Fluorometric method for the determination of lapachol in serum. **Anal. Chem**, v. 41, n. 13, p. 1854–1855, Nov 1969.
- [172] ALCANFÔR, S. K. B.; CARDOSO, S. V.; DE LIMA, C. G. Fluorimetric studies of some quinones and quinonoid compounds after reduction reaction. **Anal. Chim. Acta**, v. 289, n. 3, p. 273–290, May 1994.
- [173] NGAMENI, E.; TONLE, I. K.; NANSEU, C. P.; WANDJI, R. Voltammetry Study of 2-Hydroxy-3-isopropenyl-1,4-naphthoquinone Using a Carbon Paste Electrode. **Electroanalysis**, v. 12, n.11, p. 847-852, Jul 2000.
- [174] ABREU, F. C.; GOULART, M. O. F.; BRETT, A. M. O. Reduction of Lapachones in Aqueous Media at a Glassy Carbon Electrode. **Electroanalysis**, v. 14, n.1, p. 29-34, Jan 2002.
- [175] GOULART, M. O. F.; FALKOWSKI, P.; OSSOWSKI, T.; LIWO, A. Electrochemical study of oxygen interaction with lapachol and its radical anions. **Bioelectrochem**, v. 59, n. (1-2), p. 85–87, Abr 2003.
- [176] OLIVEIRA-BRETT, A. M.; GOULART, M. O. F.; ABREU, F. C. Reduction of lapachones and their reaction with L-cysteine and mercaptoethanol on glassy carbon electrodes. **Bioelectrochem**, v. 56, n. (1-2), p. 53– 55, May 2002.
- [177] NITSCHKE, M.; PASTORE, G. M. Biossurfactantes: propriedades e aplicações. **Quim. Nova**, v. 25, n.5, p. 772-776, Mar 2002.
- [178] VANDAMME, T. F. Microemulsions as ocular drug delivery systems: recent developments and future challenges. **Prog. Retin. Eye. Res**, v. 21, n. 1, p.15-34, Jan 2002.
- [179] BERGAMINI, M. F.; SANTOS, A. L.; STRADIOTTO, N. R.; ZANONI, M. V. B. A disposable electrochemical sensor for the rapid

- determination of levodopa. **J. Pharm. Bio. Anal**, v. 39, n. (1-2), p. 54-59, Sep 2005.
- [180] BERGAMINI, M. F.; ZANONI, M. V. B. Anodic stripping voltammetric determination of autothiomalate in urine using a screen-printed carbon electrode. **Electroanalysis**, v. 18, n. 11, p. 1457-1462, Nov 2006.
- [181] HOYER, B.; JENSEN, N. Stabilization of the voltammetric serotonin signal by surfactants. **Electrochem. Com**, v. 8, n. 2, p. 323-328, Feb 2006.
- [182] JARA-ULLOA, P.; NÚÑEZ-VERGARA, L. J.; SQUELLA, J. A. Micellar effects on the reduction of 4-nitroimidazole derivative: detection and quantification of the nitroradical anion. **Electroanalysis**, v. 19, p. 1490-1495, 2007.
- [183] GUIN, P. S.; DAS, S.; MANDAL, P. C. Electrochemical Reduction of Quinones in Different Media: A Review. **Int. J. Electrochem**, v. 2011, p. 1-22, Jan 2011.
- [184] OSSOWSKI, T.; GOULART, M. O. F.; DE ABREU, F. C.; SANT'ANA, A. E. G.; MIRANDA, P. R. B.; COSTA, C. O.; LIWO, A.; FALKOWSKI, P.; ZARZECZANSKA, D. Determination of the pKa values of some biologically active and inactive hydroxyquinones. **J. Braz. Chem. Soc**, v. 19, n. 1, p. 175-183, Jan 2008.
- [185] FERREIRA, T. L.; PAIXÃO, T. R. L. C.; RICHTER, E. M.; EL SEOUD, O. A.; BERTOTTI, M. Use of Microdevices To Determine the Diffusion Coefficient of Electrochemically Generated Species: Application to Binary Solvent Mixtures and Micellar Solutions. **J. Phys. Chem. B**, v. 111, n. 43, p. 12478-12484, Oct 2007.
- [186] DOS REIS, A. P.; TARLEY, C. R. T.; MANIASSO, N.; KUBOTA, L. T. Exploiting micellar environment for simultaneous electrochemical determination of ascorbic acid and dopamine. **Talanta**, v. 67, n. 4, p. 829-835, Oct 2005.
- [187] DE SOUZA, D.; CODOGNOTO, L.; MALAGUTTI, A. R.; TOLEDO, R. A.; PEDROSA, V. A.; OLIVEIRA, R. T. S.; MAZO, L. H.; AVACA, L. A.; MACHADO, S. A. S. Voltametria de onda quadrada. Segunda Parte: Aplicações. **Quim. Nova**, v. 27, n. 5, p. 790-797, Jun 2004.
- [188] CABRAL, M. F.; DE SOUZA, D.; ALVES, C. R.; MACHADO, S. A. S. Estudo do comportamento eletroquímico do herbicida ametrina utilizando a técnica de voltametria de onda quadrada. **Ecl. Quim**, v. 28, n. 2, p. 41-47, Apr 2003.
- [189] VAZ, C. M. P.; CRESTANA, S.; MACHADO, S. A. S.; MAZO, L. H.; AVACA, L. A. Electroanalytical Determination of the Herbicide Atrazine in Natural Waters. **Int. J. Environ. Anal. Chem**, v. 62, n.11, p. 65-76, Sep 1996.

A

Published papers



Revista Virtual de Química

ISSN 1984-6835

Artigo

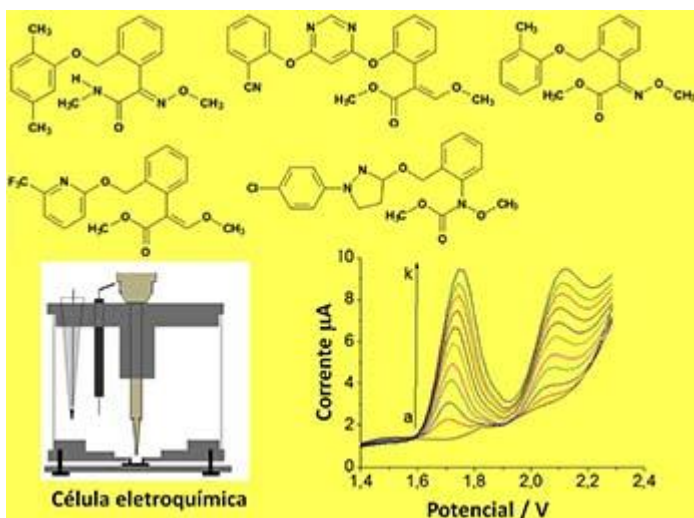
Abordagens Eletroanalíticas para a Determinação de Agrotóxicos da Classe das Estrobilurinas

Almeida, J. M. S.; Dornellas, R. M.; da Silva, A. R.; Aucélio, R. Q.*

Rev. Virtual Quim., 2015, 7 (5), 1709-1727. Data de publicação na Web: 13 de julho de 2015

<http://www.uff.br/rvq>

Graphical abstract



Electrooxidation of trifloxystrobin at the boron-doped diamond electrode: electrochemical mechanism, quantitative determination and degradation studies

Joseany M. S. Almeida^a, Carlos A. T. Toloza^a, Rafael M. Dornellas^b, Andrea R. da Silva^c and Ricardo Q. Aucélio^a

^aChemistry Department, Pontifícia Universidade Católica do Rio de Janeiro (PUC-Rio), Rio de Janeiro, Brazil;

^bChemistry Institute, Universidade Federal de Uberlândia, Uberlândia, Brazil; ^cCentro Federal de Educação Tecnológica Celso Suckow da Fonseca (CEFET/RJ), Valença, Brazil

Microchemical Journal 133 (2017) 629–637



Contents lists available at ScienceDirect

Microchemical Journal

journal homepage: www.elsevier.com/locate/microc



Voltammetric determination of lapachol in the presence of lapachones and in ethanolic extract of *Tabebuia impetiginosa* using an epoxy-graphite composite electrode



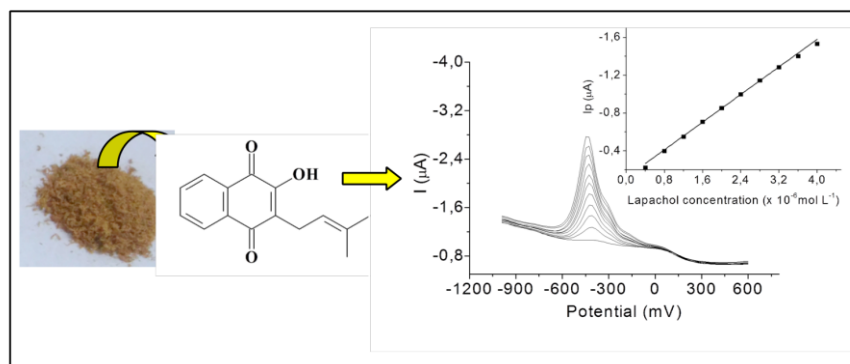
Joseany M.S. Almeida^a, Abel I. Balbin-Tamayo^b, Carlos A.T. Toloza^a, Isabela D.O. Figueira^a, Aurora Pérez-Gramatges^a, Andrea R. da Silva^c, Ricardo Q. Aucélio^{a,*}

^a Chemistry Department, Pontifícia Universidade Católica do Rio de Janeiro (PUC-Rio), Rio de Janeiro-RJ 22453-900, Brazil

^b Facultad de Química, Universidad de La Habana, Zapata y G, Vedado, Plaza, La Habana 10400, Cuba

^c Centro Federal de Educação Tecnológica Celso Suckow da Fonseca (CEFET/RJ), Valença-RJ 27600-000, Brazil

Graphical abstract



B

Participation in Congress

1- Apresentação de Poster / Painel no(a) **SIFEE- Simpósio Fluminense de Eletroquímica e Eletroanalítica, 2014. (Simpósio). Determinação voltamétrica de trifloxistrobina utilizando eletrodo de diamante dopado com boro.**

2- Apresentação de Poster / Painel no(a) **ISE- International Society of Electrochemistry, 2014. (Congresso). Voltammetric determination of trifloxystrobin in orange juice and water samples using the boron-doped diamond electrode.**

3- Apresentação de Poster / Painel no(a) **SIBEE- Simpósio Brasileiro de Eletroquímica e Eletroanalítica, 2015. (Simpósio). Determinação de gentamicina por amperometria num sistema de análise por injeção em batelada usando eletrodo de diamante dopado com boro.**

4- Apresentação de Poster / Painel no(a) **ENQA- Encontro Brasileiro de Química Analítica, 2016. (Congresso). Sensor eletroquímico para determinação voltamétrica de histamina.**

5- Apresentação de Poster / Painel no(a) **ENQA- Encontro Brasileiro de Química Analítica, 2016. (Congresso). Compósito de epóxi-grafite como sensor eletroquímico para determinação voltamétrica de lapachol.**

6- Apresentação de Poster / Painel no(a) **IUPAQ/SBQ – 46th World Chemistry Congress, 40^a Reunião Anual da Sociedade Brasileira de Química and IUPAC 49th General Assembly, 2017 (Congresso). Use of solid-phase extraction using an aminoglycoside selective molecular imprinting polymer for the determination of gentamicin by amperometry at a boron-doped diamond electrode.**